The Ohio State University
1314 Kinnear Road
Columbus, Ohio 43212-1154

Adaptive Array For Weak Interfering Signals – Geostationary Satellite Experiments

A Thesis

Presented in Partial Fulfillment of the Requirements for

the Degree Master of Science in the

Graduate School of the Ohio State University

by

Karl Steadman, B.S.E.E.

* * * * *

The Ohio State University

1989

Master's Examination Committee:

Professor Randolph L. Moses

Professor Aharon A. Ksienski

Approved by:

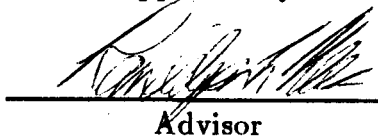

Advisor
Department of Electrical Engineering

ACKNOWLEDGEMENTS

I would like to express my sincere thanks to my advisors Dr. Eric K. Walton, Dr. Inder J. Gupta, and Prof. Randy Moses for their excellent technical assistance during this project. I would also like to thank Mr. Donald E. Henry and Mr. Wayne Cornell for their helpful assistance during the experimental phase of this work.

I would also like to thank Dr. E.F. Miller and Mr. Cliff Arth of NASA - Lewis Research Center, Cleveland, Ohio. This work was supported by NASA - Lewis Research Center under Grant NAG3-536 to The Ohio State University.

Finally, I wish to thank my family and friends for their support while this thesis was being prepared.

VITA

[redacted] ..... Born: [redacted].

May, 1987 ..... B.S.E.E., Rensselaer Polytechnic Institute, Troy, New York.

August, 1987—Present ..... Graduate Research Associate, The Ohio State University, Columbus, Ohio.

FIELD OF STUDY

Major Field: Electrical Engineering

TABLE OF CONTENTS

LIST OF TABLES

LIST OF FIGURES

CHAPTER I

INTRODUCTION

A major problem in satellite communications is interference caused by transmissions from satellites adjacent to the desired signal satellite in geostationary orbit. These transmissions enter the receive system through the sidelobes of the earth station receive antenna and interfere with the communication link. This problem has recently become more serious due to the crowding of the geostationary satellite orbit (GSO)[1] and the move towards reduced angular separations between satellites. Indeed, it is this type of interference which limits the capacity of the geostationary orbit [7].

Because the interfering signals enter the receive system through the receive antenna sidelobes, as shown in Figure 1, the signal-to-interference ratio (SIR) in the receiver is in the 10-30 dB range. The signal-to-noise ratio (SNR) in the receiver is generally 12-25 dB, which means the interference may be below the system noise level. Although weak, these signals because of their coherent nature and similar spectral characteristics with the desired signal may cause objectionable interference, and thus should be further suppressed.

One method to overcome this problem is to suppress the interference at the

[1]The geostationary satellite orbit can be described as an imaginary circle in the equatorial plane, approximately 36,000 km above the surface of the Earth. A satellite placed there orbits the Earth at the same angular velocity as the Earth rotates on its axis, so that it appears to be stationary to an observer on the Earth.

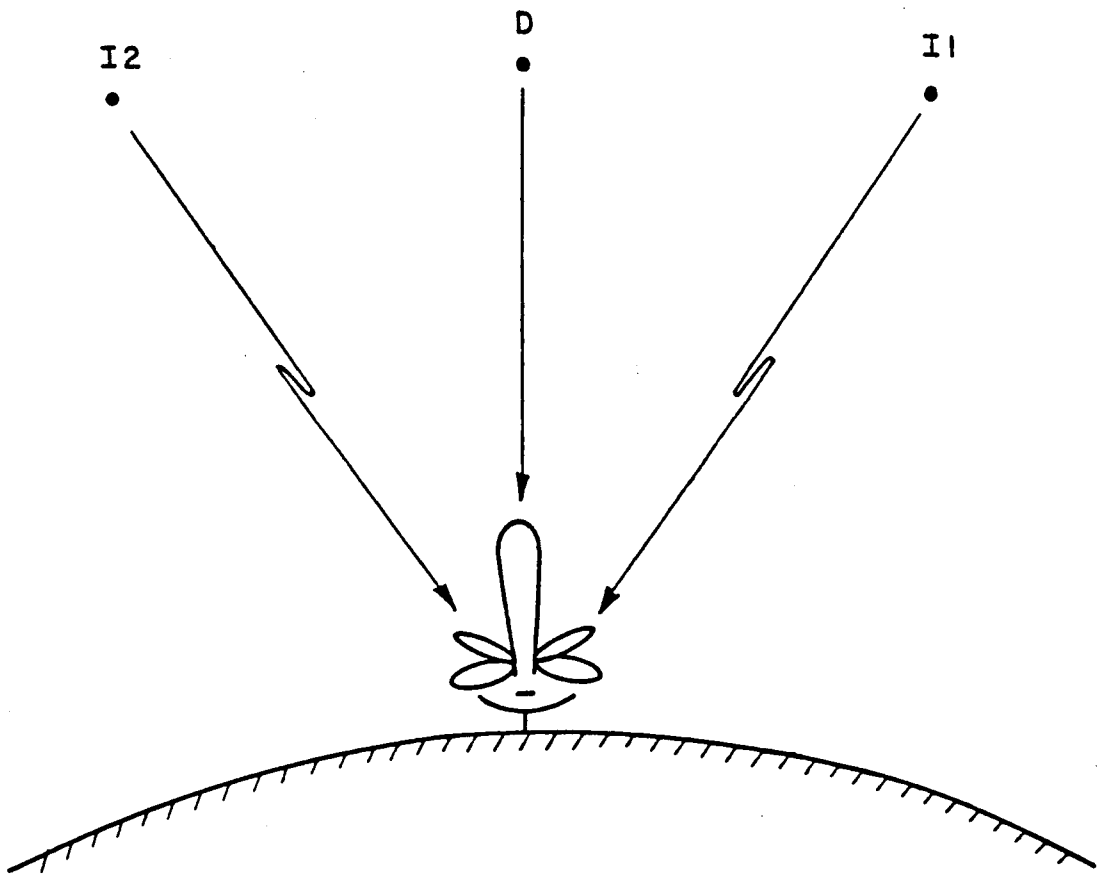

Figure 1: Earth station receiving a desired signal and interfering signals.

earth station receive site. Adaptive antenna arrays [1-4] have commonly been used to suppress interfering signals at the receive site. An adaptive array is an antenna array, which through feedback control, changes its pattern in response to the signal and interference environment in order to optimize a designated type of performance, such as the desired signal-to-interference plus noise ratio. It does so by steering pattern nulls in the directions of interfering signals and a pattern maximum in the direction of the desired signal. However, conventional adaptive arrays are traditionally designed to operate in the presence of strong interference (intentional jamming) and are unable to suppress weak interfering signals. This is because in the presence of weak interference it is the noise, rather than the interfering signals, which controls the array weights. Therefore, the array adapts to minimize the noise and the interference remains unsuppressed.

Recently, Gupta and Ksienski [5] have proposed modifications to the feedback loops which control the weights in a conventional adaptive array, that enable the suppression of weak interfering signals. In the modified feedback loops, the effect of noise on the array weights is reduced by reducing the correlation between the noise components of the two inputs to the feedback loop correlator. Two spatially separate antennas are used in each feedback loop to reduce the correlation of externally generated cosmic, atmospheric, and terrestial thermal noise. Further, two separate amplifiers are used in each feedback loop to decorrelate internally generated thermal noise. It was shown analytically that the modified adaptive array can provide the required interference suppression [5]. Later, Ward et al. built an experimental adaptive array system to verify the theoretical analysis [6,19].

In the experimental system built by Ward et al., bench generated pulse modulated sinusoids were used to study the performance of the experimental system [6]. The frequency of the sinusoidal signals was 69 MHz. Thus, the system perfor-

mance was evaluated for very narrowband signals under a controlled environment. Using the experimental system it was shown that one can indeed suppress weak interfering signals to the required level. However, in practice the signals received from geostationary satellites will be at much higher frequency and will have certain bandwidths associated with them.

The purpose of this thesis is to evaluate the performance of the experimental system using signals from an existing geostationary satellite interference environment. To do this, an earth station antenna was built to receive signals from various geostationary satellites. In these experiments the received signals will have a frequency of approximately 4 GHz (C-band) and have a bandwidth of over 35 MHz. These signals are downconverted to a 69 MHz intermediate frequency in the experimental system. Using the downconverted signals, the performance of the experimental system for various signal scenarios is evaluated. In this situation, due to the inherent thermal noise, qualitative instead of quantitative test results are presented. It is shown that the experimental system can null up to two interfering signals well below the noise level. However, to avoid the cancellation of the desired signal, one needs to use a steering vector [18]. Various methods to obtain an estimate of the steering vector are proposed.

The remainder of this thesis is arranged as follows. The experimental system built by Ward et al. is described in Chapter II. The experimental results are also summarized in that chapter. Chapter III discusses the antenna system built to receive signals from the GSO. It is a 30 ft diameter parabolic reflector with multiple feeds. Individual feed elements and their radiation patterns are also included in Chapter III. Chapter IV contains a discussion of the radio frequency (RF) circuitry built to process the GSO signals. The method used to coherently downconvert all the satellite signals is also discussed in that chapter. Using the RF circuitry the

antenna patterns of the 30 ft parabolic antenna for various feed locations were measured. These patterns are included to show that with the antenna configuration employed, one can study the performance of the experimental system under different signal scenarios. Chapter V describes system calibration, various test scenarios and experimental results. Finally, Chapter VI contains a summary, general conclusions, and some suggestions for future investigation.

CHAPTER II

THE ORIGINAL EXPERIMENTAL SYSTEM

2.1 Introduction

The experimental system built by Ward et al. [6,19] is a sidelobe canceler with two auxiliary channels. The modified feedback loops as proposed by Gupta and Ksienski [5] are used to control the weights of the auxiliary channels. In the modified feedback loops, two spatially separated antennas followed by their own individual amplifiers are used with each auxiliary channel to decorrelate the noise in the feedback loops. Thus, the experimental system uses five antenna elements, one for the main channel and two each for the two auxiliary channels. The main antenna is pointed in the desired signal direction, which is assumed to be known accurately. The auxiliary antennas are pointed in the general direction of the interfering signals. The auxiliary antennas are located such that the two antennas associated with a given auxiliary channel receive the directional signal nearly equal in phase while the external noise received by the two antennas is only partially correlated.

Instead of using actual antennas the original experimental system simulated the signals received by the five antennas. Thus, evaluating the performance of the system under a controlled environment. The signal scenario was assumed to consist of a desired signal and as many as two interfering signals. These signals were bench generated pulse modulated sinusoidal signals. A brief description of the

experimental system along with a summary of the experimental results obtained by Ward et al. using bench generated signals is given in this chapter. First, a brief discussion of a sidelobe canceler is given.

2.2 Structure of a Sidelobe Canceler

A conventional sidelobe canceler consists of a single high-gain antenna (or main antenna) to which a number of lower gain auxiliary antenna elements are added. The auxiliary antenna element outputs as shown in Figure 2 are adaptively weighted and then added to the high-gain antenna output. The weight values are adjusted in amplitude and in phase as an adaptive optimization problem. By controlling the weights on the auxiliary elements, interference in the sidelobes of the high-gain element may be nulled.

The sidelobe canceler uses the auxiliary antennas to create independent, equal amplitude and opposite phase replicas of the sidelobes of the main antenna, such that when the weighted auxiliary elements signals are summed with the main element signal to form the array output, the interfering signals are canceled. A sidelobe canceler with N auxiliary antennas, or channels, has N degrees of freedom. In other words, the sidelobe canceler is able to null as many as N interfering signals. The experimental system built by Ward et al. has two auxiliary channels. Thus, it can suppress up to two incident interfering signals. The signal-to-interference plus noise ratio performance of a sidelobe canceler is the same as that of an Applebaum array [3].

Figure 3 shows a typical feedback loop of a conventional sidelobe canceler. The sidelobe canceler attempts to maximize the desired signal-to-noise plus interference (SINR) at the array output by minimizing an error term, the correlation. In the sidelobe canceler the desired signal is 'desirable' while the interference and

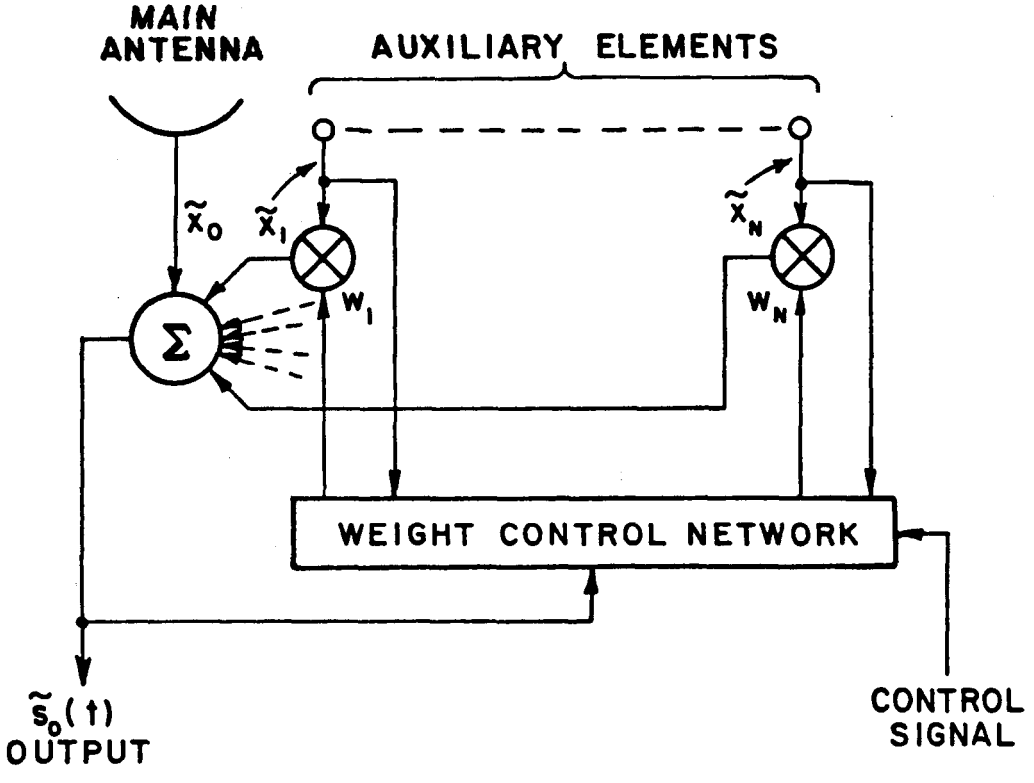

Figure 2: A sidelobe canceler.

noise components are 'undesirable'. The correlation is formed from the auxiliary channel and the array output. In the conventional sidelobe canceler, when the interference is weak or the auxiliary elements gain is low, the auxiliary element and the array output correlation is dominated by the noise components. Thus, the weights of the auxiliary channels is dictated by the system noise and the interference remains unsuppressed. To avoid this problem, Gupta and Ksienski proposed a modifed feedback loop. Figure 4 shows the modified feedback loop. Note that

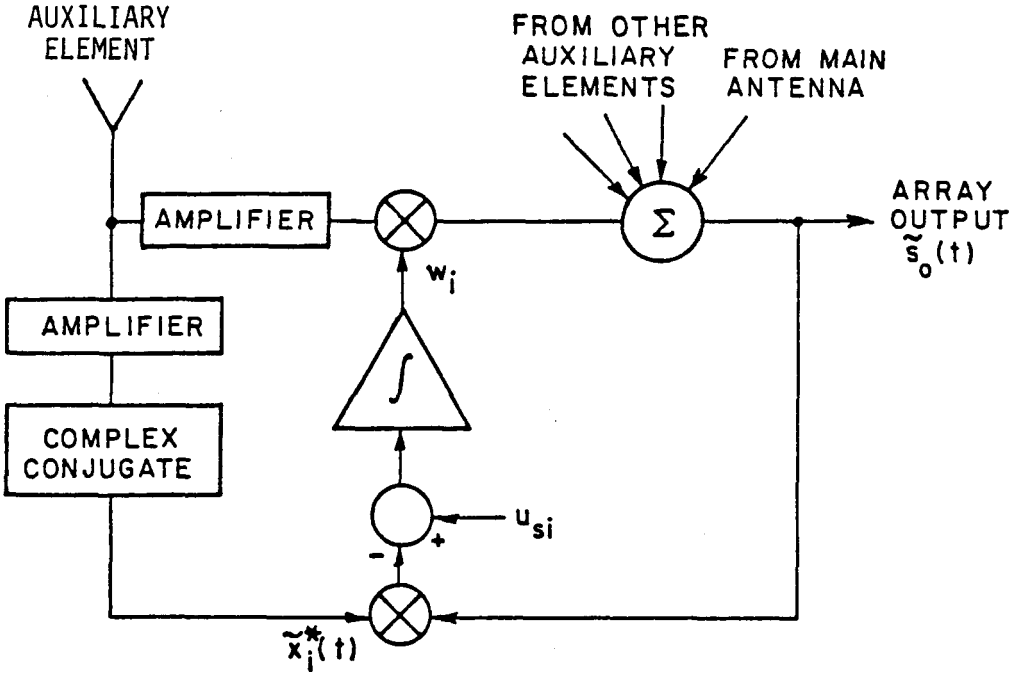

Figure 3: The conventional sidelobe canceler.

in the modified feedback loops, the effect of noise on the array weights is reduced by reducing the correlation between the noise components of the two branches of each loop. Note that two spatially separate antennas, each followed its individual amplifier, are used in each loop to decorrelate both externally and internally generated noise. The external noise is comprised of galactic, atmospheric, and terrestial thermal noise. The spatial separation between the two auxiliary channel antennas guarantees that the external noise entering the two antennas is only par-

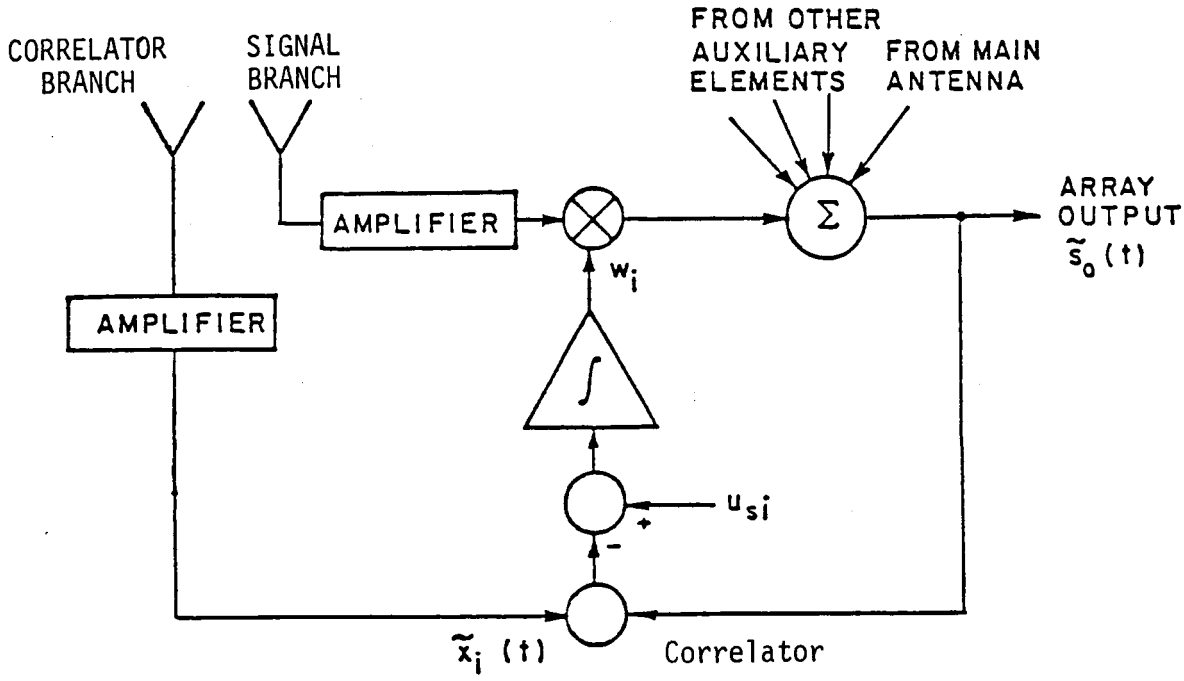

Figure 4: Modified adaptive array feedback loop.

tially correlated. For directive antennas, one can achieve the noise decorrelation by pointing the two antennas in different directions. The auxiliary antennas are located such that each antenna in the pair associated with a feedback loop receives the signals from the interfering sources in nearly equal phases.

For clarity, the antenna whose output is connected to the correlator in the feedback loop will be called the 'correlator branch' while the other antenna whose output is adaptively weighted will be called the 'signal branch'. Thus, the modified

feedback loops decorrelate the system noise in the correlator branch from the system noise in the signal branch of each loop. The original experimental system is described next.

2.3 The Experimental System

The experimental system built by Ward et al. [6,19] is a sidelobe canceler with two auxiliary channels. Modified feedback loops, such as the one shown in Figure 4, are used to control the weights of the auxiliary channel signals. The total number of antennas in the system is five, one for the main antenna and a pair of antennas feeding each auxiliary channel. For the purposes of parameter control and performance evaluation, the system does not use actual antennas. Instead, the signals which would have been received by the five element antenna array are synthesized in the experimental system. The incident signal scenario is assumed to consist of a desired signal and up to two interfering signals, whose sources may be located at arbitrary angular separations from the desired signal source.

A block diagram of the experimental system is shown in Figure 5. The first block on the left is the signal simulator. The signal simulator synthesizes the desired signal and the two interfering signals incident on the array. The array simulator, the next block to the right, accepts the signals generated by the signal simulator and combines them to form the signals received at each array element. Thus the array simulator has three inputs for the three incident signals, and five outputs corresponding to the five antenna elements of the array.

The next block, the array processor, weights the auxiliary signal branch and forms the adapted array output. Figure 6 shows the subsystems significant to the array processor. Only one implemented modified feedback loop is shown. The system operates at 69 MHz (or approximately 70 MHz for wide-band signals), with

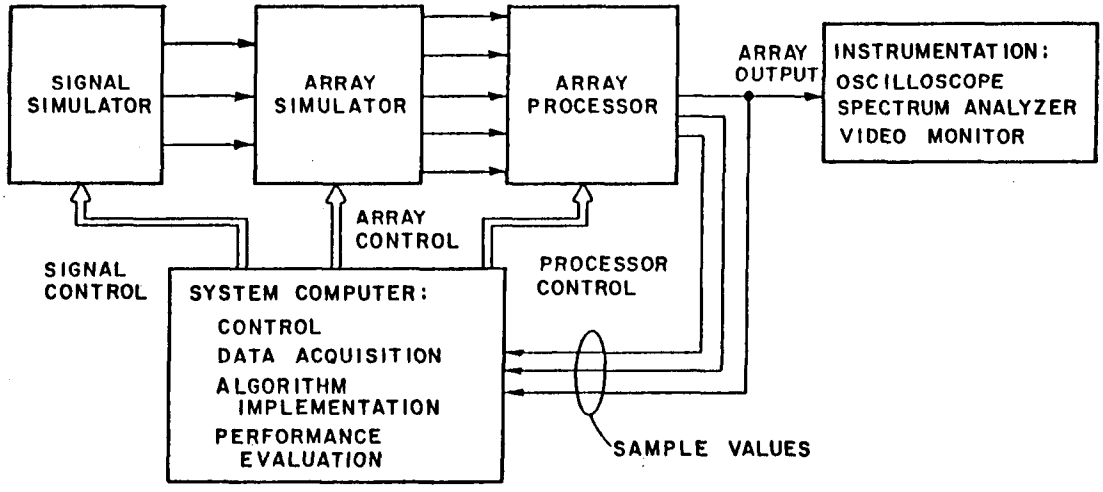

Figure 5: Block diagram of the experimental system.

a bandwidth of 6 MHz. A digital computer (PDP-11/23) is used to implement the weight control algorithms, to control the various system components, and to evaluate the system performance. A brief description of these three blocks are given below.

2.3.1 The Signal Simulator

The bench generated desired signal and the two interfering signals are produced in the signal simulator. In order to measure adaptive array performance characteristics such as interference suppression, output signal-to-noise ratio, and output signal-to-interference plus noise ratio, it is necessary to measure separately the desired signal power, the interference power, and the noise power present at

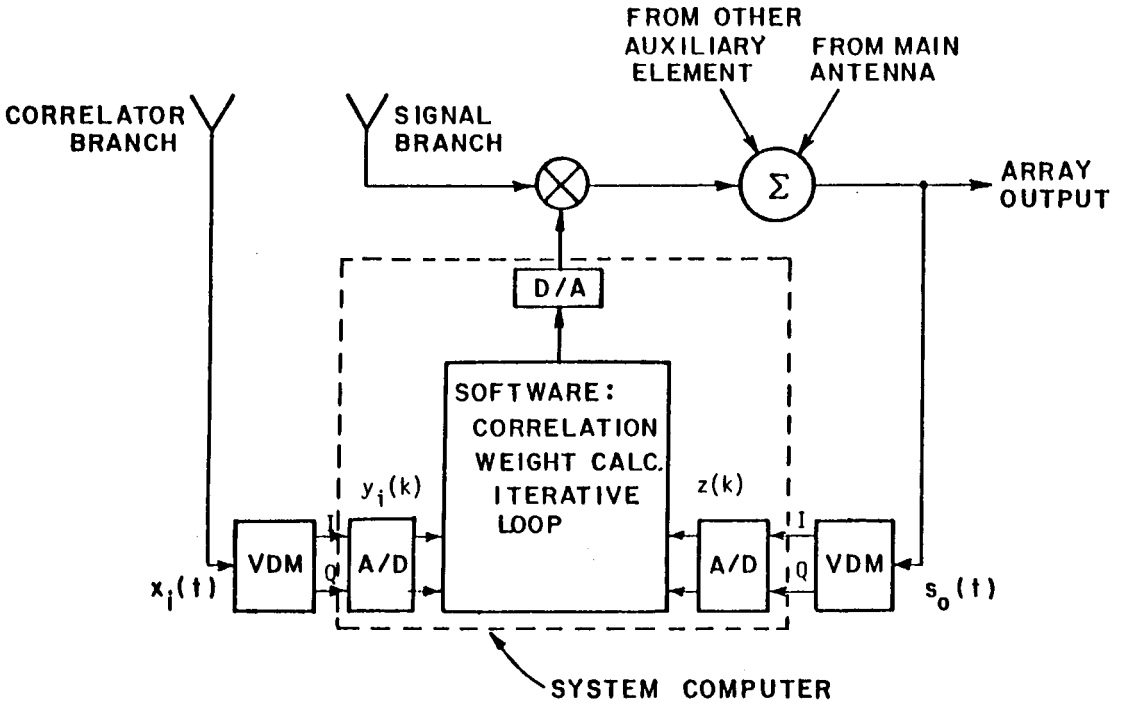

Figure 6: The system implementation of a modified feedback loop.

each of the array branches and at the array output. Pulse modulated sinusoids are used as the desired signal and the interfering signals to accomplish this objective. The modulation on one interfering signal is staggered from the modulation on the other interfering signal, and from the desired signal modulation, such that each signal occupies a different portion of the pulse repetition period. There is also a portion of each period when no signal (only noise) is present. The desired and interfering signals are therefore all uncorrelated with each other (for all interelement time delays of interest). To summarize, a complete pulse modulated waveform contains the desired signal, the two interfering signals, and the additive noise. Figure 7 shows the envelope of a typical pulse modulated signal. The incident signals

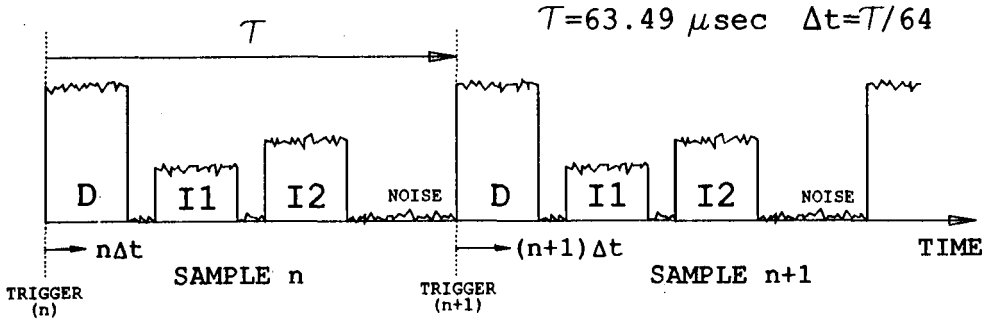

Figure 7: Diagram of the envelope of a pulse modulated sinusoidal signal and the sampling scheme.

produced by the signal simulator are transferred to the array simulator which is described next.

2.3.2 The Array Simulator

Figure 8 shows a detailed block diagram of the array simulator. In the array simulator, the incident signals are combined and thermal noise is added to form the signals received at each array element, such that each element signal contains a component due to the desired signal, components due to both interfering signals, and additive thermal noise. Thus the array simulator has three inputs for the three incident signals, and five outputs corresponding to the five antenna elements of the array. The five elements are designated as the Main channel, Signal Branch 1 and

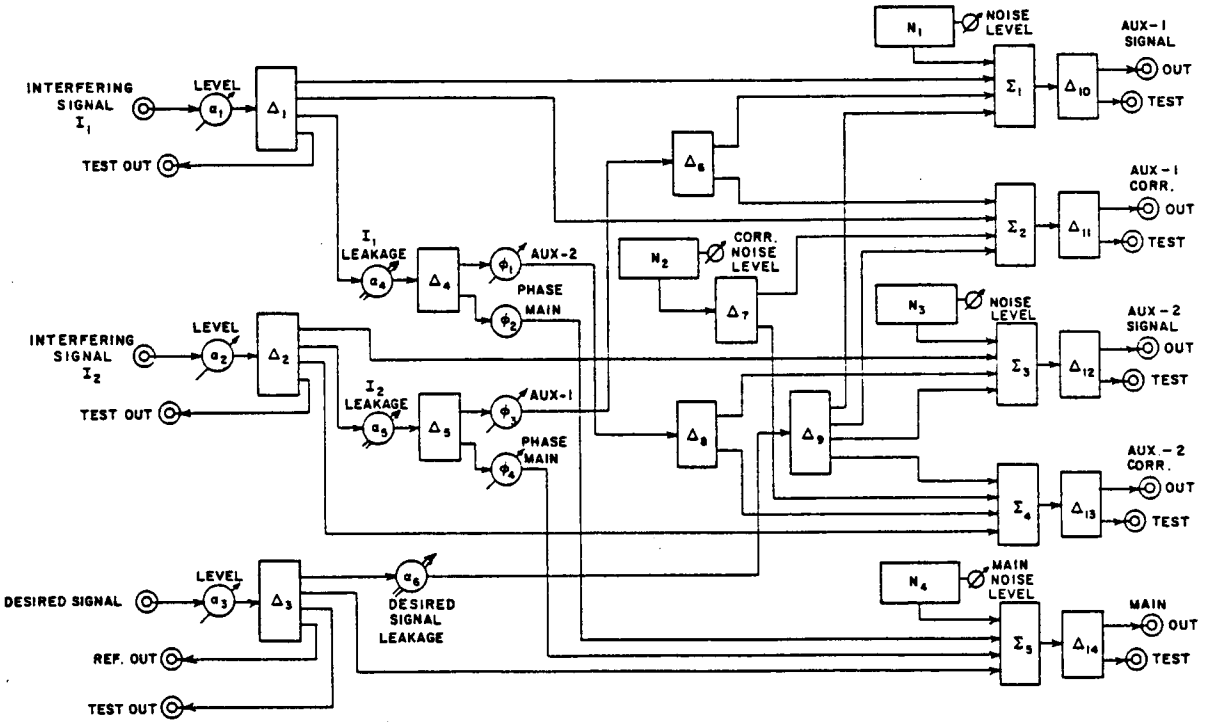

Figure 8: Array simulator detailed block diagram.

Correlator Branch 1 for auxiliary channel 1, and Signal Branch 2 and Correlator Branch 2 for auxiliary channel 2. The main channel output is the signal received at the main antenna. The other outputs are the signals received by the auxiliary antennas of the modified feedback loops of the two auxiliary channel sidelobe canceler. The blocks labeled N_1 through N_4 are the noise sources. Note that the noise components injected into the auxiliary signal branches and the main channel are all from different noise sources, and thus uncorrelated. Furthermore, the noise components in the auxiliary correlator branches originate from another noise source, and are therefore uncorrelated with the noise components of all the signal branches. In Figure 8, the Δ's are zero-phase power dividers. The Σ's

represent summing junctions, which are zero-phase power dividers connected as summers. The α's are variable attenuators and the ϕ's denote variable phase shifters.

The phase shifters simulate variations of the interfering signal directions of arrival by varying the interelement phase shifts between interfering signal components of different array elements. There are no phase shifters associated with the desired signal because it is assumed to arrive from broadside and thus is received with the same phase at each array element. Variable attenuators are used to control the amount of each incident signal received at each output channel. This is analogous to varying the gains of the main and auxiliary antennas in the directions of the incident signals. Once the desired scenario is set, the array simulator outputs are fed to the array processor, where the auxiliary channel weights are determined. The array processor is discussed next.

2.3.3 The Array Processor

A detailed block diagram of the array processor is shown in Figure 9. Note that the auxiliary channel correlator branch signals are downconverted to baseband and quadrature detected by the vector demodulators (VDMs), as is the array output. These baseband voltages are simultaneously sampled, analog-to-digital (A/D) converted and read by the system computer, which implements the weight control equation and calculates the array weights. The new weights are then digital-to-analog (D/A) converted and applied to the auxiliary signal branches as I and Q control voltages of the two vector modulators (VMODs). The weighted auxiliary elements are summed with the main signal branch to form the array output. In the array processor, the I and Q outputs of each vector demodulator are processed prior to being sampled. A low pass filter first removes the second

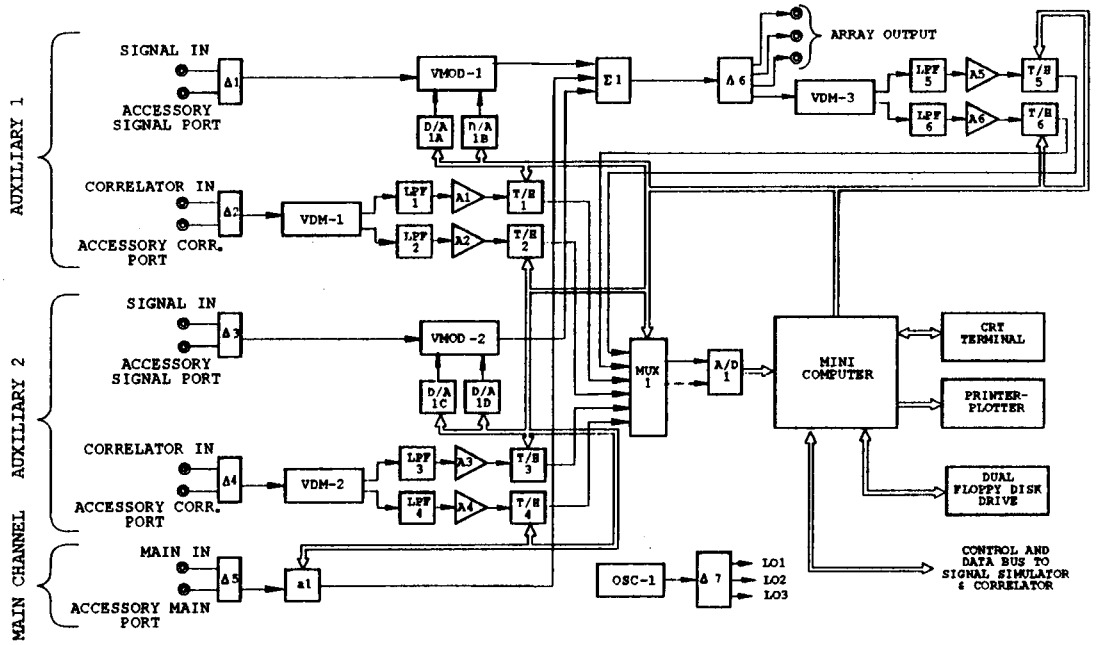

Figure 9: The detailed block diagram of the array processor.

harmonic. The resultant baseband signals are then amplified to utilize the full dynamic range of the system A/D converter. Track and hold devices allow the multiplexing of all six VDM outputs to the single A/D converter, so that they can be sampled simultaneously. This preserves the signal and noise correlation between the samples of different branches. The track/hold devices of the array processor are triggered in synchronism with the pulse modulated signal envelope. Because of A/D conversion speed limitations, successive samples are not taken in the same pulse repetition period (τ), as can be seen in Figure 7. Instead, successive samples are from different pulse repetition periods, but separated by only a small time interval ($\Delta t \approx 1.0\ \mu$sec) from the start of a pulse repetition period.

Thus, an effective sampling rate (1.0 MHz) much higher than the sampling rate possible in real time (15.75 KHz) is achieved. By varying the delay from the start of a period to the sampling instant, a sequence of samples covering the whole waveform is provided to the system computer. By averaging over a complete pulse modulated waveform period (64 samples), as far as the adaptive array is concerned, the desired and interfering signals appear to be simultaneously present. Thus, the pulse modulation scheme is exploited solely for performance evaluation, and not used in determining the auxiliary channel weights.

Note that the system is a hybrid system. This is because analog weights are applied to analog signals, but the weights are calculated from discrete time samples of the element signals and the array output. The correlation between the correlator branch and the array output is estimated from the sampled data in software, which then updates the array weights. The discrete form of the modified feedback loop algorithm is described next.

2.4 The Modified Feedback Loop Algorithm

The I and Q weights of each auxiliary element are computed according to a discrete time form of the Applebaum control equation [3] and are given by

$$w_{iI}(n+1) = w_{iI}(n) - \gamma Re(c_i - u_{si}) \tag{2.1}$$

$$w_{iQ}(n+1) = w_{iQ}(n) + \gamma Im(c_i - u_{si}) \tag{2.2}$$

where w_{iI} and w_{iQ} are the in-phase and quadrature weights of the i^{th} auxiliary element, γ is the loop gain, u_{si} is the i^{th} component of the steering vector, and c_i is the correlation between the array output signal and the i^{th} auxiliary correlator branch signal. The loop gain, γ, determines the speed of response of the system.

It is chosen as a compromise between response time and weight variance while ensuring that the weights remain stable. The correlation, c_i, is defined as

$$c_i = \frac{1}{N} \sum_{k=1}^{N} y_i(k) z^*(k) \tag{2.3}$$

where N is the number of samples used for the correlation estimate, and $y_i(k)$, $z(k)$ are, respectively the complex samples of the signals received by the i^{th} auxiliary correlator branch and the signals at the array output. Here, * denotes the complex conjugate. Also,

$$y_i(k) = y_{iI}(k) + j y_{iQ}(k) \tag{2.4}$$

where $y_{iI}(k)$ and $y_{iQ}(k)$ are samples taken from the I and Q outputs of the i^{th} auxiliary element vector demodulator. Similarly for the array output

$$z(k) = z_I(k) + j z_Q(k). \tag{2.5}$$

The steering vector is defined as

$$u_{si} = \frac{1}{N} \sum_{k=1}^{N} y_{di}(k) z_d^*(k) \tag{2.6}$$

where N is the number of samples used for the correlation estimate, and $y_{di}(k)$, $z_d(k)$ are respectively the complex samples received in the i^{th} auxiliary element and the array output due to the desired signal only. The steering vector components u_{si} prevent the array weights from moving to cancel the desired signal, and can be calculated using the angle of arrival of the desired signal which is assumed to be known exactly. The number of samples N is chosen so that the correlations are averages over several periods of the received signals. Also, note that the system noise at the array output is uncorrelated with the system noise in the auxiliary correlator branches. Thus, if the number of samples is large enough for an accurate

correlation estimate, the weights will essentially be independent of the noise power in the various branches and the array will respond to the weak interfering signals.

By implementing the weight control equation in software, many problems often encountered with analog feedback loops, especially at low signal levels, are avoided. These include effects of DC offset voltages, stray coupling and feedthrough associated with the correlator multiplier, and leakage and DC offset voltages in analog integrators. Also, the use of a digital computer in the experimental system provides great flexibility, not only in algorithm implementation, but also in system calibration and quantitative performance evaluation. The next section summarizes the results obtained by Ward et al.

2.5 Experimental Results Using Bench Generated Signals

A series of tests were performed to evaluate the performance of the experimental system [6]. Prior to each experiment, a calibration sequence was executed to compensate for DC offset voltages and feedback loop differential phase shifts. A summary of the results obtained with bench generated sinusoidal signals is given below.

1. Interference suppression is independent of the angle of arrival of the interfering signal. This will be the case as long as the auxiliary antenna elements are pointed in the general directions of the interference and the interfering signals are not within the main beam of the main antenna.

2. Interference suppression increases as the INR in the main channel increases, as shown in Figure 10.

3. Output SIR is constant as the INR in the main channel increases, as shown in Figure 10.

4. Interference suppression is essentially independent of the auxiliary ele-

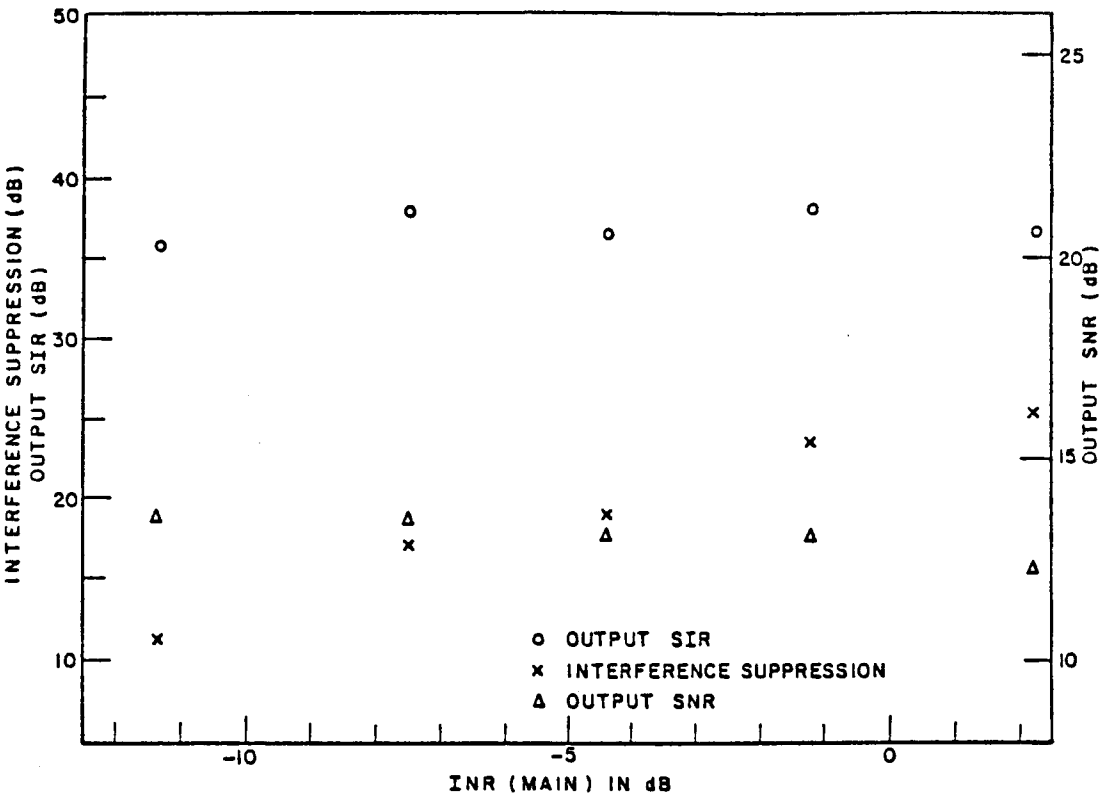

Figure 10: Performance versus INR(main channel) after adaptation. Two interfering signals, INR_1(aux-1) = INR_2(aux-2) = 8.8 dB, SNR(main channel) = 13.6 dB.

ment gain (see Figure 11), as long as the gain is large enough to keep the weights from becoming too large for the system to accommodate, and the system noise is decorrelated. If the noise is not decorrelated, interference suppression will increase with auxiliary element gain.

5. The output SNR with two interfering signals is lower than with one interfering signal due to the weighted auxiliary branches contributing more noise.

6. A slight degradation of the interference suppression was observed with two interfering signal versus only one. This degradation is most likely because both degrees of freedom in the array are used to cancel the two interfering signals.

7. The adaptive antenna array is able to suppress two interfering signals below the thermal noise level, as shown in Figures 10 and 11. As can be seen from

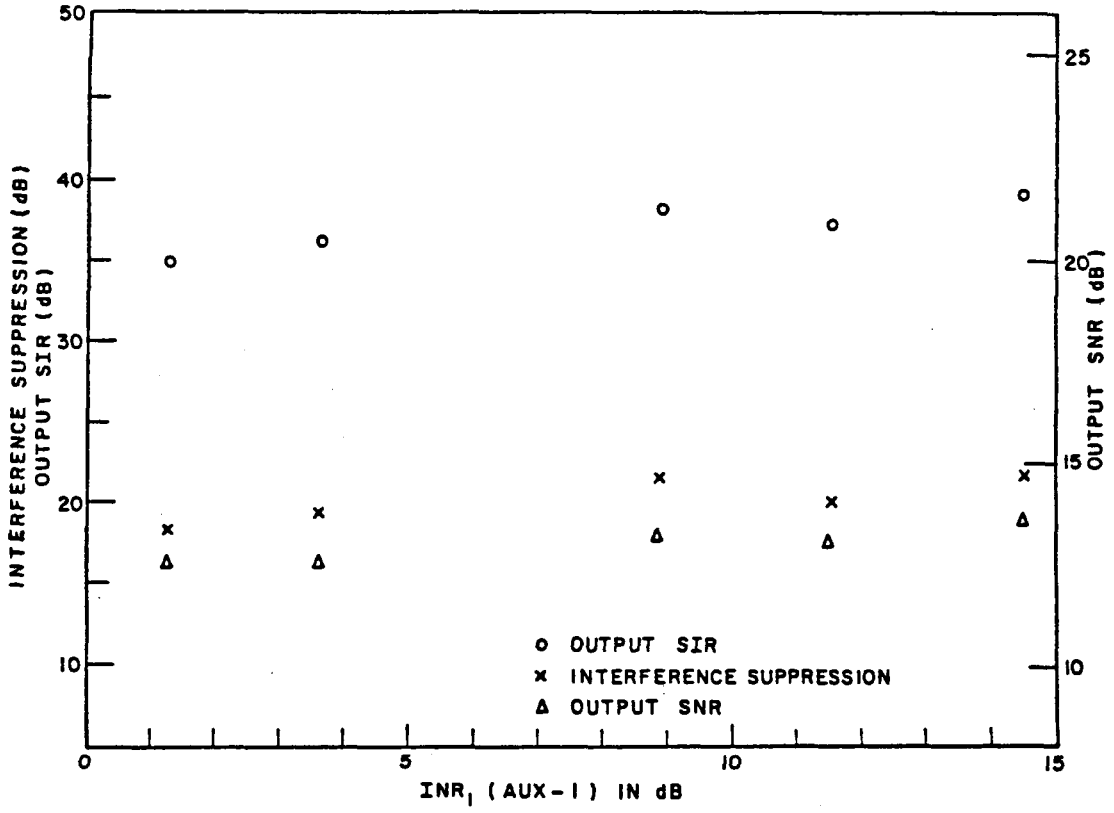

Figure 11: Performance versus INR_1(aux-1) after adaptation. Two interfering signals, INR_1(aux-1) = INR_2(aux-2), INR_1(main channel) = INR_2(main channel) = -6.5 dB. SNR(main channel) = 13.6 dB.

these two figures the output SIR is at least 35 dB.

8. Errors in the DC offset estimate which is used as a correction to the received data and the correlation of the strong desired signal with the auxiliary noise components were observed to contribute, respectively, to performance variations and weight jitter.

These experiments were limited to a very narrow bandwidth since pulse modulated sinusoids were used. However, in an actual communication link, such as with broadcast satellite FM television signals, the bandwidth can exceed 30 MHz. In the experimental system, which has a 69 MHz center frequency, this translates to a percentage of bandwidth of over 50%. However, in the fixed satellite down-

link band from 3.7-4.2 GHz this percentage of bandwidth is less than 1%. Thus a single complex weight value set by the array processor should suppress a wide-band signal at the 69 MHz intermediate frequency. Nevertheless we would want to experimentally verify that this is true in practice. Moreover, evaluating the performance of the experimental system with actual satellite signals would reinforce the operation of the modified feedback loops. Specifically, we would wish to determine if any system particularities were overlooked in a true satellite communication link environment. Therefore, the system was modified to receive signals from satellites in the geostationary orbit. These modifications are described in the next chapters.

2.6 Summary

In this chapter, the experimental adaptive array system built by Ward et al. was described. The system is a modified sidelobe canceler with two auxiliary elements, so up to two interfering signals can be suppressed. The five element antenna array configuration for a modified sidelobe canceler was described. Two spatially separate antenna elements are used with each auxiliary channel to receive the signals from the interfering sources nearly in phase while the noise between them is only partially correlated. The results of the performance evaluation of the experimental system using pulse modulated sinusoids were outlined. These results showed that using modified feedback loops one can suppress as many as two interfering signals below the system noise level. Thus, the experimental system built by Ward et al. verified previous theoretical work.

The next chapter discusses the antenna system built to receive the geostationary satellite signals. This will allow the experimental system to be tested with wide-band signals in an actual satellite interference environment.

CHAPTER III

THE ANTENNA CONFIGURATION

3.1 Introduction

The experimental system as described in the last chapter uses five antenna elements: one for the main channel and two for each auxiliary channel. The main channel antenna designated as the main antenna is pointed in the direction of the desired signal, which is assumed to be known accurately. The auxiliary antennas are pointed in the general direction of the interfering signals. The auxiliary antenna pair associated with an auxiliary channel is located such that the directional signals incident on the two antennas are received nearly in phase while the noise entering the two antennas are only partially correlated.

These five antenna elements should be designed to receive signals from satellites in geostationary orbit (GSO). The center frequency of these signals is approximately 4 GHz. Normally, parabolic reflector antennas are used to receive signals from geostationary satellites. Thus, one would normally need five parabolic reflectors in the front end of the experimental system, which is not very practical. Alternatively, as suggested by Gupta [20], one can use multiple feeds with a single parabolic reflector. In the case of a parabolic reflector, by moving the feed in the focal plane, one can steer the main beam in different directions. Thus, one can use a parabolic reflector with five feeds as a front end to the experimental system. One of these feeds (the main feed) is used to receive the signals from the

desired satellite source, while the other feeds should be located such that reflector antenna beams associated with these feeds are pointed in the general direction of the interfering satellite sources. Note that the main feed will also receive signals from the interfering satellites through the sidelobes of the reflector antenna. The details of the parabolic reflector used with the experimental system are given in this chapter. The type of feed used and their distribution in the focal plane are also discussed. Some measured and calculated radiation patterns of the feeds, as well as of the reflector antenna, are included. The parabolic reflector used with the experimental system is discussed first.

3.2 The 30 Foot Parabolic Reflector

The antenna used for the adaptive array experiment is a 30 foot diameter (D) center fed parabolic reflector with a focal distance (F) of 12.5 feet. The parabolic reflector was constructed for another research project and was available for use for this experimental system. Servo controlled mounts position the parabolic reflector in azimuth and elevation. These mounts are designed to have a resolution of 0.1° or better even in 35 mph winds [9]. In practice, during calm winds the parabolic reflector was able to obtain a 0.05° resolution even with gear backlash.

Using the dimensions of the parabolic reflector, and an operating frequency of 3.95 GHz, certain parameters can be calculated, as shown in Table 1 [16]. In these calculations the electric field taper is modeled by the equation $E(r) = 1 - 2 \times r^2/3$, where r is the radial distance from the center of the reflector.

Note that the reflector has a very narrow main beam and very low sidelobes. The first sidelobe is 23 dB down from the peak of the main beam. At 3.95 GHz, the first sidelobe of this reflector antenna is 0.8° away from the boresight. The same can be seen in the plot of Figure 12. In the figure, the calculated radiation

Table 1: The performance estimates of the 30 ft (9.14 meter) diameter parabolic reflector antenna.

Parameter	Equation	Value
Parabolic dish depth (d)	$D^2/(16 \times F)$	1.37 m (4.5 ft)
F/D ratio	F/D	0.42
Gain	$(2.2D/\lambda)^2$	48.5 dBi
Half Power Beam Width (HPBW)	$\frac{65^\circ\lambda}{D}$	0.54°
Beam Width First Nulls (BWFN)	$\frac{145^\circ\lambda}{D}$	1.20°
First sidelobe level	—	-23 dB
Effective aperture	$0.5 \times \pi \times D^2/4$	32.8 m^2 (353 ft^2)

pattern for the parabolic reflector antenna at 3.95 GHz is shown. This pattern was computed using the Ohio State University ElectroScience Laboratory's NEC Reflector Antenna Code [10,11]. In the pattern calculation, aperture blockage due to the feed, surface irregularities and scattering due to the four struts are not included. Next, it will be shown that this parabolic reflector with multiple feeds can meet all the requirements of the experimental system.

3.3 The Preliminary Feed Distribution for the Parabolic Reflector Antenna

In the above section, the radiation pattern of the 30 ft diameter parabolic reflector was discussed. By laterally displacing a feed in the focal plane of the parabolic reflector, or defocusing a feed, one can steer the main beam of the antenna off-axis and over a required angular region. Thus, by displacing the feeds associated with the auxiliary channel a known angular distance from the focus one can point their respective main beams in the general direction of the interfering sources.

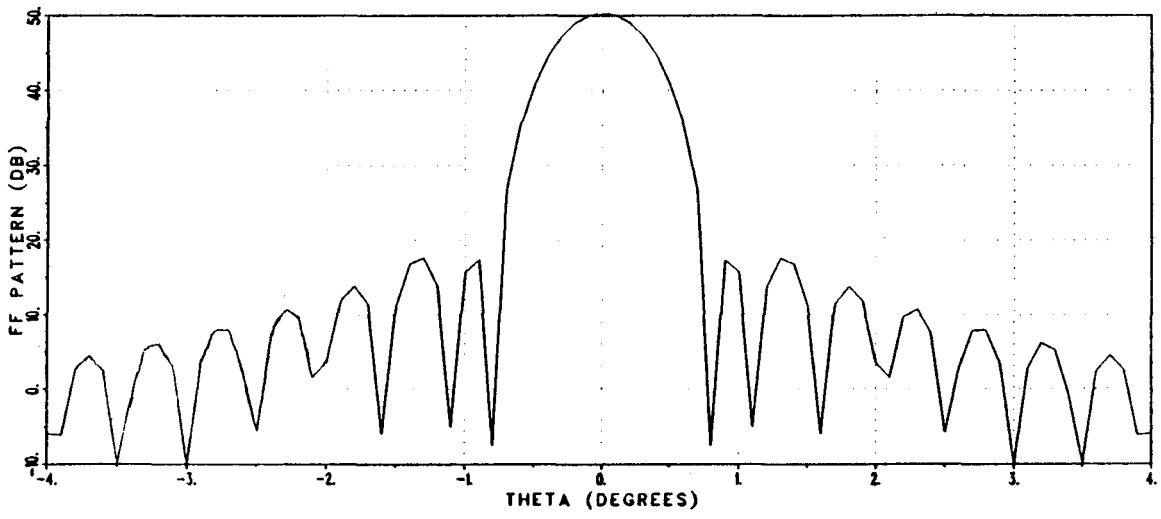

Figure 12: The radiation pattern of a focus fed 30 ft parabolic reflector antenna.

Figure 13 shows how the five feeds could be distributed. The X axis, as shown, coincides with the plane of the geostationary arc. The center feed is at the focus of the parabolic reflector. To the left and right of the center feed are a pair of feeds corresponding to each auxiliary channel. Note that each of the two feeds of an auxiliary channel are also displaced along the Y axis. Therefore, the beam associated with each auxiliary branch is pointed away from the GSO in opposite directions. This procedure is used to achieve external noise decorrelation in the two branches of each auxiliary channel. Below, we investigate the antenna patterns associated with the defocused feeds of each auxiliary channel to determine if this distribution of feeds can be used to receive signals from two geostationary satellites representing two interfering signal sources.

Again, the Ohio State University ElectroScience Laboratory's NEC Reflector Antenna Code is used to compute the antenna patterns for the 30 ft diameter reflector antenna at 3.95 GHz. The patterns are taken along the X axis which

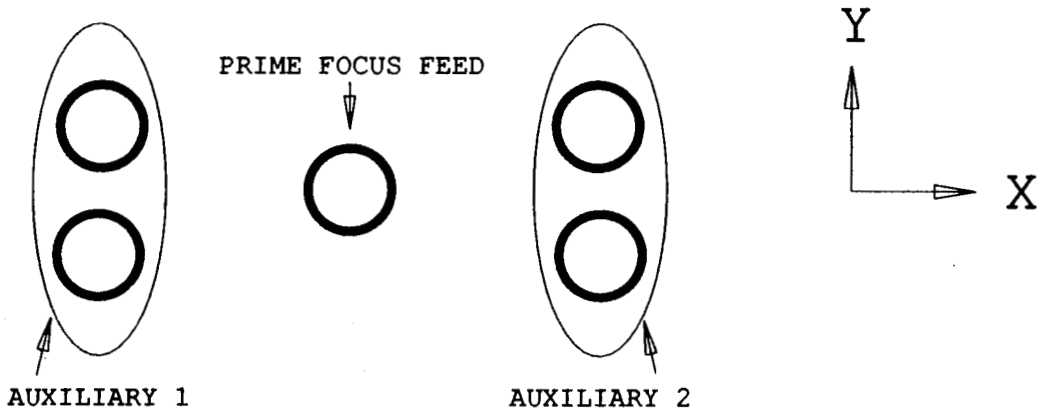

Figure 13: The preliminary feed distribution.

corresponds to the GSO. As before, the effects of feed blockage, strut scattering, and surface deformations are not taken into account. Figures 14 and 15 show, the parabolic reflector antenna pattern when the feed is displaced +2 and -2 wavelengths from the focal point along the X axis, respectively. From these two figures one can see that the antenna patterns are shifted by $\pm 1.9°$ off-axis, as expected. Note that the sidelobes are at least 14 dB down. Also, in each case the 10 dB beamwidth is 1.2°. Thus, this scheme will only be useful if the interfering satellites sources are between 1.3° and 2.5° from the desired satellite source. Normally, the spacing between the satellites is more than 2.5°. One can increase the displacement of the auxiliary feeds to receive signals from satellites which are more widely spaced. For example, Figure 16 shows the antenna pattern of the reflector when a feed is displaced three wavelengths from the focal point. In this case, the antenna will only receive signals from satellite sources with an angular displacement between 2.1° and 3.5° from the desired satellite source. Since geostationary

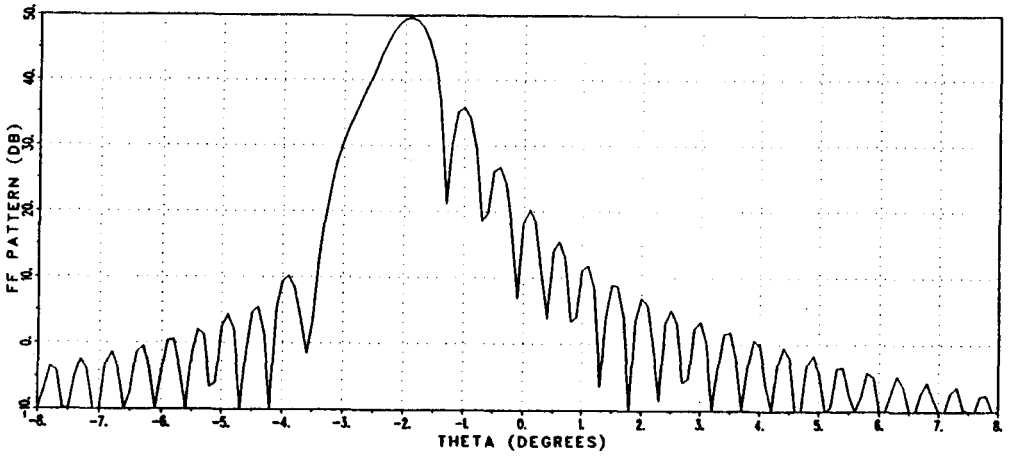

Figure 14: The radiation pattern (cut along the GSO) for a 30 ft. parabolic reflector antenna without aperture blockage with a feed displaced 2λ from the focus.

satellites are not evenly separated in the GSO, fixing the position of the auxiliary channel feeds is not practical. Moreover, since the main beams are very narrow, the defocused feeds have to be positioned very precisely in order for the satellite source to be within an associated main beam.

To allow more flexibility in the pointing of the auxiliary beams, the feeds associated with each auxiliary channel are installed on a movable platform. This movable platform displaces the feeds along the X axis while in the focal plane of the parabolic reflector antenna. The movable platform also provides the user with control over the received signal level in the auxiliaries. For example, by not pointing the main beam of an auxiliary channel directly at the interfering source, one can decrease the interference level received by the auxiliary channel. In other words, one has the ability to change the INR in the auxiliary channels as needed for a specific interference scenario.

Another important consideration, which was alluded to previously, is the low

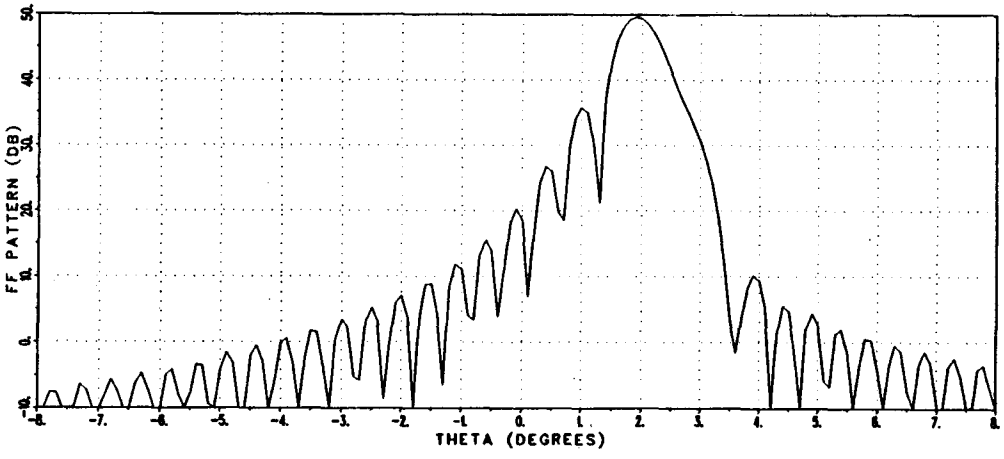

Figure 15: The radiation pattern (cut along the GSO) for a 30 ft. parabolic reflector antenna without aperture blockage with a feed displaced -2λ from the focus.

sidelobe level for the focus-fed 30 ft diameter parabolic reflector antenna. Since the minimum satellite separation is 2.0°, the main feed of the 30 ft diameter parabolic reflector will in essence receive only a desired satellite signal and no other interfering satellite signals.[1] To establish a desired signal-to-interference ratio (SIR) in the main channel, controlled sidelobes are added to the main beam to create deliberate interference in the main channel. To do this two more feeds are included with the five feed adaptive array. These two feeds are designated as

[1]Commonly a 3 meter diameter parabolic antenna is used commercially to receive GSO television receive only signals. In comparison to a 30 ft parabolic reflector a 3-m parabolic reflector antenna will have a much broader main beam with a BWFN of $\approx 3.63°$ at 4 GHz assuming a 50% aperture efficiency. Thus, a 3-m reflector antenna will receive an interfering signal in its main beam if the angular separation between the desired source and the interfering source is less than 1.81°. Furthermore, a 3-m diameter parabolic reflector antenna, in contrast to the 30 ft parabolic reflector antenna will have a reduction in gain and a corresponding increase in sidelobe level. Thus, a 3 meter antenna can also receive significant amounts of interference from widely spaced satellites.

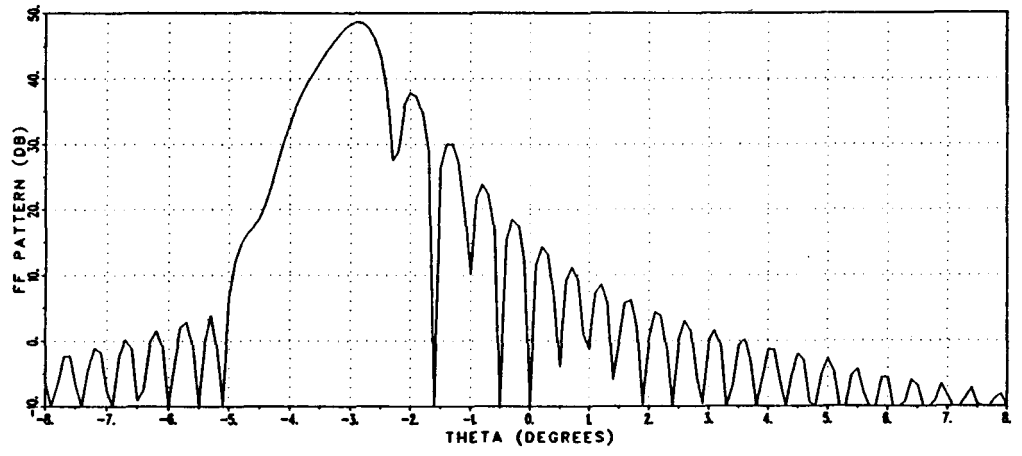

Figure 16: The radiation pattern (cut along the GSO) for a 30 ft. parabolic reflector antenna without aperture blockage with a feed displaced 3λ from the focus.

'Offset Feed #1' and 'Offset Feed #2'. Both, Offset Feed #1 and Offset Feed #2, are positioned in the focal plane of the parabolic reflector such that their associated main beams are pointed in the general direction of an interfering signal. Thus, the main channel output for the array processor is the sum of the signals received by the Offset Feed #1, the prime focus feed, and the Offset Feed #2. The next section details the layout of these seven feeds of the parabolic reflector antenna.

3.4 The Feed Distribution used for the Parabolic Reflector Antenna

The signal scenario and feed distribution is shown in Figure 17. Note that there are a total of seven feeds with two clusters of three feeds each. In this figure, D represents the desired signal and I_1 and I_2 represent two interfering signals. Because of the narrow beamwidths, each of the feeds shown effectively receives

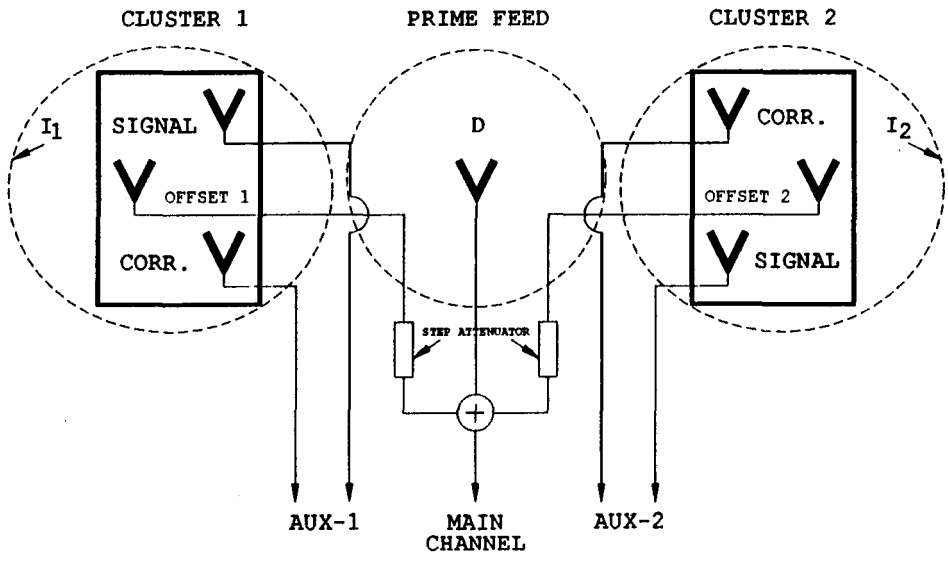

Figure 17: The signal and feed distribution.

only one signal.[2] For example, the three feeds in cluster 1 receive only I_1 and noise. The desired signal is received by the prime feed which is at the focal point of the parabolic reflector. Since this feed is not defocused, its associated antenna pattern will be the most directive and thus have the largest gain. The two feed clusters will each receive an interfering signal. Thus Signal 1 and Correlator 1 of Auxiliary channel 1 and the Offset Feed #1 receive interference from interfering source I_1 while Signal 2 and Correlator 2 of Auxiliary channel 2 and the Offset Feed #2 receive interference from interfering source I_2. Each of the feed clusters can be moved independently in relation to the angle of arrival of each interfering

[2]It should be noted that in practice each feed will also receive signals from other sources through its sidelobes.

signal.

The Signal feed and the Correlator feed for each auxiliary channel are located symmetrically along a line perpendicular to the plane of the signal sources. This ensures that the phases of the three incident signals received by Signal 1 feed are nearly equal to the phases of the signals received at Correlator 1 feed. Because of the separation between Signal 1 feed and Correlator 1 feed, the external noise received at Signal 1 feed is only partially correlated with the antenna noise received at Correlator 1 feed. Thus, Signal 1 and Correlator 1 feeds form appropriate inputs to a modified feedback loop and comprise one auxiliary element of the sidelobe canceler. Similarly, Signal 2 and Correlator 2 feeds form the inputs to the other modified feedback loop of the adaptive array. Since the feeds on the feed cluster are defocused their associated antenna patterns have less directivity relative to the associated prime feed antenna pattern.

The signals received by Offset Feed #1 and Offset Feed #2 are combined using a summer with the signal received by the prime feed. Figure 17 shows explicitly the summer which combines the received signals from the desired signal source as well as the two interfering signal sources. Step attenuators are used in each Offset Feed branch to allow the user to control the amount of each interference in the main channel. This gives the user freedom to change the signal interference scenario within the dynamic range of the system. Moreover, since the level of the original sidelobes are so low, the induced sidelobes establish the apparent sidelobe level of the parabolic reflector antenna.

In the experimental adaptive array the seven feeds of the parabolic reflector antenna are distributed on a feed platform. The actual physical design and dimensions of the feed platform are described next.

3.5 The Feed Platform

The design of the feed platform was implemented using computer aided design (CAD). Using CAD, any potential collision of the movable platforms with any other mechanical item was investigated. The layout of the feed platform produced by CAD is shown in Figure 18. A top view and two side views are shown. The physical distribution of the feeds on the feed platform is the same as in Figure 17. Throughout the platform design readily available mechanical components were incorporated.

A commercial television antenna rotator is used to move the feed clusters. Each feed cluster is installed on a 3/16 inch aluminium plate. Each plate slides on two 5/8 inch diameter stainless steel rods by employing four pillow blocks. The pillow blocks provide a low friction interface between the flat metal plate and the polished rods. Normally, pillow blocks are used for circular instead of linear motion. However, since the feed clusters move infrequently and at a slow speed in practice, the pillow blocks are adequate. A set of pulleys and wheels transform the circular motion of the rotator to the linear motion of the feed cluster. During an adaptive array experiment, the position of the feed cluster is adjusted from inside the building using the control boxes of the television antenna rotators.

Presently, the satellites in the Western Hemisphere are spaced 2.0° to 4.5° from each other. The Canadian satellites are spaced most widely at 4.5°. The feed platform was designed in such a way as to achieve the required linear displacement of the feed clusters in order to fulfill the above angle separation. The relationship between the squint angle (θ) for a parabolic reflector and the distance a feed is displaced from the focal point (X) is given by

$$\theta = \tan^{-1}(X/F) \tag{3.1}$$

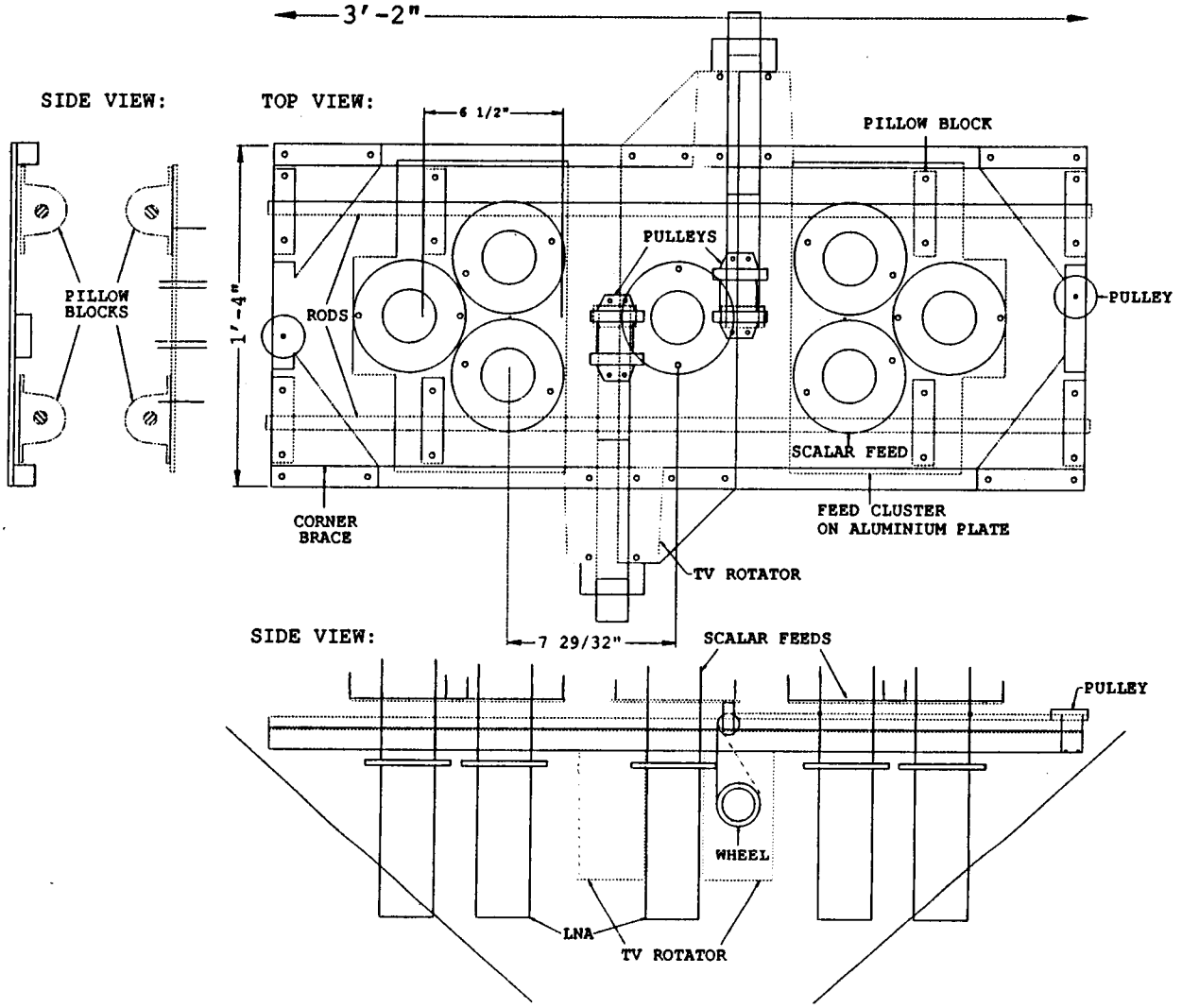

Figure 18: The feed platform layout.

where F is the focal distance. From the preceding equation the desired total length of the feed platform can be calculated. If the feed platform is made too long it would have less structurally integrity, be very heavy, and cause unnecessary aperture blockage. For this reason, the length of the feed platform was set at 3 feet 2 inches. This corresponds to a maximum skew angle of 3.8° for each feed cluster. Because there is a feed at the focal point of the parabolic reflector, the minimum skew angle for a feed cluster is 2.2°. Thus, by moving the feed clusters one can move the beam between 2.2° and 3.8°.

The offset antenna beam squint angle resolution of the rotator/feed cluster system can now be calculated as

$$\frac{3.8° - 2.0°}{360°} \times 5° = 0.025°. \tag{3.2}$$

As can be noted in Equation (3.2), the squint angle resolution, as a function of the 5° resolution of the television antenna rotators and the 2.0° to 3.8° squint angle range, is 0.025°. Nylon rope was used to pull the feed cluster platforms. Because of slack in the rope, there is a small degree of uncertainty in the actual position of the feed cluster. However, the exact position of a feed cluster is not critical when performing experiments since it is the specific power levels of an interference scenario which are of prime importance.

The feed platform structure is constructed of aluminium. Aluminum is used because it is light in weight and does not rust. Additionally, stainless steel hardware is incorporated throughout. Braces are installed at the feed platform corners. These structural braces provide integrity so that the feed platform does not twist in its long dimension. Further integrity is provided by balancing all mechanical objects. During the design process, all heavy items were positioned symmetrically near the center of the platform. For example, the rotators are installed the

same distance away from the center but on diagonally opposite sides of the feed platform. Moreover the rotators, which are the heaviest of the items on the feed platform, are positioned close to the feed platform center. The feeds used in the experimental system are discussed next.

3.6 The Parabolic Reflector Feeds

The feeds used in the experimental system are circular waveguides with a flange and chokes, and are commonly known as scalar feeds. These feeds are similar to a corrugated horn with a 90° flare angle. The actual dimensions of a feed are shown in Figure 19. These particular scalar feeds were purchased from Chaparral Communications, which is located in the San Jose, California area. The center, circular waveguide which projects out of the flange structure is commonly called the throat. As can be noted on the diagram, the corrugations, or rings, are about a quarter wavelength deep. These rings act like RF chokes, thus preventing the electric field from diffracting over the edges of the scalar feed; hence, there is a reduction in the level of the sidelobes. The rings also reduce the surface currents around the edges of the scalar feed. Thus the feed has a broad 10 dB beamwidth with a steep pattern rolloff. As a consequence, the scalar feed has a very good front-to-back ratio which further results in a high aperture efficiency. The dimensions of the rings in the scalar feed are adjusted so that the E and H plane patterns are similar in the main beam region. Within the scalar feed there is a transformation from a circular throat waveguide to a rectangular WR-229 waveguide. Thus the scalar feed is linearly polarized. The scalar feed has a low specified VSWR (1.25:1) from 3.7-4.2 GHz [14-17]. Before installing the feeds on the feed platform of the parabolic reflector two modifications to the scalar feeds were performed. These are described below.

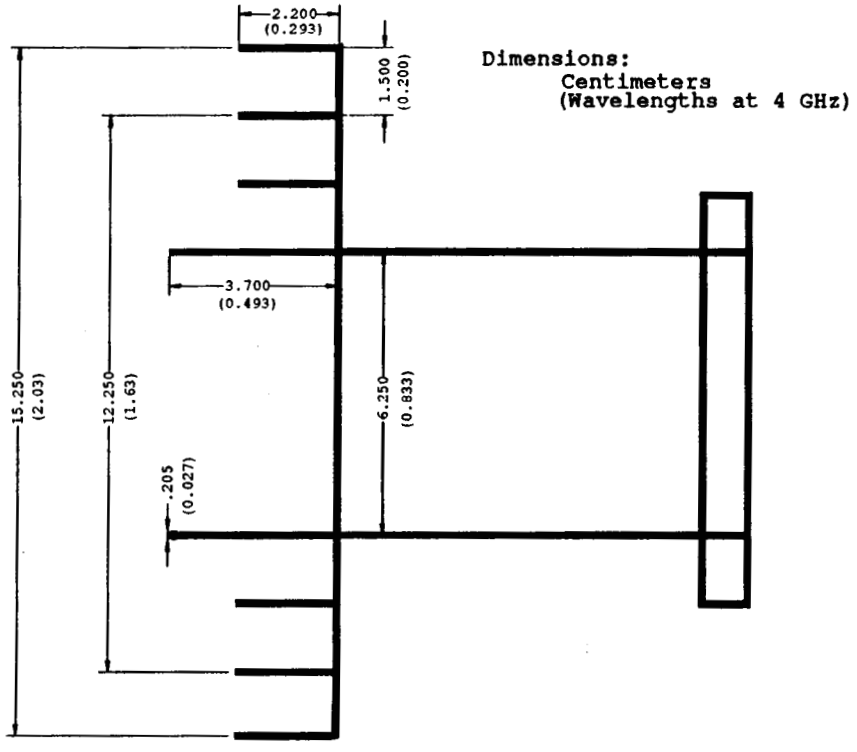

Figure 19: The dimensions of the scalar feed manufactured by Chaparral Communications.

3.7 Scalar Feed Modifications

In the experimental sidelobe canceler, the antenna beams associated with the two auxiliary branch feeds of an auxiliary channel and one of the main channel feeds (an Offset Feed) are required to be pointed in the general direction of an interfering satellite. For this to be the case, all three scalar feeds must be clustered together. The two feeds that comprise the auxiliary channel should be located such that both receive the interfering signal while the noise received by them is relatively uncorrelated. Since the feeds cannot physically overlap, the three feeds should be displaced away from the position of maximum received signal. A one inch linear displacement away from the parabolic reflector focal point corresponds

approximately to a 0.30° change in the antenna beam direction. Since each scalar feed has a radius of 3.00 inches, the minimum distance between the centers of two scalar feeds will be twice this quantity, or 6.00 inches and each feed will be 3.46 inches away from the position of the maximum received signal. Thus, each antenna beam is approximately 1.04° away from the maximum received signal. This results in a 15.0 dB loss in signal strength. In order to maintain a respectable signal strength in the auxiliaries it is desirable to decrease this antenna beam squint angle. This in turn requires that the radius of the scalar feed be physically reduced.

One can reduce the physical dimensions of the feed by removing the outer ring. By cutting off the outer ring, the radius of the feed will be reduced to 2.41 inches. However, the removal of the outer ring could affect the feed pattern. To obtain some insight in the degradation in the feed pattern, the feed pattern of the scalar feed was computed using a body of revolution code [12] developed at the Ohio State ElectroScience Laboratory. This computation was done at 4.0 GHz. The E and H-plane feed patterns are shown in Figures 20 and 21, respectively. Note that the removal of the outer ring does not change the feed characteristics significantly. In the region which illuminates the 30 ft parabolic reflector, there is an insignificant difference between the two ring and the three ring scalar feeds. The back lobes of the two ring scalar feed are approximately 1.0 dB higher than that of the three ring scalar feed. However, since the backlobes are low and do not illuminate the parabolic reflector, their effect is not important. With the outer ring cut off, the centers of the scalar feeds of an auxiliary channel are separated by 1.63 wavelengths at 4.0 GHz, thus providing significant external noise decorrelation. However, there is still a reduction of 9.6 dB in signal strength because the auxiliary channel feeds are defocused perpendicular to the plane of the GSO.

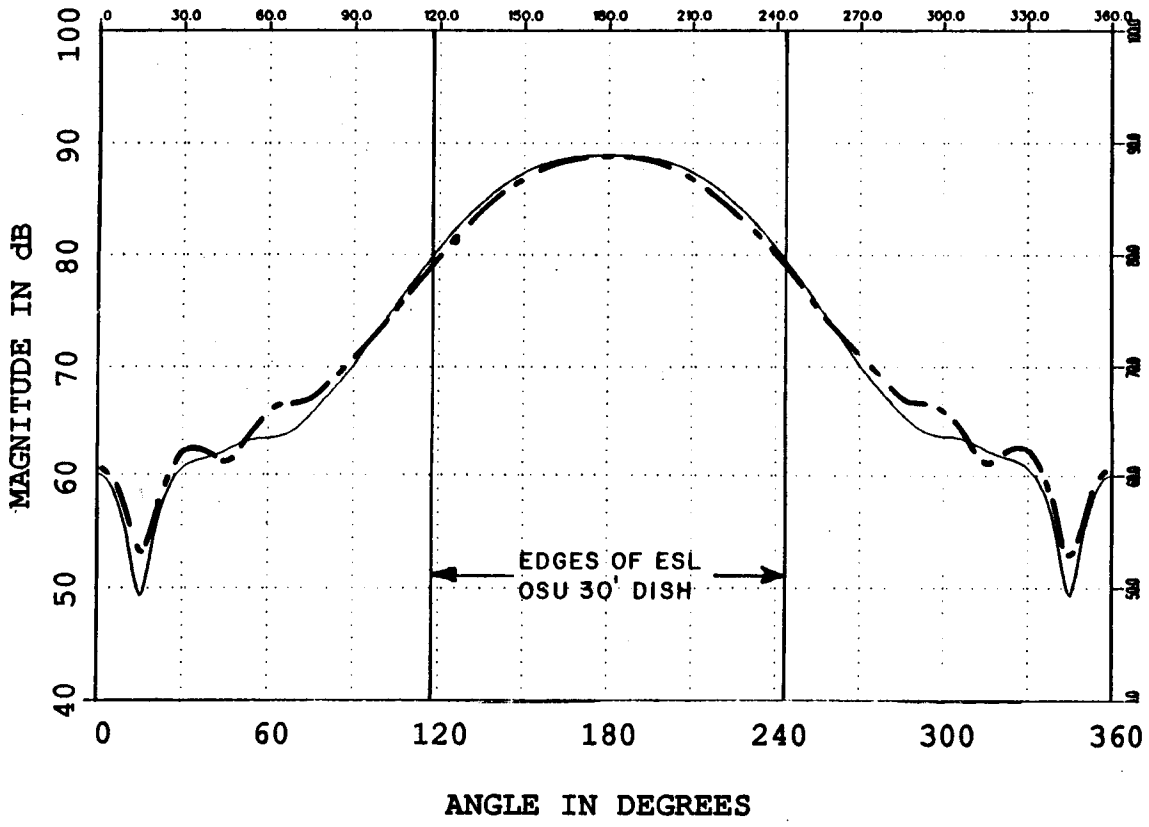

Figure 20: The E-plane pattern for a scalar feed with two (dashed curve) and three rings (solid curve).

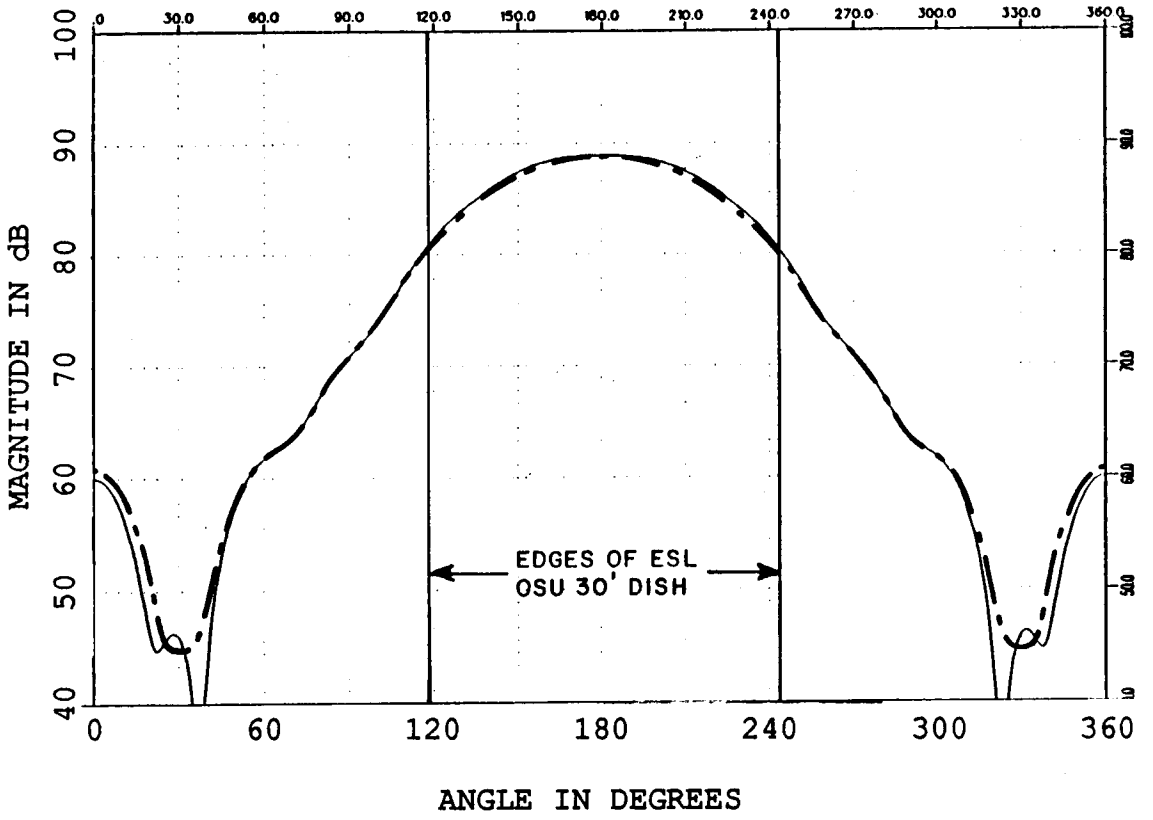

Figure 21: The H-plane pattern for a scalar feed with two (dashed curve) and three rings (solid curve).

The second modification was made to obtain the desired aperture illumination for the 30 ft parabolic reflector. The aperture illumination of a reflector is dictated by the desired signal-to-noise ratio to be obtained from the reflector antenna. A major contributor to the antenna noise is the surface of the Earth (at a temperature of approximately 290 K) 'illuminated' by the scalar feed. Increasing the feed taper reduces the feed pattern spillover, which consequently reduces the overall antenna noise temperature. However, an increase in the feed taper reduces the aperture efficiency and thus reduces the gain of the parabolic reflector. To obtain an optimal signal-to-noise ratio, the rule of thumb is to design the illuminating power pattern of the feed to be 10 dB down at the reflector edges with respect to its center. The height of a scalar feed throat varies the beamwidth, and thus varies its power pattern taper. The height of the scalar feed throat was adjusted to achieve the desired taper.

The scalar feeds purchased were designed for center fed parabolic reflectors with an F/D ratio of 0.36. However the parabolic reflector used in the adaptive array has an F/D ratio of 0.42, a more shallow parabolic reflector. Using a device called a Polar Axis/Scalar Gauge,^{TM} manufactured by Chaparral Communications, the correct throat height for a scalar feed can be determined for a given F/D ratio. For an F/D ratio of 0.42 the height of the throat should be the same height as the other rings of the scalar feed.

Figures 22 and 23 show the effect of shortening the throat height versus the original throat height. Figure 22 shows the E-plane pattern and Figure 23 shows the H-plane pattern. These patterns were also obtained using the body of revolution code. From these figures it can be seen that after modifying the throat, the desired 10 dB taper is obtained for a 30 ft center fed parabolic reflector. Specifically, the power pattern is down 12 dB at the parabolic reflector edges.

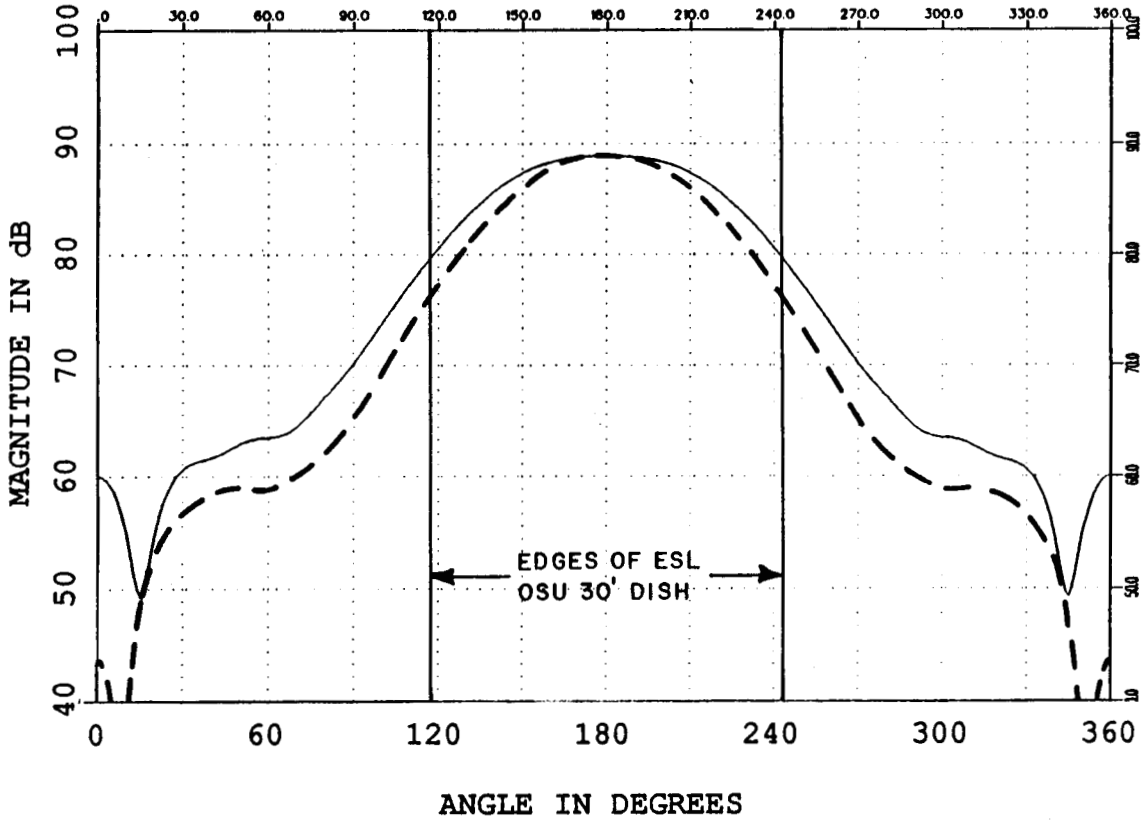

Figure 22: The E-plane pattern for a scalar feed when the throat is shortened (dashed curve) (height=2.2 cm) and its original height (solid curve) (height=3.7 cm).

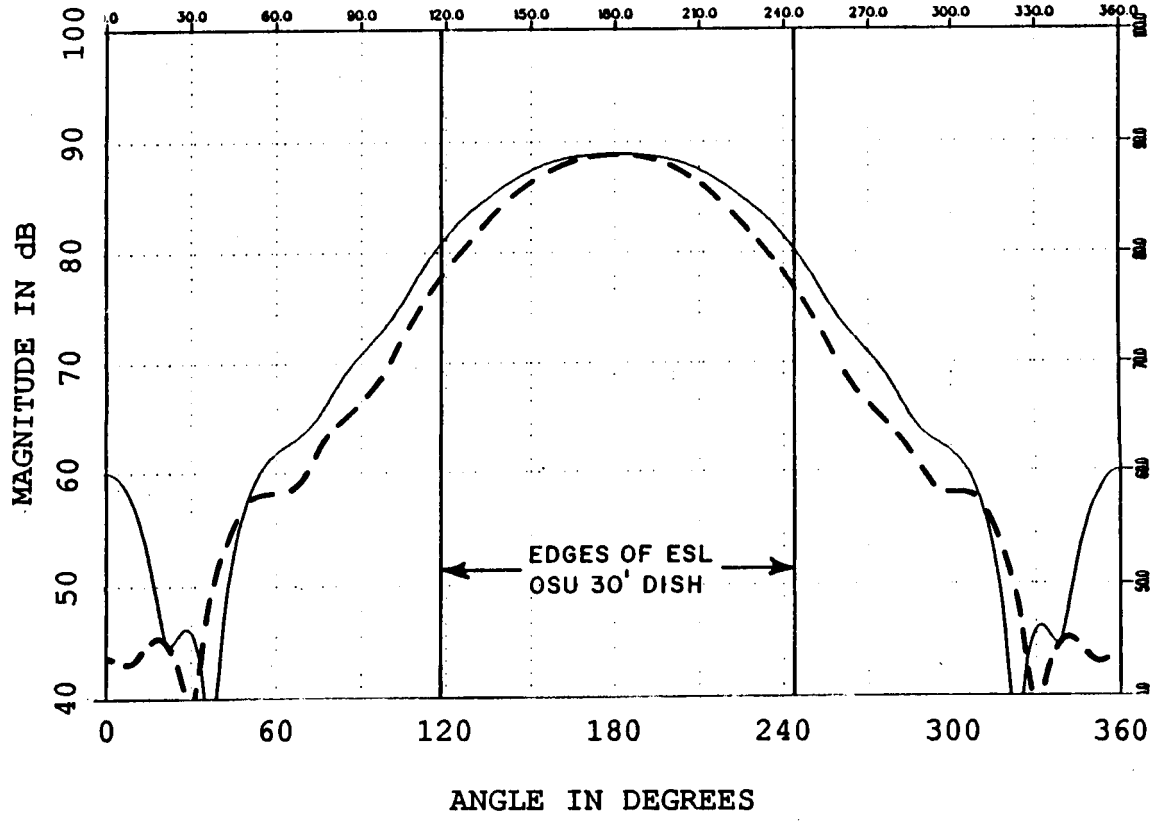

Figure 23: The H-plane pattern for a scalar feed when the throat is shortened (dashed curve) (height=2.2 cm) and its original height (solid curve) (height=3.7 cm).

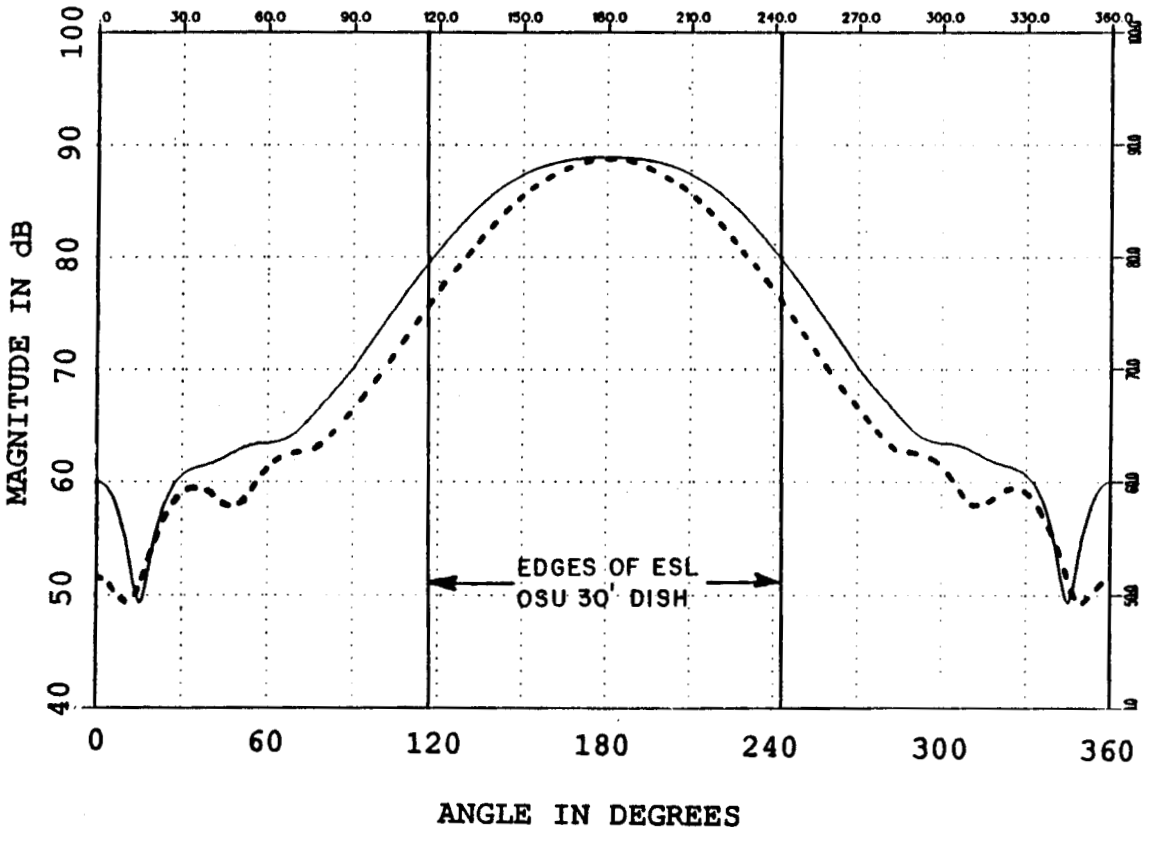

Figure 24: The E-plane pattern for a scalar feed for the unmodified feed (solid curve) and the same feed after the outside ring is cut off and the throat is shortened (height=2.2 cm) (dotted curve).

Figures 24 and 25, compare respectively the E and H-plane patterns between the original feeds and the feeds whose one ring is cut off and the throat shortened. From these figure it can be seen that the two modifications obtain the desired 10 dB taper for a 30 ft parabolic reflector without significantly degrading the feed performance. In order to ensure that the calculated performance of the feeds is accurate, the radiation patterns of the feed were also measured after the above mentioned modification. The procedure used to measure the radiation patterns and the measured patterns are described next.

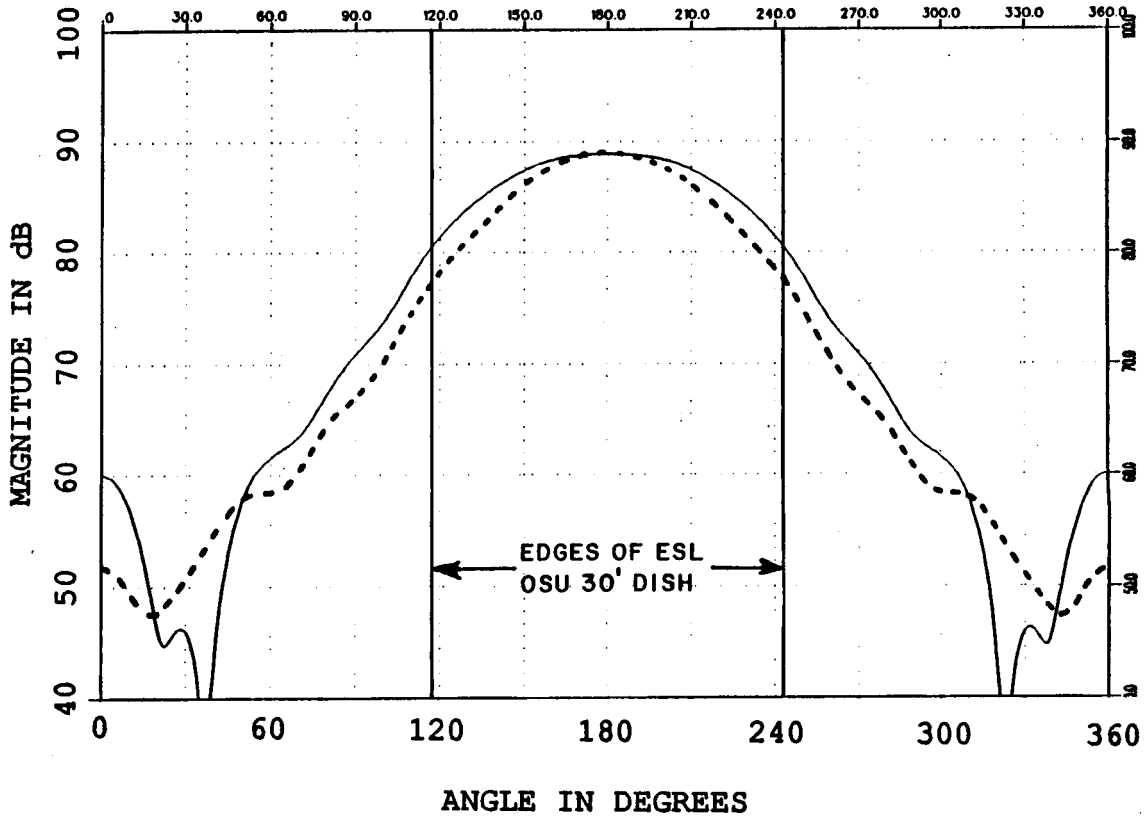

Figure 25: The H-plane pattern for a scalar feed for the unmodified feed (solid curve) and the same feed after the outside ring is cut off and the throat is shortened (height=2.2 cm) (dotted curve).

3.7.1 Measured Patterns of the Modified Feeds

The radiation patterns of the modified feeds were measured in the Ohio State University ElectroScience Laboratory compact range [21]. The compact range is a room lined with microwave absorbing material. In this room, at a region in front of a specially designed reflector there is a uniform plane wave (a synthesized far-field condition). The scalar feed being tested was installed on a pedestal in this region. The pedestal rotates the feed a full three hundred and sixty degrees in 1° increments, and the far-field pattern of the scalar feed is measured. The compact range was used to measure antenna patterns in both the E and H planes. The scalar feed was connected to its standard LNA for these experiments. Attenuators were installed in both the receiving and transmitting lines of the compact range system to avoid saturation of the measurement system. Since the compact range has a very sensitive receiver, a high amount of attenuation (50 dB) was required. These patterns were taken at 3.977 GHz.

Figures 26 and 27 show the E and H-plane patterns respectively for the modified scalar feed. In the experiments, the isolation between orthogonal linear polarizations was found to be at least 25 dB. These plots correspond well with those obtained in the theoretical study. In both cases the feed patterns are not absolute but relative measurements. Two differences can be noted between the theoretical and experimental tests. First, since the scalar feed was not perfectly lined up in reference to the 180° position of the compact range, the resulting plots are not exactly symmetric about the phase center. Second, the curve for the theoretical case is more smooth than the one for the experimental case. This could be due to noise or clutter in the compact range system. Again note that the modified feeds have the desired characteristics.

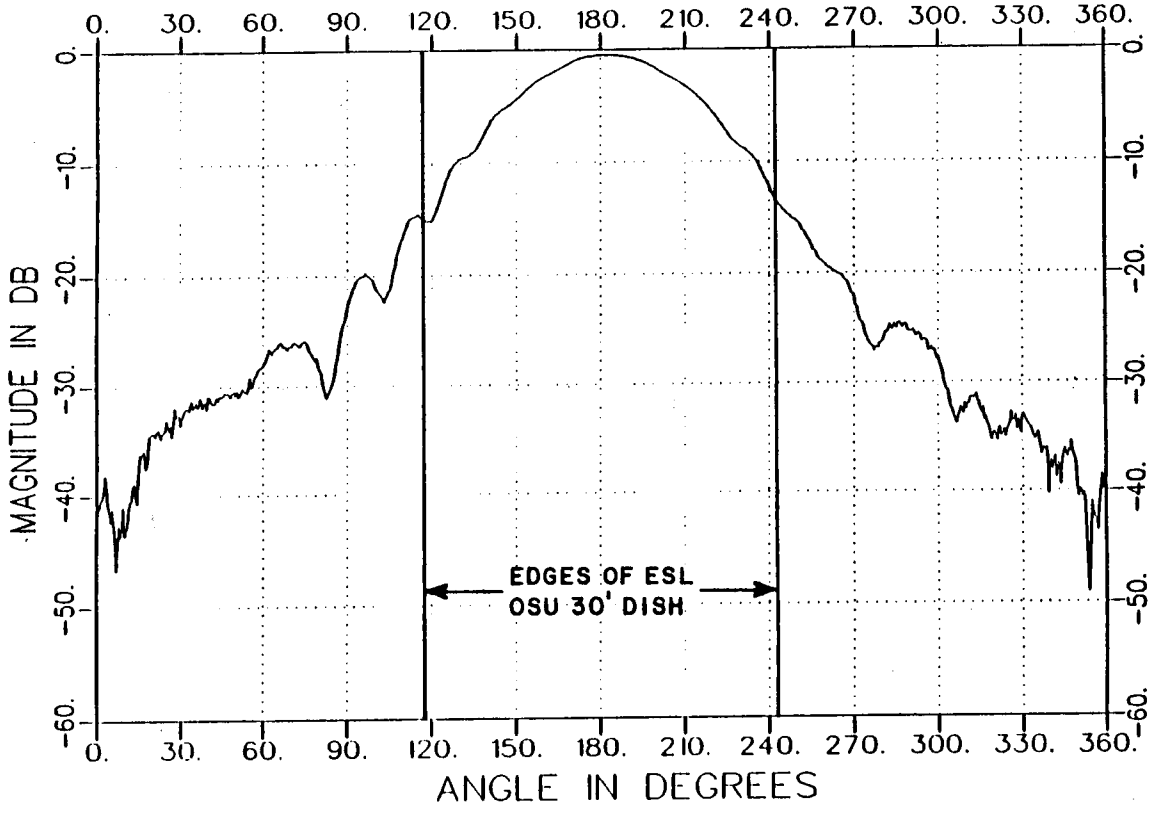

Figure 26: The E-plane pattern for a scalar feed as measured in the ESL/OSU compact range after the outside ring is cut off and the throat was shortened (height=2.2 cm).

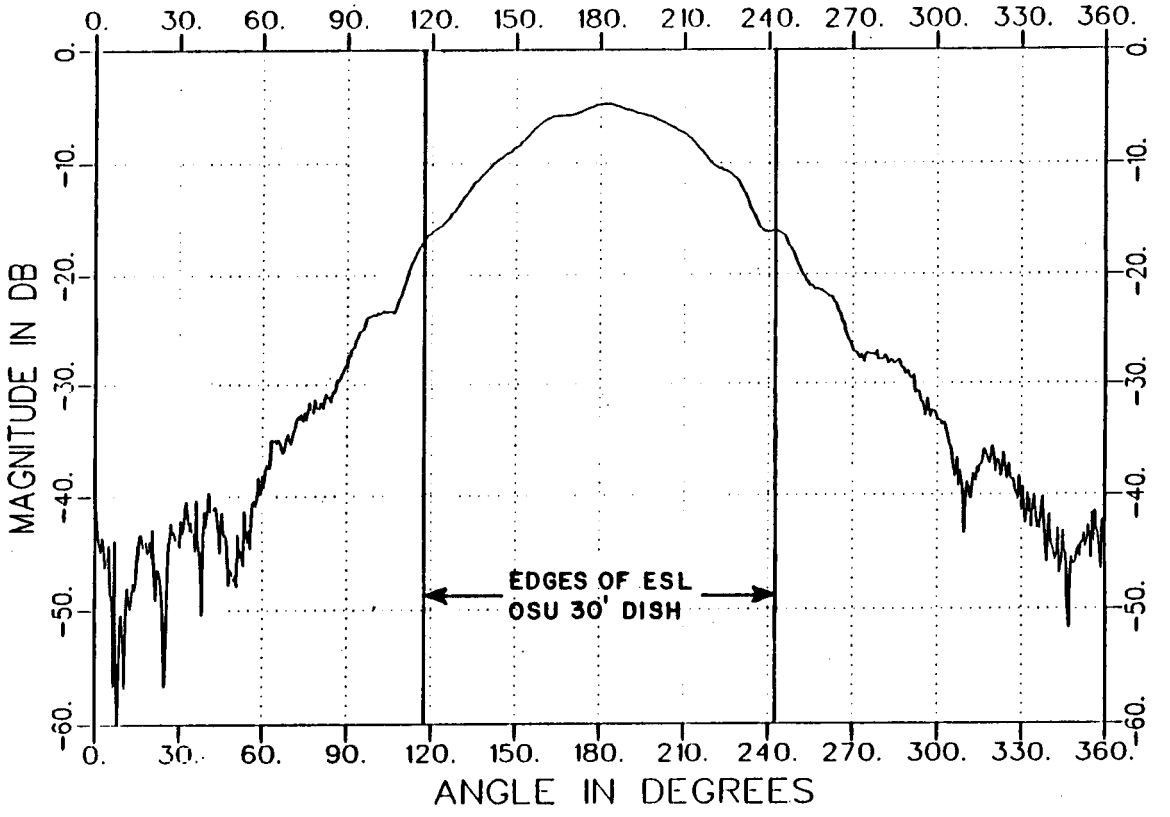

Figure 27: The H-plane pattern for a scalar feed as measured in the ESL/OSU compact range after the outside ring is cut off and the throat was shortened (height=2.2 cm).

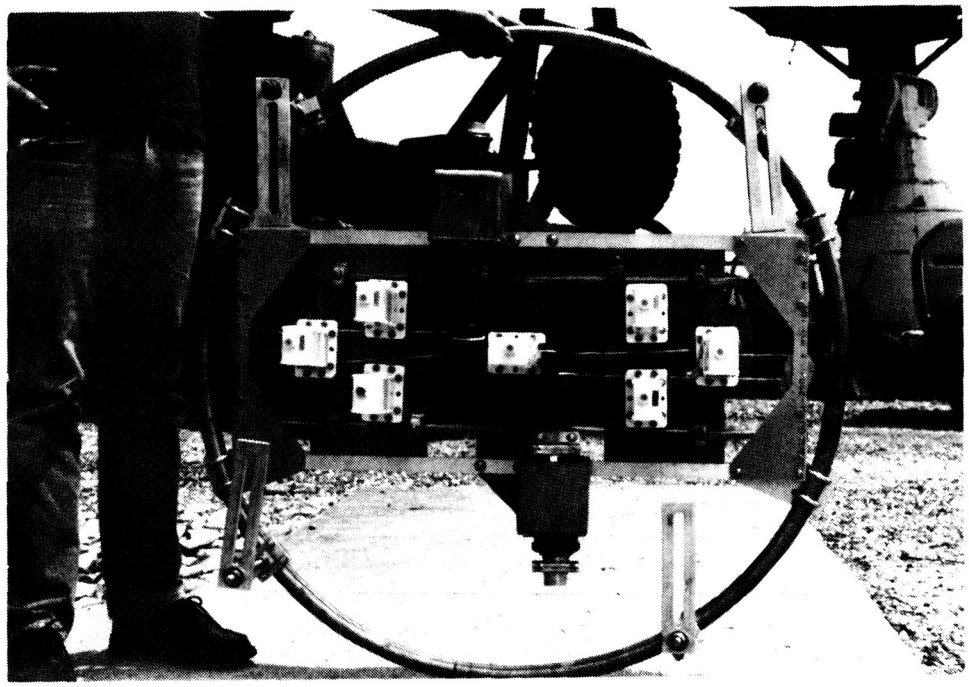

Figure 28: A picture of the feed platform and the ring, a bottom view.

3.8 Orientation of the Feed Platform to Match the Polarizations of each Feed with a Satellite

Each scalar feed can be installed in either the vertical or horizontal polarization configuration. Two adjacent satellites normally transmit a given channel at opposite senses of polarity. In an adaptive array experiment all of the scalar feeds are installed so that their polarizations match those of the geostationary satellites to be used. Further, the entire feed platform can rotate. This adjustment is necessary so that the polarizations of the scalar feeds coincide with the geostationary arc. The feed platform is positioned within a stainless steel pipe bent into a circle. A picture of this ring and feed platform is shown in Figure 28. Other views of the feed platform are shown in Figures 29 and 30. The feed platform is fastened to this ring with U-bolts. Loosening these U-bolts and rotating the feed platform by hand, allows the platform to be oriented for a set of one desired and two interfer-

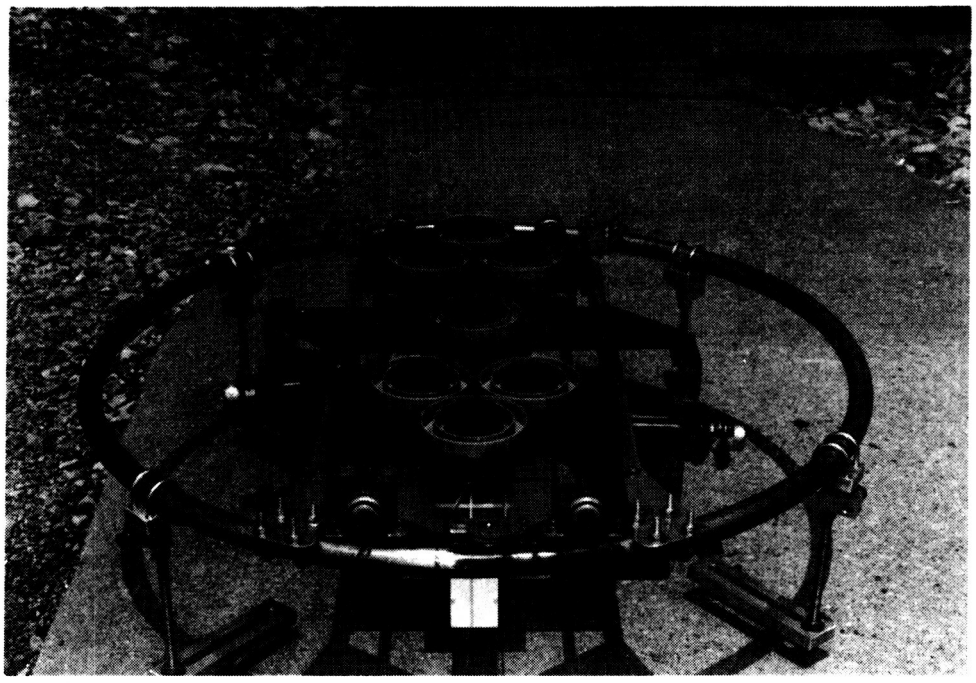

Figure 29: A picture of the feed platform and the ring, a top view.

Figure 30: A picture of the feed platform and the ring, a side view.

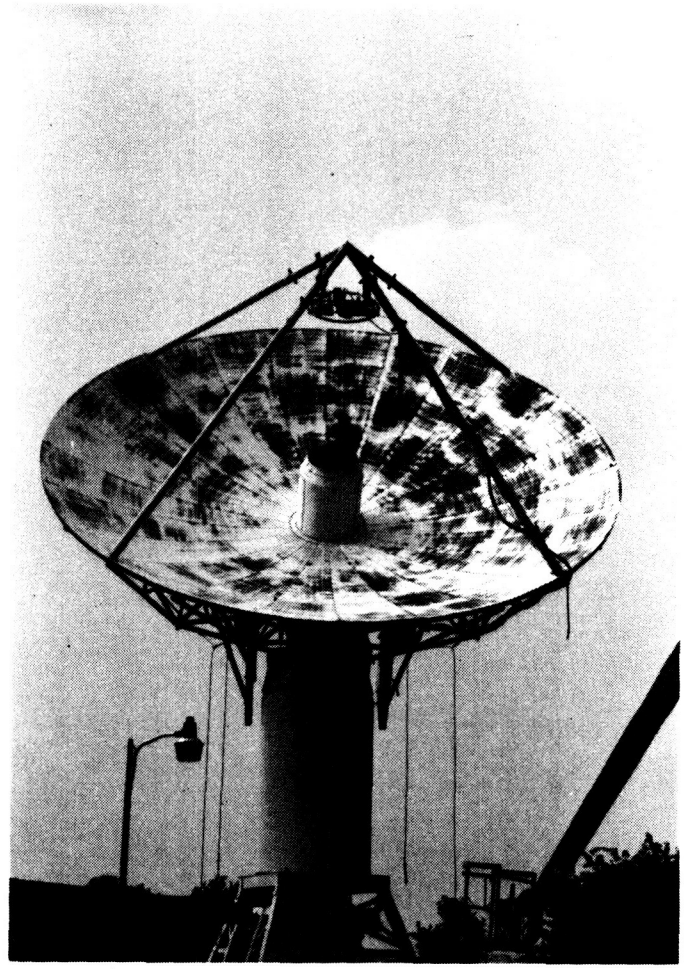

Figure 31: A picture of the parabolic reflector and the feed platform.

ing satellites. Finally, Figure 31 shows a picture of the parabolic reflector antenna with the feed platform in place.

When correctly adjusted, the feed platform is tangent to the geostationary arc. Figure 32 shows the geostationary arc as viewed from Columbus, Ohio. The axes on the figure depict the elevation angle versus the azimuth angle for a parabolic reflector antenna pointed at a geostationary satellite. Thus, the position of the parabolic reflector can be determined from a satellite's corresponding longitude. The longitudes of various geostationary satellites are readily available in the lit-

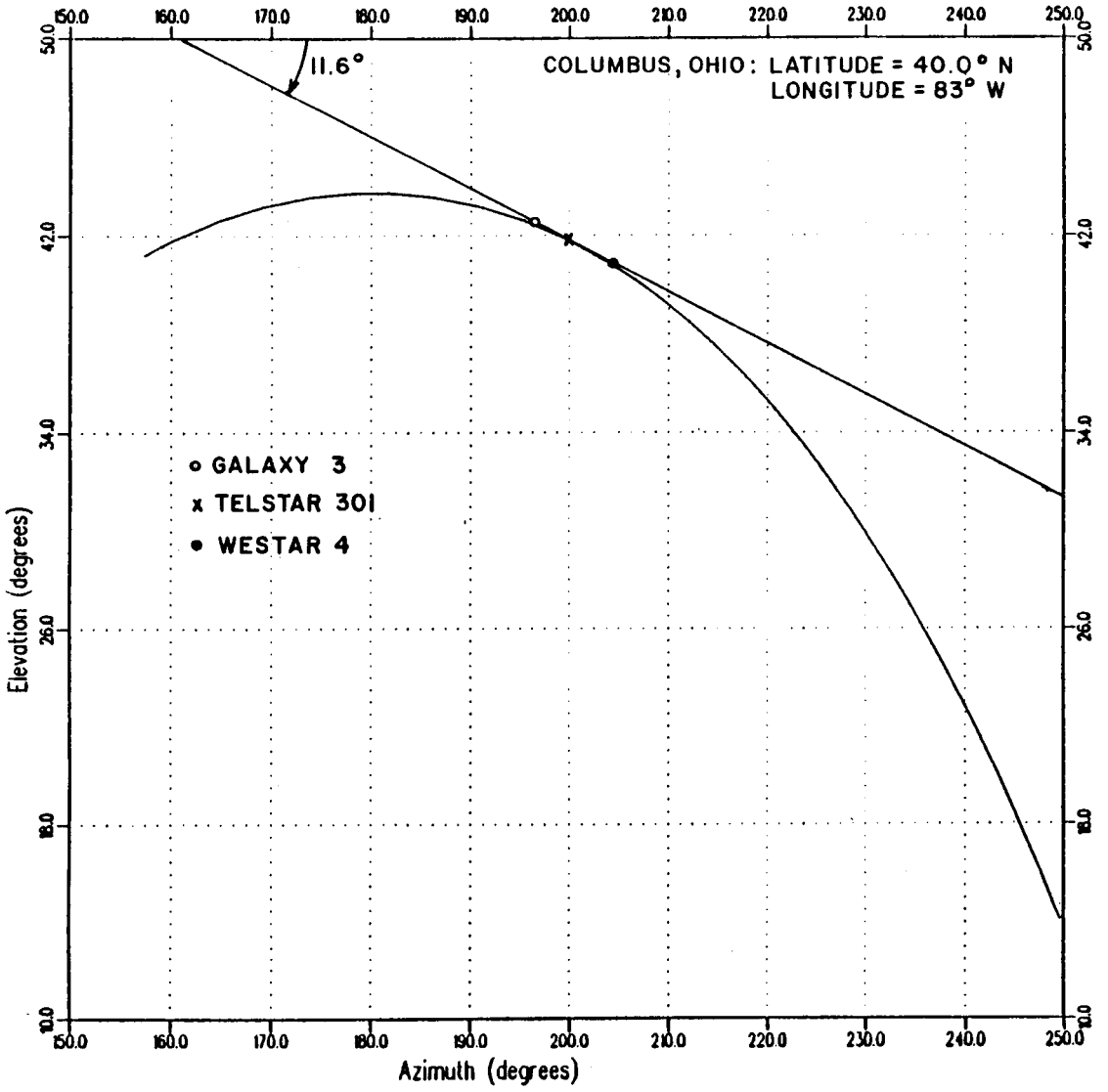

Figure 32: The geostationary arc viewed from Columbus, Ohio.

erature [13]. Figure 32 shows the azimuth and elevation for the satellites which were accessed for this adaptive array experiment. As can be noted on the figure, the correct inclination angle of the feed platform is 11.6°. This calculated value agrees, within measurement error, with the 12.0° angle which was determined experimentally. A summary of this chapter is given next.

3.9 Summary

In this chapter, the antenna system used to receive signals from various geostationary satellites was described. It is a 30 ft diameter parabolic reflector antenna with seven feeds. These feeds are mounted on a 38 inch by 16 inch platform located at the focal plane of the parabolic reflector. Two clusters of three feeds each are used to receive signals from interfering satellites while the seventh feed located at the focal point is used to receive the signal from the desired satellite. The specifications and the radiation characteristics of individual feeds were also discussed. Some modification to the orginal scalar feeds were also presented.

The signals received from the seven feeds should be processed before these signals can be used with the adaptive array processor whose intermediate frequency is 69 MHz. The front end used to process the satellite signals received by the various feeds is discussed in the next chapter.

CHAPTER IV

THE RECEIVE SYSTEM

4.1 Introduction

The seven feed parabolic reflector antenna described in the last chapter is used to receive signals from television receive only (TVRO) geostationary satellites. These signals are amplified and downconverted to a center frequency of 69 MHz by the receive system in order to be used directly with the adaptive array processor. In this way, the performance of the experimental system can be evaluated with actual satellite signals. In this chapter the electrical subsystems of the satellite experimental receive system are described. First there is a general overview of each subsystem. After this overview, each subsystem is described in detail with an emphasis on hardware implementation. The subsystems are broken into three areas: 1) the low-noise amplifier, 2) the downconverter chassis, which includes the downconverters and their related components, and 3) the subsystems in the main building, which include the array processor, the satellite TV receiver, and the test equipment. A detailed description of the various modifications made in the commercial downconverter is also given. Finally, the antenna patterns for the experimental system are investigated.

4.2 The Receive System Block Diagram

The receive system block diagram is shown in Figure 33. In the following discussion the blocks of the satellite receive system are described from right to left, as the signal travels from the system front-end to the test equipment. Note that the first stage on the diagram contains the feeds which, as described previously, convert the downlinked electromagnetic waves into electrical signals. Following each feed, the received signal is transferred directly to a low-noise amplifier (LNA). The LNA is used to preamplify the incoming signal and to establish the system signal-to-noise ratio due to its substantial gain. The amplified signal is carried by a 39 foot long RG-9/U coaxial cable to a chamber, called the tub, just below the parabolic reflector. The loss in this RG-9/U cable at 4 GHz is 7 dB. However, since the signal-to-noise ratio is determined by the LNA, the power loss of this cable does not appreciably affect the overall receive system signal-to-noise ratio.

Inside the tub is the downconverter chassis. The tub provides a barrier to harsh weather elements. Signals received by the feeds enter the tub through watertight bulkhead connectors and passed into downconverters. Note that there are five downconverters on the downconverter chassis. Each downconverter is comprised of a balanced mixer, a filter, and an amplifier. The mixer converts a signal within the 3.7-4.2 GHz band down to the 70 MHz intermediate frequency (IF). A known frequency is injected into the mixer from a local oscillator (LO). The resulting signal then passes through a bandpass filter with a center frequency of 70 MHz and a 3 dB bandwidth of 35 MHz. The signal is than amplified to counteract mixer and filter losses. The output impedance of the downconverter is 75 ohms. However, the coaxial cable which was previously available had a 50 ohm impedance. A transformer is used to match the two impedances.

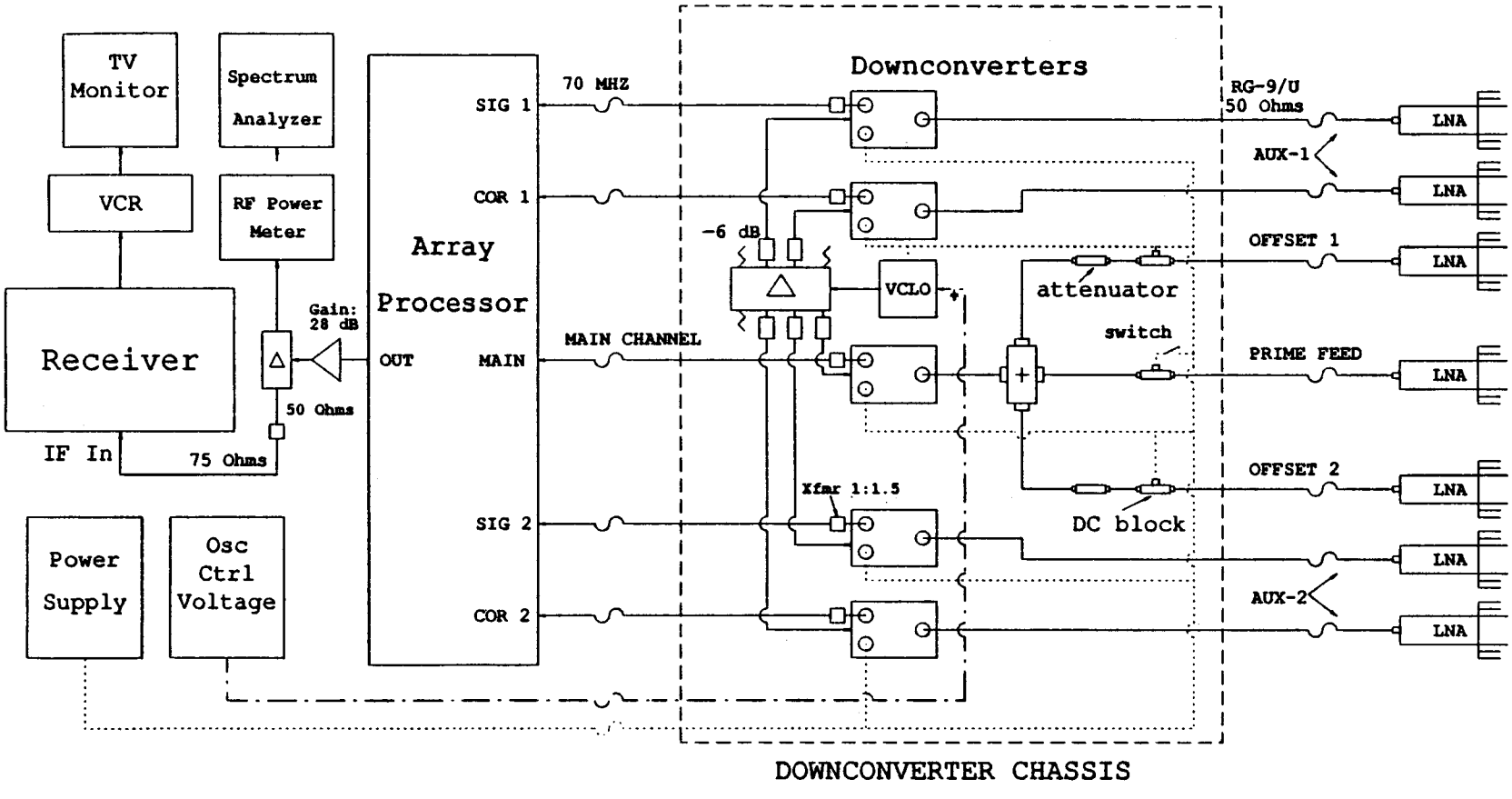

Figure 33: The receive system block diagram.

The frequency of the LO is voltage controlled (VCLO). In order for each of the downconverters to have the same phase reference, a common VCLO is used. As can be seen on the system block diagram, an eight port power divider is used in this design. All unused outputs are terminated.

From the downconverter chassis, all the received signals are carried from the tub by RG-58/U coaxial cable into the main building. The array processor is located inside this building. The satellite signals are fed into the array processor. The output of the array processor is transferred through a power divider to a commercially available satellite TV receiver. The other output of the power divider drives the RF power meter. The satellite receiver has an input impedance of 75 ohms, while the array processor has a 50 ohm impedance. Therefore, a transformer is used to match the impedance of the receiver with the impedance of the array processor. Through FM demodulation the satellite receiver produces a composite video signal. This signal can be recorded by a video cassette recorder (VCR), viewed on a television (TV) monitor, or analyzed by a spectrum analyzer.

Note that the amplified signals received by three feeds are summed to form the main channel. Attenuators in series with the Offset Feeds are used to control the amplitude of the interference in the main channel in known, fixed steps. A set of four relays, configured as shown in Figure 34, provide four combinations of attenuation. For easy adjustment of this attenuation, the relays are controlled from inside the main building.

The LNAs require DC power to operate. The DC supply voltage for these electrical components is carried along the same RG-9/U coaxial cable which was described previously to carry the received satellite signals. Since one cable carries both the radio frequency (RF) signal and the DC supply power, only one cable per LNA is required. As described previously, attenuators are included in the Offset

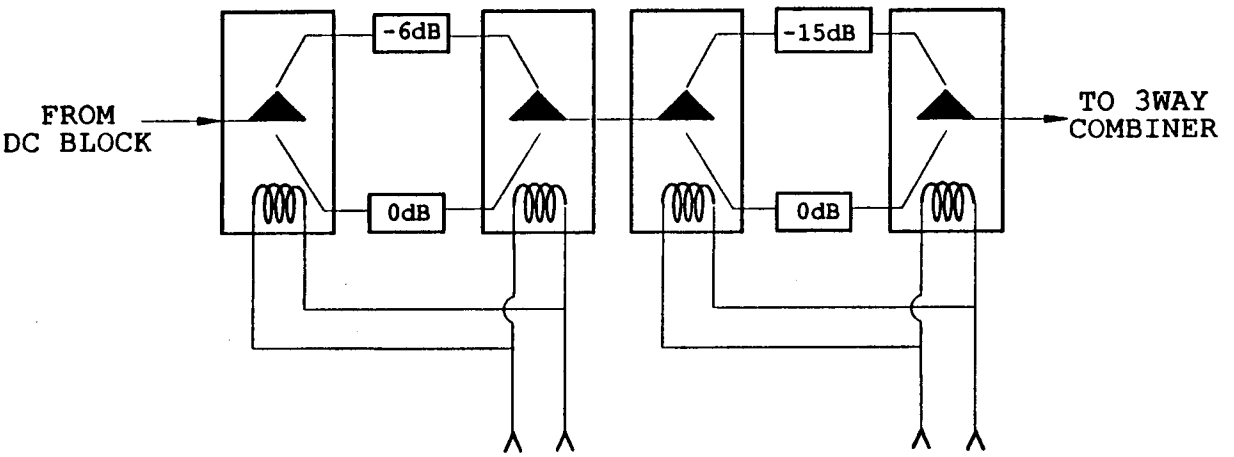

Figure 34: The configuration of the four relays.

Feeds of the main channel of the receive system. Because this attenuator attempts to attenuate both the DC power supply voltage as well as the RF signal a DC block is placed between the LNA and the attenuator. Using a DC block, the DC power supply voltage is blocked from traveling into the attenuator. For proper operation, the downconverter in the main channel was modified so that it would no longer output a DC voltage at its RF input port. A 16 volt direct current power supply provides the power for the downconverters, LNAs, and VCLO. In practice the maximum current drawn from this power supply is 1.6 amperes.

The signals in the main channel are controlled by three switches in series with the three main signal power supply branches. These switches are located inside the main building. Since a switch turns off the DC power to a LNA, it effectively removes its corresponding signal from the main channel. Through the control of three such switches, the operator can easily receive only a desired signal, only an interfering signal, both a desired and an interfering signal, or other combinations of these three signals in the main signal branch. These switches provide a quick

method of system demonstration. Interference suppression can also be determined by comparing the interference power before and after adaptation while the desired signal is turned off. In the next sections a detailed description is given of each subsystem of the receive system.

4.3 The Low-Noise Amplifier

The LNAs are 'off the shelf' consumer items. Table 2 shows the LNA manufacturer and their specifications. These specific LNAs were chosen because of quick delivery time and low price. The specifications of this LNA are representative of what can be found in broadcast satellite television receive only systems.

Table 2: The specifications of the LNA.

Manufacturer:	NORSAT International, Inc; Surrey, B.C. Canada
Gain:	49 dB at 4 GHz $\cdots$ measured
Temperature:	75 K $\cdots$ manufacturer's specification
Bandwidth:	957 MHz $\cdots$ measured

Figure 35 shows a plot of the gain of a typical LNA versus frequency. The gain was measured using an HP 8510 Network Analyzer. Note that for the frequencies of interest (3.7-4.2 GHz) the amplifier gain is approximately 49 dB. In Appendix A the system link calculations are carried out. From these calculations it can be seen that an LNA with 49 dB gain is adequate for proper operation of the system.

4.4 Downconverter Chassis

Figures 36 and 37 show the top and side views respectively of the downconverter chassis. As mentioned before, the downconverter chassis is housed in the

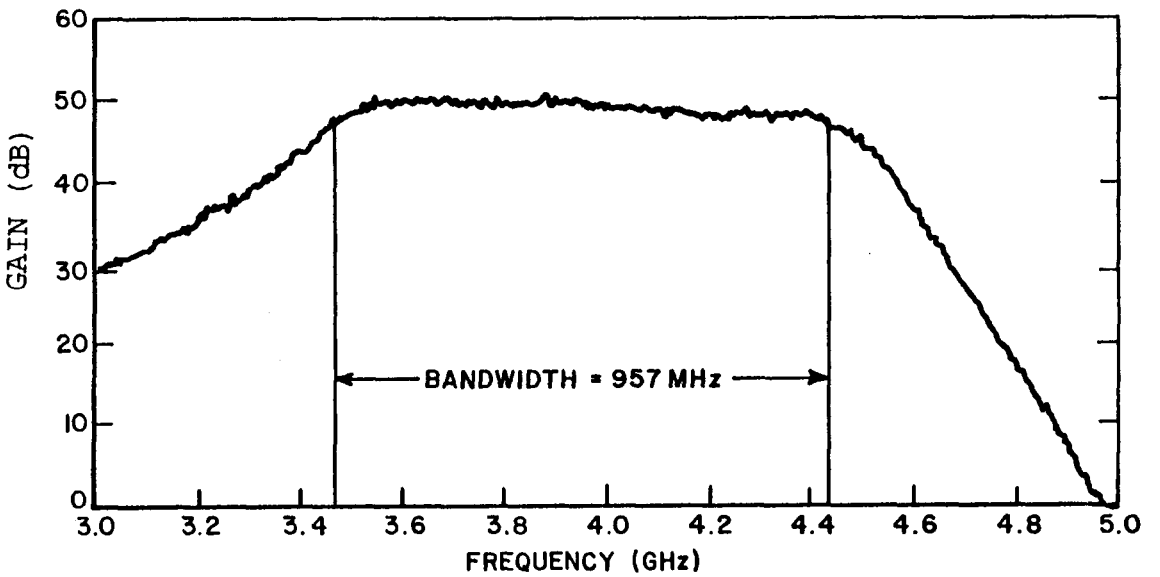

Figure 35: The gain of a typical LNA.

tub of the parabolic reflector. Note that the downconverter chassis contains five downconverters, a local oscillator, two power dividers, and five transformers. A description of these components is given below. Before installing the downconverters on the chassis, some modifications to the commercially available downconverters were made. These modifications are described in this section. Various steps taken to reduce the radio frequency interference (RFI) are also discussed.

4.4.1 The Downconverter

The five downconverters are also 'off the shelf' consumer items. Table 3 shows the specifications for the downconverters. The intermediate frequency, impedance, and output power level of the downconverter are matched with that of the satellite TV receiver developed by the same manufacturer.

An experiment was conducted to determine the gain linearity of a typical downconverter. The experimental setup is shown in Figure 38. Typically the

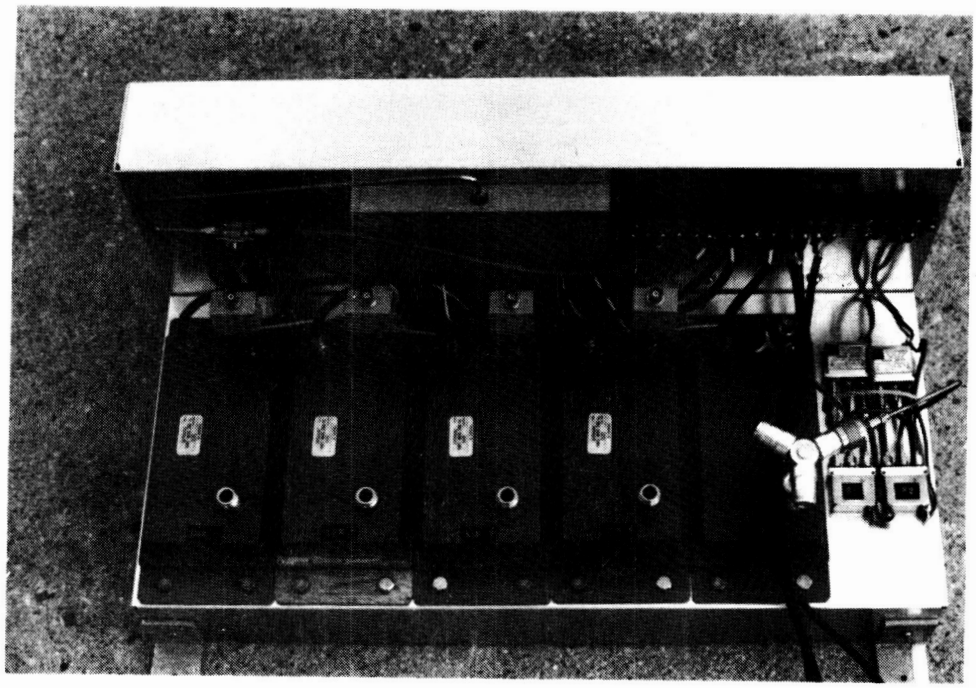

Figure 36: A picture of the downconverter chassis - a top view.

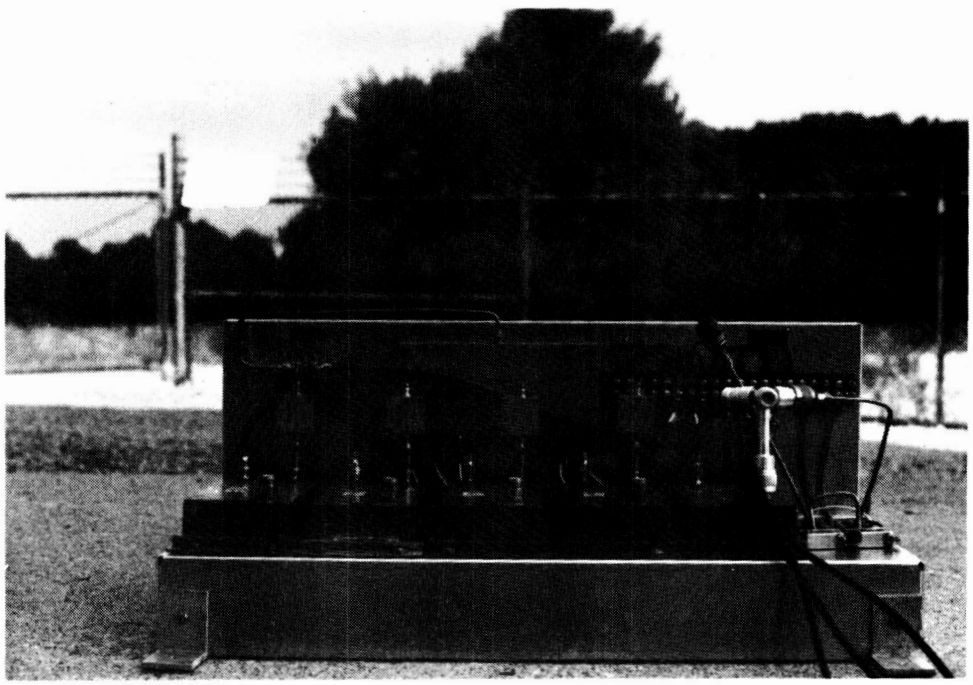

Figure 37: A picture of the downconverter chassis - a side view.

Table 3: The specifications of the downconverter.

Manufacturer:	R.L. Drake, Ohio
Input Frequency:	3.7 - 4.2 GHz
Input level:	-55 dbm to -30 dbm at 50 ohms
Noise Figure:	15 dB nominal
Image Rejection:	20 dB $\cdots$ nominal; 15 dB $\cdots$ measured
IF output Freq:	70 MHz
IF output Impedance:	75 ohms
Supply Voltage:	14.5 - 18 volts DC

upper limit of the gain linearity is specified by the 1 dB gain compression point. The 1 dB gain compression point is that point where the output power increase is 1 dB less than the increase in input power. As can be seen in Figure 39 the 1 dB gain compression point is at an input power of -20 dBm. The -20 dBm value is less restrictive than the -30 dBm value which is specified by the manufacturer. The result of this experiment shows that the downconverter can operate linearly up to an input power of -20 dBm. However in this system, -40 dBm is the strongest input power to the downconverter. Thus, the downconverter should provide the desired performance. Note that the gain of the downconverter is 20 dB; the gain of the other downconverters range from 12-20 dB.

From the previous specifications, the allowable system signal levels can be determined. For standardized comparison purposes the signal levels will be referenced to the antenna. The maximum advisable input power at the antenna is constrained by the 1 dB gain compression point of the downconverter, which is -20 dBm in this case. Between the downconverter and the antenna there is an

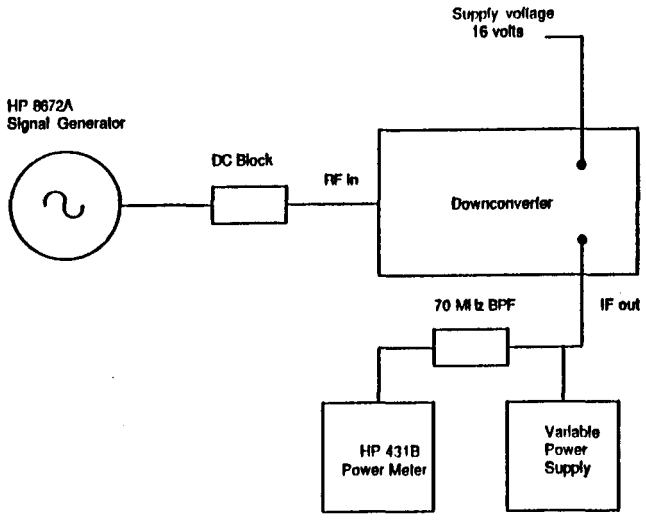

Figure 38: The experimental setup to determine the gain of a downconverter.

LNA, which has a gain of 49 dB, and a connecting cable which have a loss of 7 dB, giving a net gain of 42 dB. Thus, the maximum input power at the antenna is approximately -62 dBm. On the other hand, the minimum detectable signal level of the array processor is -60 dBm as set by its vector demodulators. Thus the system sensitivity, or minimum input power at the antenna, for the case where the downconverter has a gain of 20 dB is -122 dBm. Hence, the overall system dynamic range, referenced to the antenna, is -122 dBm to -62 dBm, excluding system noise. The system noise power when referenced to the antenna, which is calculated in Appendix A, is -103 dBm for a 32 MIlz bandwidth. Next, some modifications made to the commercially available downconverters are discussed.

4.4.2 Downconverter Modification

Initially, each downconverter had an individual internal voltage controlled local oscillator (VCLO) whose frequency was controlled by the satellite receiver. As usually is the case, the downconverter/receiver system was designed for only one

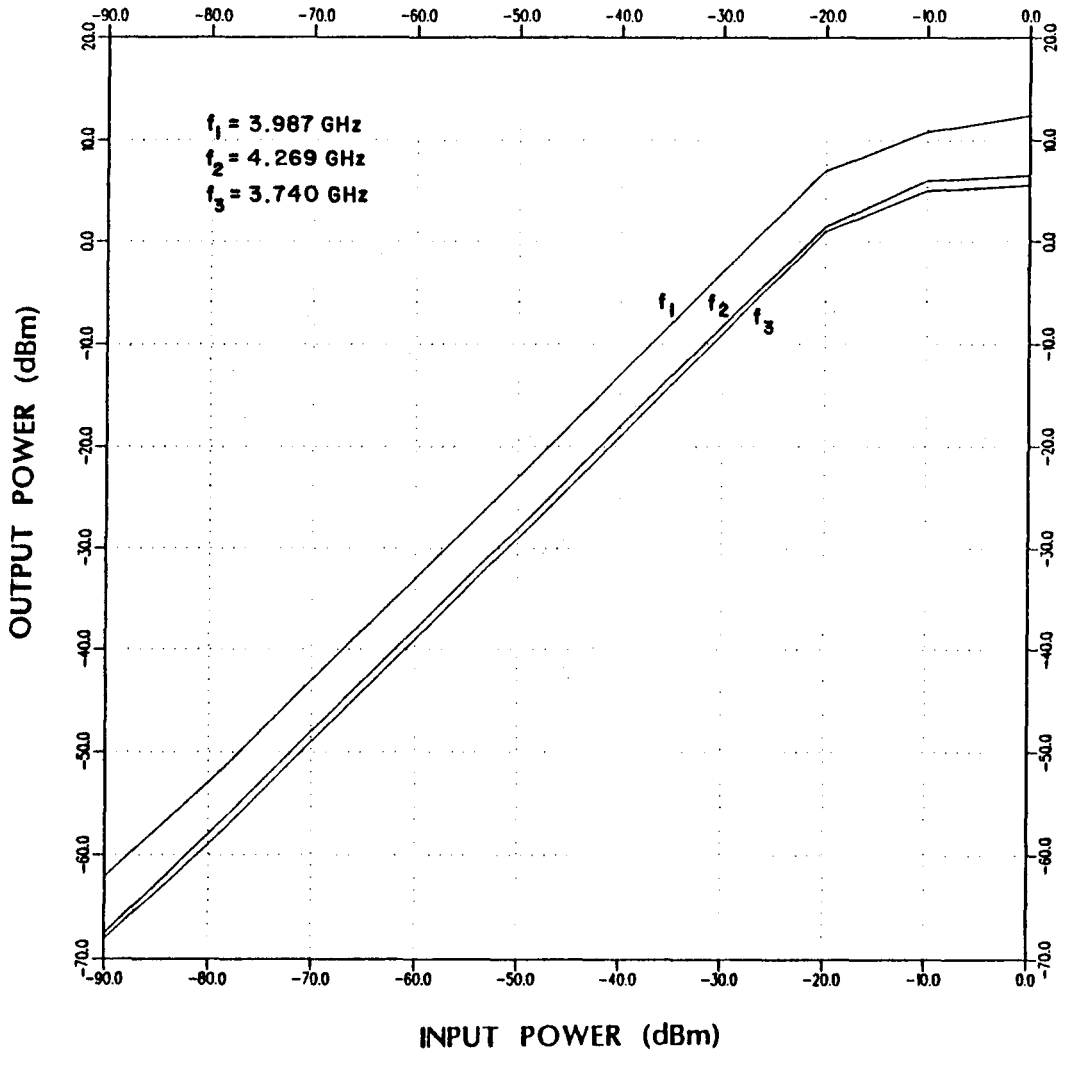

Figure 39: The output power of a downconverter for a given input power.

downconverter per receiver. However, in this experimental system with its special characteristics there are five downconverters which all must use a coherent local oscillator. Thus the downconverters had to be modified. Two possible methods of modification were investigated. One method consisted of locking together all five downconverter LOs in phase. The second method was to employ a separate VCLO for all five downconverters. Since the downconverter local oscillators are operating in the 4 GHz range, the design of the required phase lock circuitry is not trivial.

Thus, the second option of employing a separate VCLO was pursued.

In order to use an independent VCLO, the downconverters had to be modified. First, the oscillator in each downconverter was disabled. This was accomplished by unsoldering and removing all of the electrical components associated with the oscillator. Previously the signal from the oscillator was injected into the mixer through a loose coupling of two wires. The length and the separation of these wires were adjusted so as to provide a good match between the oscillator and the mixer. The externally injected LO signal uses the same injection method.

The external LO signal had to be fed into the mixer section of the downconverter. For this reason, a hole was drilled through the downconverter case and a bulkhead SMA connector was installed. Semi-rigid 0.141 inch diameter coaxial cable was used as the transmission line for the injected LO signal inside the downconverter's metal box. The placement of the bulkhead connector and the use of this coaxial cable were chosen to ensure the least effect on the balance of the mixer and other high frequency circuits. These circuits, being microstrip, would be adversely affected if a long piece of metal ran closely adjacent to them. A short section (0.5 inch) of wire was installed at the far end of this semi-rigid coaxial cable at the point of mixer injection. Using a network analyzer (HP 8510), the loop was manually adjusted until the lowest possible voltage standing wave ratio (VSWR) was recorded across the required frequency range. From this trial and error process, it was determined that a very loose coupling worked best, and that replacing the loose coupling with a small capacitor was unsatisfactory. A VSWR of 2.0:1 or less was the criterion used for a good match.

An anomaly in the operation of the downconverter was observed after the case top of the downconverter was securely fastened. After the top was installed, the VSWR at the LO port rose to a very high value within the LO passband. It

was theorized that the metal case of the downconverter, because of its size, was actually a resonant cavity. Fastening a strip of microwave absorbing material on the cover of the metal box remedied this effect. A comparison of VSWR versus frequency for one of the downconverters with and without this microwave absorber is shown in Figure 40. This graph is typical for all of the downconverters.

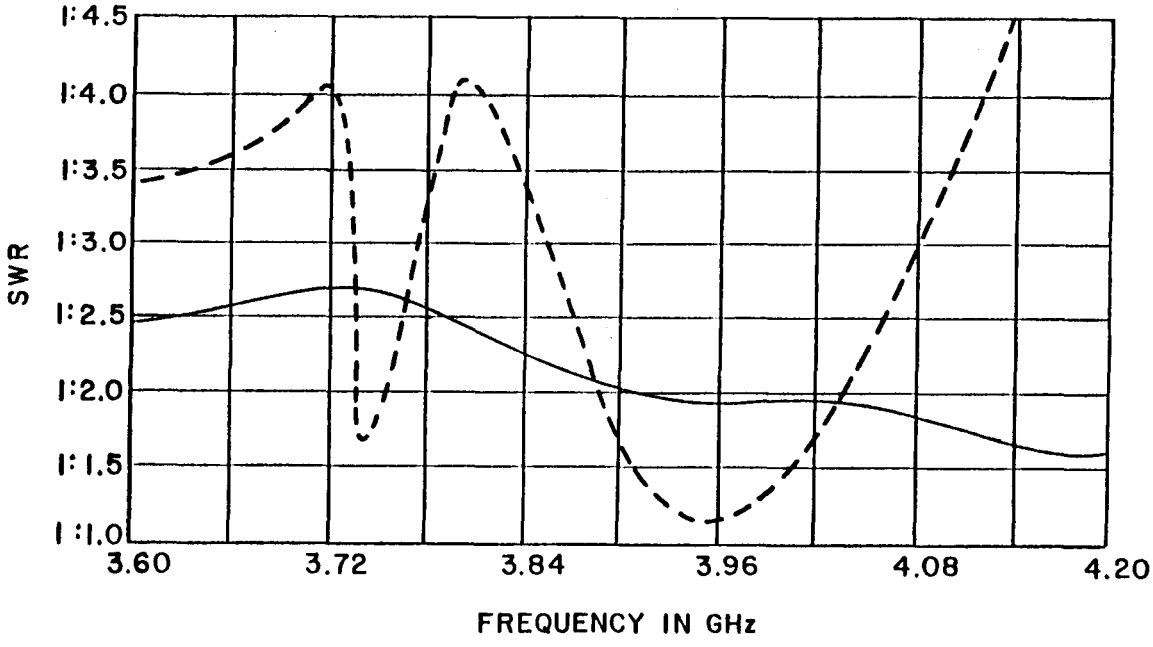

Figure 40: VSWR of a downconverter with (the solid curve) and without (the dashed curve) the microwave absorbing material.

4.4.3 RFI Reduction

After the downconverters were installed on the downconverter chassis it was discovered that a local 70 MHz signal leaked into the downconverters. It was observed that within a half mile of where this experiment is performed there is a transmitter and antenna for a commercial television station. It happens to be Channel 4 which transmits in the 66-72 MHz band, which is within the downcon-

verter IF passband. Thus, there is a need for very good electrical shielding in the downconverter.

The downconverter is enclosed in an aluminum box. It is rectangular in shape and has a removable top plate that allows access to the circuitry. The box has a groove around its circumference where the two pieces of metal meet. A rubber gasket sits in this groove. The rubber gasket creates a watertight mechanical joint; but on the other hand, the case is insulated electrically from the case top of the downconverter. Thus the 70 MIlz signal was able to leak into the downconverter box. Replacing the rubber gasket with a strip of wire braid solved this aspect of the problem. Moreover, rubbing steel wool on both portions of the metallic joint removed any oxidation and paint which further decreased the radio frequency interference from the Channel 4 transmitter.

RF energy was also observed on the DC line which powered the downconverters. A 0.01 microfarad disc capacitor was used to bypass this RF energy to ground at the point where the DC entered the box through a feedthrough connector. All of the connectors feeding into the box were tightened to insure a better electrical connection between the shield of each connector and the downconverter box.

It was found that the interference still was able to get inside the downconverter box by entering through the LO port. Excellent shielding was obtained here by connecting the power divider to the downconverter using semi-rigid 50 ohm cables with SMA connectors on either end.

Finally, the RFI which still existed was traced to the VCLO. To reduce the remaining RFI, the DC voltage which applies power to the VCLO was capacitively bypassed in the same fashion as was done for the downconverters. In addition, a feedthrough capacitor was installed on the input voltage control line for the voltage controlled oscillator. The feedthrough capacitor provides 40 dB attenuation to the

70 MHz interfering signal. Originally, a capacitor was not present there since, if present, the voltage controlled oscillator could not change its frequency at a rapid rate. A bypass capacitor acts like a lowpass filter, so it does not allow rapid changes in the oscillator control voltage.

After making the preceding modifications, the 70 MHz signal was not perceptible above the noise level when viewed by a spectrum analyzer. Weak local interference was also caused by FM commercial stations above 88 MHz, as well as TV Channel 6 (82-86 MHz). A bandpass filter was installed in the main channel. The filter was designed to have a passband 32 MHz wide centered at 70 MHz and a steep enough skirt to suppress a 90 MHz signal by 19 dB. Using this filter, interference due to commercial FM stations does not visually contaminate the desired signal and was measured to be at least 40 dB less in power than the desired signal.

4.4.4 The Local Oscillator

For this design a voltage controlled 3.63-4.13 GHz oscillator was required. The required frequency range is midway between the officially designated S and C-bands. A local oscillator which met the requirements was purchased from Pacific Monolithic. Table 4 shows its specifications.

The output frequency (F in GHz) versus input control voltage (V in volts) for this VCO was experimentally found to be

$$F = .0832 \times V + 3.3161. \tag{4.1}$$

In practice, the output frequency was within ± 100 KHz of the selected frequency. This is due, in part, to the fact that the control voltage from a power supply has a small (approximately 0.1 volt peak-to-peak) amount of ripple.

An important criterion in the choice of an appropriate oscillator is its output power. This value is directly related to the LO power requirement of the mixer in

Table 4: The specifications of the voltage controlled oscillator.

Manufacturer:	Pacific Monolithic, Calif.
Output Frequency:	3.5 - 4.5 GHz
Control Voltage:	2.25 - 14.35 volts
Power output:	24.4 - 24.2 dBm
Supply Voltage:	14.5 - 18 volts DC
Pushing @ $\pm$0.5 volts:	40 KHz/V
Pulling with VSWR of 1.67:	$\pm$1.0 MHz
Phase noise @ 100 KHz:	-70 dBc/Hz
Harmonics:	-15 dBc

each downconverter. An experiment giving the conversion loss of a downconverter helped to determine this value. The conversion loss represents the loss in gain of a mixer as a function of its LO power. As shown in Figure 41 the LO power should be 0.0 dBm or higher. Since an eight way power divider and a 6 dB attenuator are used in each of the downconverter branches, the VCLO output power must be at least 20 dBm. To be conservative, the VCLO purchased has an output power of 24 dBm (.25 watts).

4.4.5 The Power Dividers

A three-way combiner is used in the main channel. This combiner is actually a reactive three-way power divider used in reverse operation. Table 5 shows the manufacturer's specifications for the three-way power divider. Figure 42 shows its insertion loss, Figure 43 the isolation between its input ports, and Figure 44 shows the phase difference between an input sum port and its output. Note that in

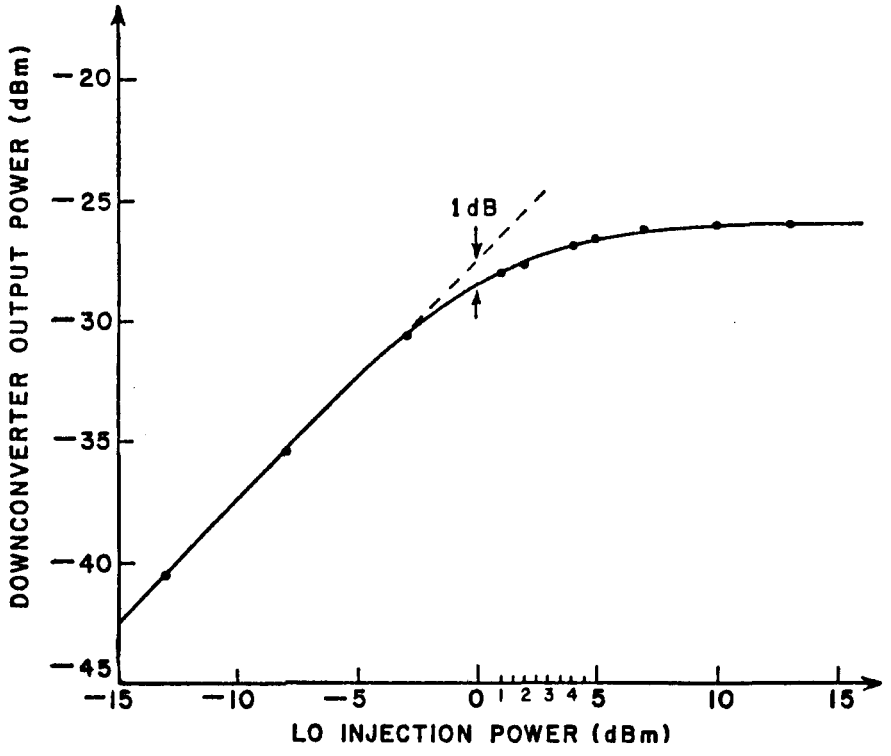

Figure 41: The downconverter output power versus input LO power for a downconverter.

the frequency range of interest, the measured values agree with the manufacturer's specifications.

An eight way power divider is used to split the voltage controlled oscillator signal. Table 6 shows its specifications. Before performing an adaptive array experiment, a phase calibration is carried out in order to counteract any phase imbalances which might exist between the different power divider output ports. This is described in more detail in Chapter V.

A 6 dB attenuator is installed between the eight way power divider and each downconverter. These attenuators improve the VSWR seen by the power divider. Using this method, the reflected power of each downconverter is attenuated by 12 dB. The unused ports of the eight way power divider were terminated with

Table 5: The specifications of the 3 way combiner.

Manufacturer:	Microlab, N.J.
Frequency range:	2.0 - 6.0 GHz
Insertion loss:	4.8 dB
Branch isolation:	9.6 dB
Impedance:	50 ohms

Table 6: The specifications of the 8 way - 0° power divider.

Manufacturer:	Mini Circuits, N.Y.
Part number:	ZB8PD-4
Frequency range:	2.0 - 4.2 GHz
Isolation:	23 dB typical
Insertion loss:	9.8 dB typical
Amplitude unbalance:	0.9 dB maximum
Input impedance:	50 ohms

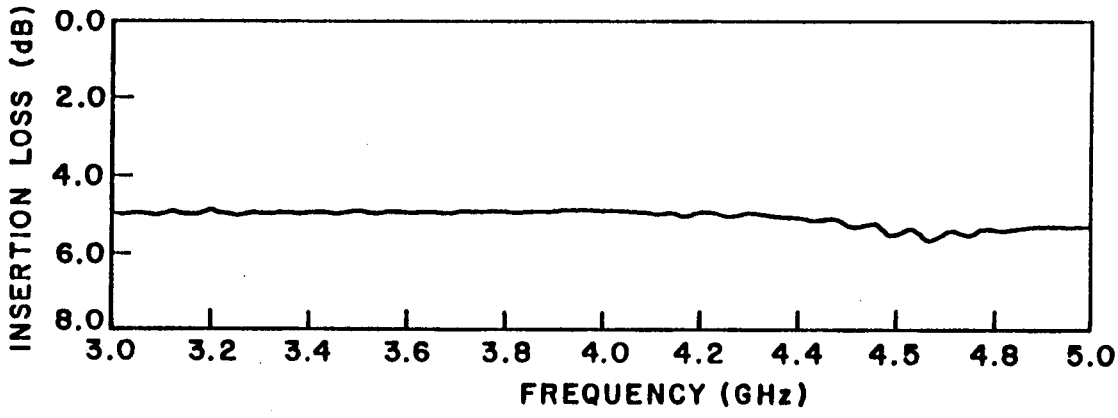

Figure 42: The insertion loss for the 3 way combiner.

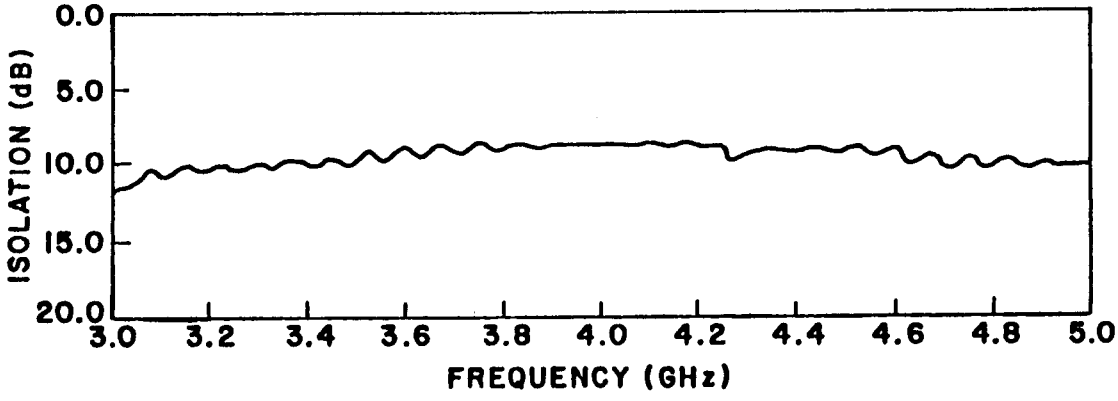

Figure 43: The isolation between input ports for the 3 way combiner.

matched loads.

4.4.6 The RF Transformer

RF transformers are used to transform an impedance of 50 ohms to 75 ohms, or vice versa. Commercial television equipment normally operates using a 75 ohm impedance, while electronic test equipment and their related devices use a 50 ohm impedance. The transformer acquired has a turns ratio of 1.225:1 and frequency range of 52-88 MHz as needed. The transformer is built by Mini-Circuits. The measured insertion loss is less than 1 dB.

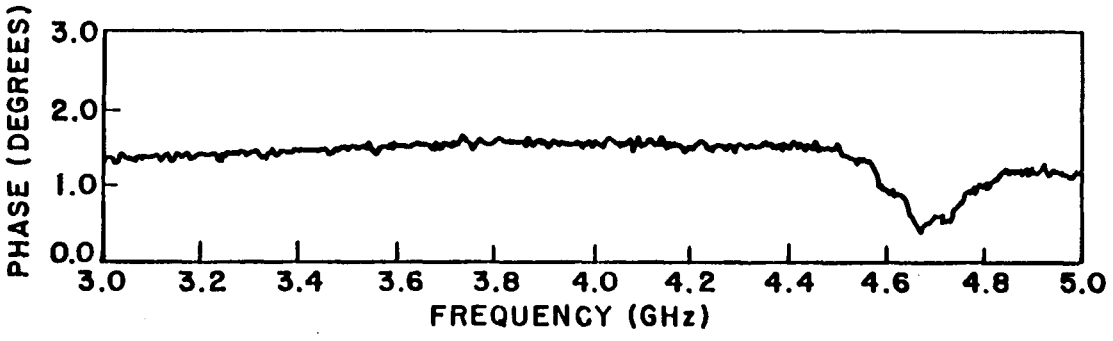

Figure 44: The phase difference between input and output ports for the 3 way combiner versus frequency.

Table 7: The specifications of the monitor tee.

Manufacturer:	Microlab/FXR, Livingston, N.J.
Model number:	HW-30N
Frequency range:	2 - 4.5 GHz
Impedance:	50 ohms
Maximum Insertion Loss:	0.2 dB
Maximum VSWR:	1.3
Minimum Isolation:	25 dB

4.4.7 The DC Block

A DC block, or series monitor tee, consists of a uniform coaxial line shunted by an auxiliary line which has a high impedance to RF and a low impedance to DC. A series capacitance in the main line passes RF but provides DC isolation. The monitor tee is used to separate DC current from a RF signal. Table 7 shows the specifications for the DC block.

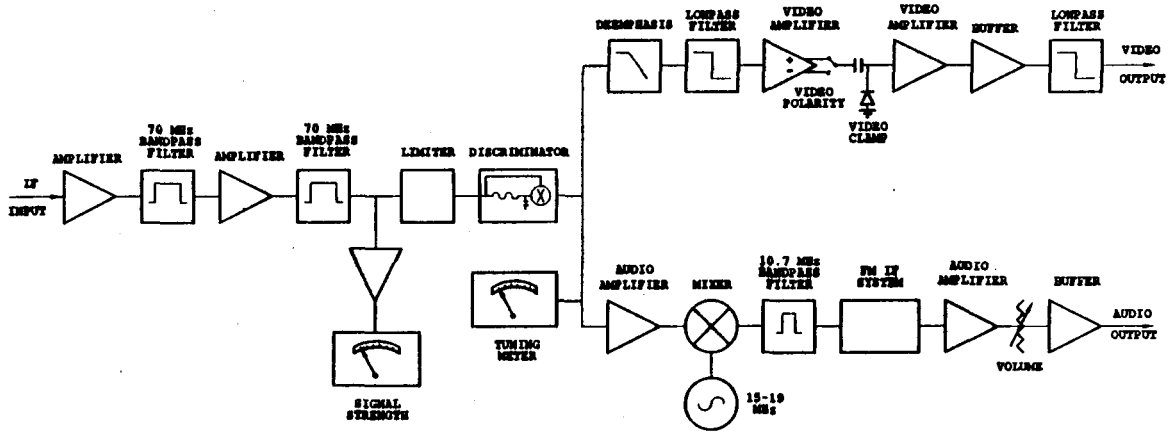

Figure 45: Block diagram for the Drake satellite receiver.

4.5 Subsystems within the Main Building

Inside the main building is the array processor. Also inside this building is the satellite TV receiver and test equipment. The test equipment is used for performance evaluation and incorporates a VCR with monitor, spectrum analyzer, and power meter. In the following three subsections these subsystems are described.

4.5.1 The Satellite TV Receiver

The receiver produces a baseband video signal by demodulating a frequency modulated (FM) television signal. After FM demodulation the video and audio information are separated by appropriate filters. The receiver demodulates the FM signal using a quadrature phase detector. An on-panel adjustment allows the user to choose any audio subcarrier between 5.5 and 8.0 MHz. The North American standard audio subcarriers are 6.2 and 6.8 MHz. Figure 45 shows a block diagram of the receiver. Table 8 shows the specifications for the satellite receiver.

Table 8: The specifications of the satellite receiver.

Manufacturer:	R. L. Drake Co., Ohio
Model number:	ESR-24
IF input frequency :	70 MHz
IF input impedance:	72 ohms
IF input level:	-35 to -5 dBm
IF Bandwidth:	25 MHz at 3 dB
Threshold:	8 dB C/N
Video De-emphasis:	CCIR 405-1, 525 lines
Video frequency Response:	20 Hz - 4.2 MHz
Video dispersion removal:	$>$ 40 dB

4.5.2 The VCR, Monitor, and Spectrum Analyzer

A television (TV) monitor and spectrum analyzer are used to analyze the array performance. The spectrum analyzer (HP 8565A) provides quantitative spectral information. The array output is examined by the spectrum analyzer prior to being frequency demodulated to the 6 MHz wide television picture bandwidth. An accurate representation of the signal powers is unobtainable after the nonlinear limiter stage of the satellite TV receiver. The TV monitor accepts NTSC (National Television Standards Committee) as well as SECAM (Séquence Couleur á Mémoire), and PAL (Phase Alternation by Line) standards. This allows reception and inspection of most downlinked video signals. A video cassette recorder (VCR) is used to record in real time the adaptation process for later review.

Table 9: The specifications of the power meter and its sensor.

Manufacturer:	Hewlett Packard
Meter model number:	HP 435A
Sensor model number:	HP 8481A
Frequency range:	10 MHz - 18 GHz
Input impedance:	50 ohms
Input power:	-30 to +20 dBm
Maximum VSWR:	1.10 at 50 MHz - 2 GHz
Accuracy full scale:	±1%

4.5.3 The Power Meter

An HP 435A RF power meter is used to acquire meaningful quantitative results. A bandpass filter with center frequency of 70 MHz and 32 MHz bandwidth is inserted in series with the power meter. The center frequency of the bandpass filter was chosen to match the center frequency of a satellite transponder. Note that this is not the center frequency of the array processor which is 69 MHz. The sensitivity of the power meter is enhanced with an amplifier having 41 dB gain. All noise measurements are done using the bandpass filter. However, it must be noted that when measuring a received signal within the satellite's passband, one is also measuring an additive noise component. To rectify this, all signal measurements are taken relative to a power measurement performed previously for only noise. Table 9 shows the specifications of the power meter and its power sensor (HP 8481A).

Using the receive system, antenna patterns of the multi-feed array can be

obtained. The next section details this process.

4.6 Antenna Patterns

When the parabolic reflector is pointed at a satellite, it is desirable to have quantitative information concerning the sidelobe levels directed at adjacent satellites. For this reason, antenna power patterns were measured for various positions of a scalar feed relative to the focal point of the parabolic reflector.

To measure the antenna power patterns, the parabolic reflector was swept past a point source in either the azimuth or elevation dimension. In this instance, the parabolic reflector was swept through a frequency modulated signal transmitted by the geostationary satellite Telstar 301. Because the satellite is a small object many wavelengths from the receiving location, the parabolic reflector is effectively sweeping across a point source. Mathematically this is a convolution of the antenna power pattern with a delta function, and thus gives the antenna power pattern.

The received satellite signal was amplified and downconverted in the same manner as previously described. A spectrum analyzer was used to measure the signal power. The spectrum analyzer is furnished with a Y axis output port. The voltage at this port varies from 0 - 0.8 volt relative to the ordinate position of the trace, at a given time (abscissa or X value). There are eight vertical divisions on the spectrum analyzer with each division set to represent five decibels. Each higher division coincides with an increase of 0.1 volt at the Y axis output port. Therefore the top to the bottom of the spectrum analyzer grid represents 40 dB, or a change of 0.8 volt. The frequency span of the spectrum analyzer was set to a low value, 100 KHz, in relation to the 35 MHz wide received signal bandwidth. By doing this the spectrum analyzer had a fixed, flat horizontal trace which varied ± 1.0 dB with time. This provided a generally constant Y axis output voltage for

any point in time. All the power patterns are normalized to 0 dB.

The antenna power pattern using the prime feed is shown in Figure 46. It can be seen that this pattern has a HPBW of about 0.5° and a 10 dB beamwidth of 1.05°, and the first sidelobe is down 17 dB from the boresight.

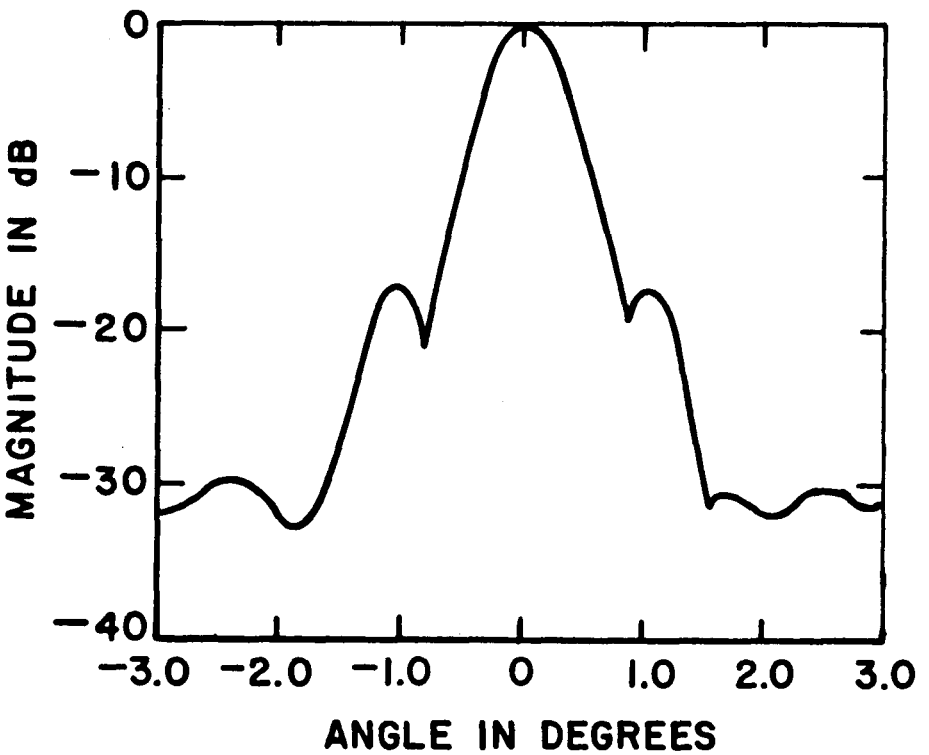

Figure 46: The antenna pattern using the prime feed.

When the feed of a parabolic reflector antenna is displaced laterally away from the focal point, the beam squints off axis in the opposite direction to the feed displacement. Such squinting is accompanied by gain loss, beam broadening and the appearance of a prominent asymmetrical first sidelobe commonly called the coma sidelobe. The amount of such degradation in performance is a function of the F/D ratio and the feed displacement. A feed displaced by 5.5 inches (1.86 wavelengths at 4.0 GHz) from the focal point squints the beam 1.8°. The measured pattern for such an offset feed is shown in Figure 47. Note that the coma sidelobe

is down 14 dB, and the 10 dB beamwidth is 1.2°. The pattern magnitude drops from its peak faster in the direction opposite to the focal point.

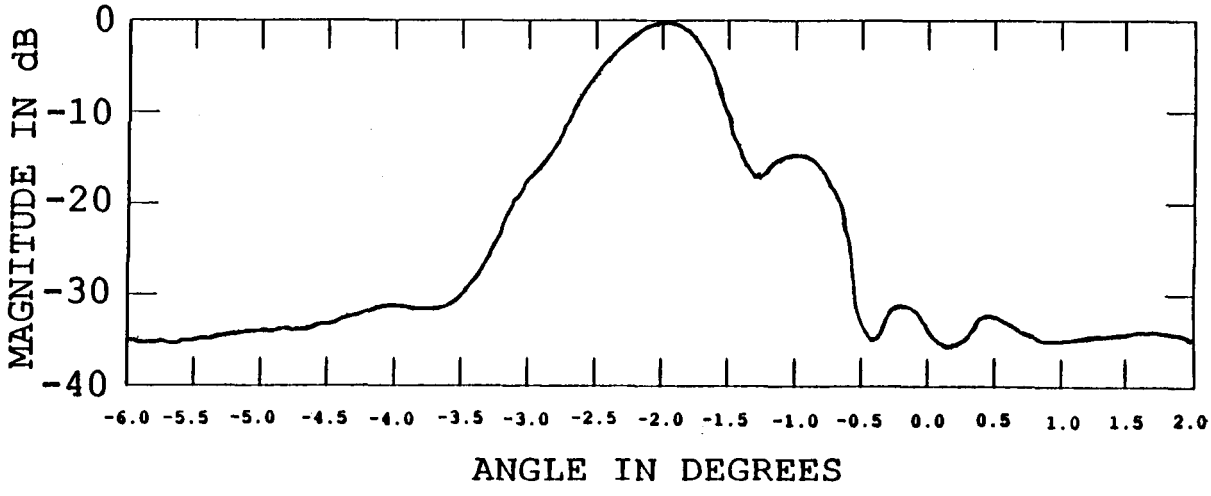

Figure 47: Antenna pattern using a laterally displaced feed positioned 5.5 inches from the prime feed.

A feed displaced 10 inches (3.39 wavelengths at 4.0 GHz) from the focal point squints the beam 3.2°. The measured pattern for such an offset feed is shown in Figure 48. Note that the coma sidelobe is down 11 dB and the 10 dB beamwidth is 1.4°. As expected, the coma sidelobe increases in level as the feed is increasingly displaced from the focal point. The above data are summarized in Table 10.

Figure 49 shows the received signal power of a scalar feed when it is displaced from the focal point within the bounds of 5.5 to 10 inches. This corresponds respectively to squint angles between 2.2° and 3.8°. In this case the signal being received is from a satellite 3° away from boresight. Since in this figure the signal level varies while the noise level is constant, in essence the gain for an auxiliary element can be adjusted by known quantities. As can be noted from the figure, if a satellite was located at 3.0° squint angle, its gain can be decreased by up to

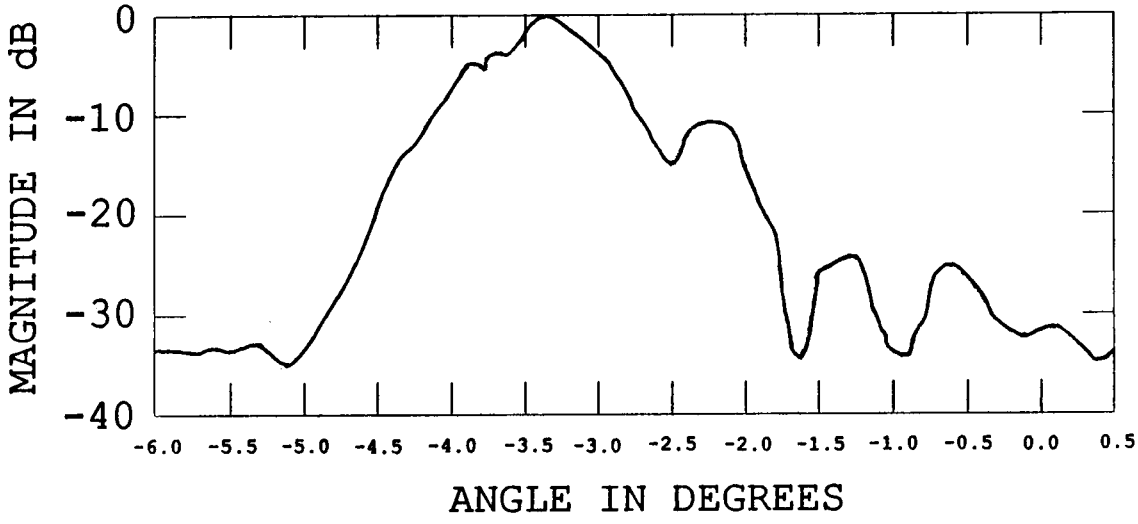

Figure 48: Antenna pattern using a laterally displaced feed positioned 10.0 inches from the prime feed.

23 dB by displacing the feed to the 2.2° skew angle position. This figure is not meant to be a power antenna pattern, but instead a representation of the control possible to the gain of an auxiliary element.

The Ohio State University ElectroScience Laboratory's NEC Reflector Antenna Code [10,11] was also used to determine the antenna patterns for the displaced feeds. The patterns were computed at 3.95 GHz with an aperture blockage

Table 10: The measured antenna pattern parameters.

Feed position	Squint Angle (degrees)	10 dB beamwidth (degrees)	Coma Lobe Referenced to main beam
Focal point	0.0	1.1	-17 dB
5.5 inches	2.1	1.2	-14 dB
10 inches	3.8	1.4	-11 dB

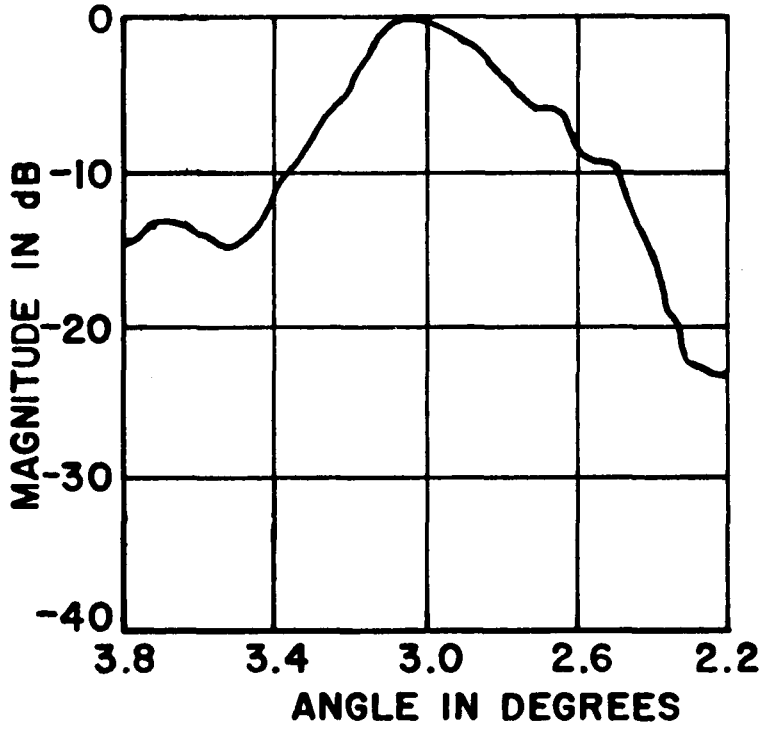

Figure 49: The received signal power level for a scalar feed which is displaced from the prime feed within the bounds of 5.5 and 10 inches (2.2° and 3.8° skew angle respectively) with the signal source being a satellite offset 3.0° from the focal point.

of 4.2 square feet (corresponding to the size of the feed platform). Typically, Aperture Integration (AI) is used to compute their far-field main-lobe and first sidelobes while Geometrical Theory of Diffraction (GTD) is used to compute the wide angle sidelobes and backlobes. The computed data are summarized in Table 11. The antenna patterns produced by the computer code have lower sidelobes and less beamwidth than do the measured patterns. This is probably because the struts of the parabolic reflector were not accounted for, the reflector surface has imperfections, the assumed and actual aperture illumination are slightly different, and the actual feed platform is not exactly at the focal point.

Because of practical mechanical limitations, the actual parabolic reflector an-

Table 11: The GTD antenna pattern parameters.

Feed position	Squint Angle (degrees)	10 dB beamwidth (degrees)	Coma Lobe Referenced to main beam
Focal point	0.0	0.9	-28 dB
5.5 inches	1.8	1.1	-13 dB
10 inches	3.8	1.4	-9 dB

tenna has less gain than an ideal one. Therefore, the actual parabolic antenna has less gain than that which was predicted analytically in Section 3.2. This degradation is due to the four struts, surface deformations, and aperture blockage. For example, the aluminum reflector surface deviates from a true paraboloid by ± 0.08 inches maximum [9]. At 4 GHz the surface deformations reduce the gain of the receiving antenna by 0.5 dB. However, the aperture blockage from the feed platform is not a serious problem for a 30 ft diameter parabolic reflector. Even with an aperture blockage of 4.2 square feet, the percentage of physical aperture blockage is only 0.5% for the 30 ft diameter parabolic reflector.

From the above antenna power patterns it is clear that using the seven feeds one can simultaneously receive signals from various geostationary satellites. By moving the two feed clusters and adjusting the reflector orientation, one can control the level of various signals in different feeds. Thus, one can test the performance of the experimental adaptive array system for various signal/interference environments. A summary of the work reported in this chapter is given next.

4.7 Summary

In this chapter, the electronics of the experimental receive system were discussed. It was shown that the system signal-to-noise ratio is set by the LNA due to its substantial gain. The downconverters were successfully modified to allow for the injection of a common local oscillator signal. A monitor, spectrum analyzer, and power meter are used for system performance evaluation. The antenna patterns of the seven feed adaptive array were presented. From the patterns it was shown that the user has ample control of the required satellite signal environment. In the next chapter, the experimental receive system is used for performance evaluation of the experimental adaptive array. Various experiments performed are described in the chapter and the results of these experiments are discussed.

C-2

CHAPTER V

EXPERIMENTS AND RESULTS

5.1 Introduction

The purpose of this chapter is to describe the experiments conducted and present the results obtained using the experimental receive system. First a description of the procedure to calibrate the experimental system is discussed. Next an overview of the electrical characteristics of the geostationary satellites used in the experiments is given. Following this, the steps undertaken to perform an experiment are described. The first set of experiments are conducted with one or two interfering signals in the absence of a strong desired signal. Since the experiments are mainly qualitative, pictures are included for one example test so the reader can evaluate the adaptive array performance. In the second set of experiments the results of having a strong desired signal present in the main channel are investigated.

5.2 Phase Compensation

In order for a modified feedback loop of the adaptive array to operate correctly, the signal components in the signal and the correlator branches of an auxiliary channel must arrive in phase. However, in general the time delay due to the cables, delay through the LNA, delay through the downconverter, and the delays due to the other hardware components in the two branches of a feedback loop

are not identical. This differential time (or phase) delay causes weight cycling during transients, which increases the adaptation time. The physical reason for weight cycling is that a differential time delay causes the adaptation of the weights to follow a circular phase path rather than path of constant phase. One can visualize the weights as spiraling in toward the optimal weight value on a complex weight plane. As the weight values travel around the optimal weight value their magnitudes exhibit an oscillatory behavior.

To keep weight transients reasonably well behaved, the band edge differential phase shift should be kept to within 45° [3]. The system software was designed to introduce a compensating phase shift in order to correct for differential time delay. A phase calibration is carried out prior to performing any adaptive array experiments. The compensating phase shift is determined from the computer samples of the quadrature vector demodulator signals for a fixed frequency, using the test configuration as shown in Figure 50. This phase shift is introduced into the software such that all subsequent data sampled at the correlator branch by the system computer are phase adjusted prior to performing the adaptive array correlation.

Using this phase compensating technique, we are unable to keep the phase matched in the two branches over a band of frequencies. This band edge differential delay decorrelates the finite bandwidth signal components, and thus there is an accompanying degradation of interference suppression. Since the percentage of bandwidth is less than one percent (see Section 2.5), the actual degradation of the output SINR is less than 1 dB after phase calibration [3].

5.3 Overview of Geostationary Satellites

In this section there is an overview of the geostationary satellites used in the adaptive array experiments. For ease of discussion, this overview is centered around

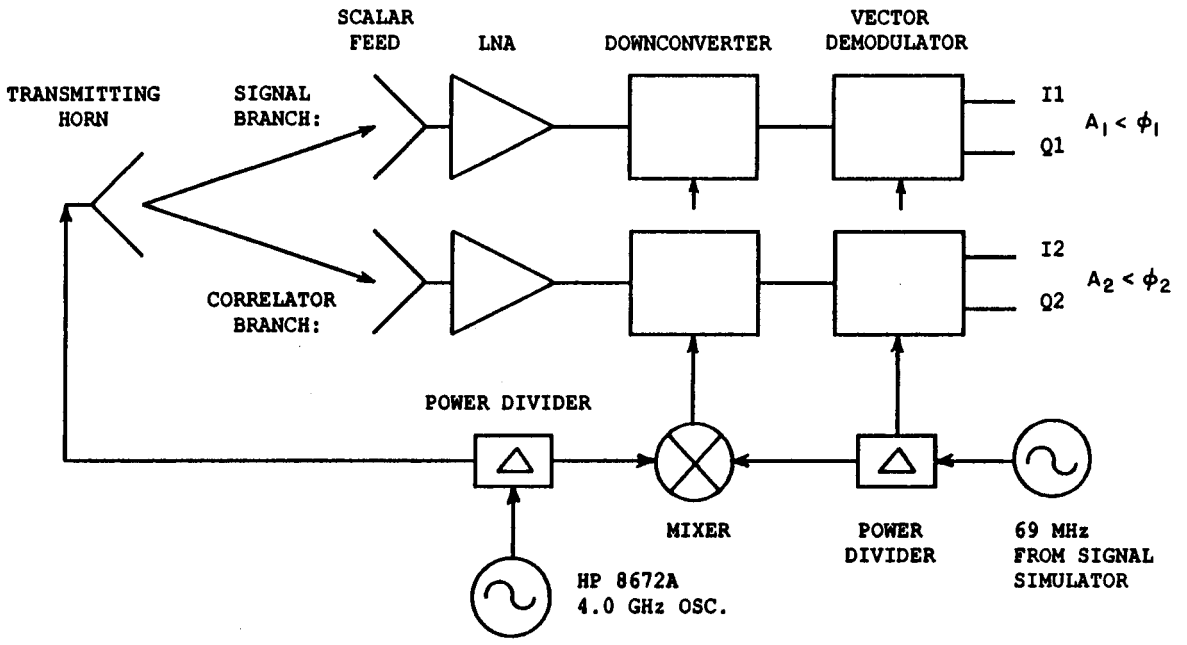

Figure 50: The test setup for phase calibration.

the geostationary satellite Telstar 301, which is located at 96° West Longitude. Telstar 301 was chosen because it has characteristics typical of the geostationary satellites in the Western Hemisphere.

Television broadcast satellites, such as Telstar 301, are repeaters in a two-way communication link. First a signal is transmitted to the satellite. This uplink is within the band from 5925-6425 MHz as shown in Figure 51. Each signal is sent on any one of the twenty-four possible interleaved channels, each with a bandwidth of 36 MHz. A 4 MHz guard band separates the individual channels. For each channel handled on-board the satellite there is an independent receiver and transmitter pair known collectively as a transponder. The uplinked signals are transmitted from the satellite back to the Earth, or downlinked, within the band from 3700-4200 MHz. By alternating between horizontal and vertical polarization, the twenty-four

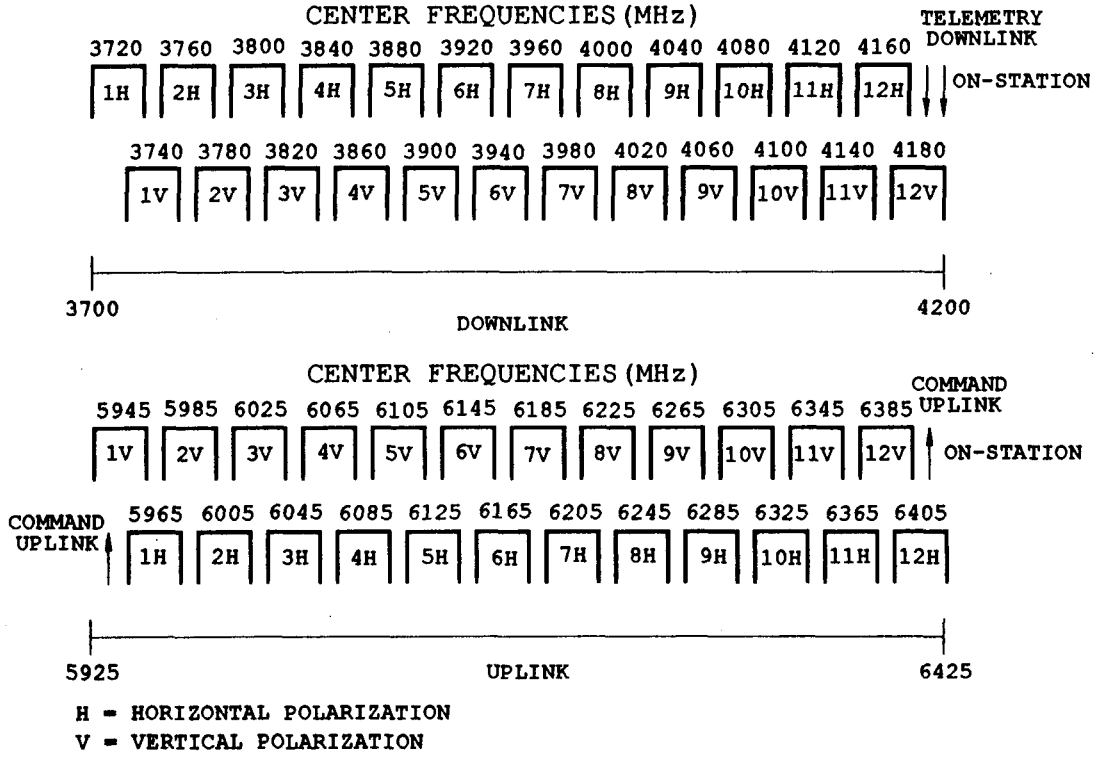

Figure 51: The channel assignment plan for Hughes Aircraft geostationary communication satellites.

36 MHz wide channels are overlapped (commonly called frequency reuse) in the total 500 MHz wide fixed satellite band. While the channels do overlap within their bandwidths, they are at orthogonal polarizations and unequal center frequencies. Cross-channel interference is therefore reduced by using both cross-polarization and channel bandwidths which do not fully overlap.

Various transponders carry different modes of communication traffic. As can be noted from Figure 52, frequency modulated television (FM TV) and frequency division multiplexed frequency modulated (FDM/FM) telephony are used. Only the FM TV is used in this adaptive array experiment. One of the transmitting antennas aboard Telstar 301 is designed to cover the Continental United States

Tr.#	*Pol.*	*Beam*	*Uplink/Downlink*	*Mode*	*Service*	*Audio*
9 (5V)	V	CONUS	6105/3880 MHz	FM TV	Wold Communications: independent TV	6.8 MHz & 5.94/6.12 MHz discrete stereo
					Auxiliary Services: Transtar	5.58/5.76 MHz stereo
					Data	7.2 MHz
10 (5H)	H	CONUS and/or Hawaii	6125/3900 MHz	FM TV	ABC NY network program feeds	6.2 & 6.8 MHz
11 (6V)	V	CONUS and/or Alaska	6145/3920 MHz	FM TV	Fox Broadcasting Corp.	6.2 & 6.7 MHz
12 (6H)	H	CONUS and/or Puerto Rico	6165/3940 MHz	FM TV	ABC L.A: network program feeds	6.2 & 6.8 MHz
13 (7V)	V	CONUS	6185/3960 MHz	FM TV	INN & SNS Occasional news & sports feeds	6.8 MHz
14 (7H)	H	CONUS and/or Hawaii	6205/3980 MHz	FM TV	Fox Broadcasting occasional video	6.8 MHz
15 (8V)	V	CONUS and/or Alaska	6225/4000 MHz	FM TV	CBS network affiliate feeds	6.2 MHz
16 (8H)	H	CONUS and/or Puerto Rico	6245/4020 MHz	FDM/FM	Telephony: TBB = Low C/N	
17 (9V)	V	CONUS	6265/4040 MHz	FDM/FM	Telephony: TBB = 8190 kHz	
18 (9H)	H	CONUS and/or Hawaii	6285/4060 MHz	FDM/FM	Telephony: TBB = 6880 kHz	
19 (10V)	V	CONUS and/or Alaska	6305/4080 MHz	FM TV	Occasional news & sports feeds	6.2 & 6.8 MHz
20 (10H)	H	CONUS and/or Puerto Rico	6325/4100 MHz	FDM/FM	Telephony: TBB = 8190 kHz	
21 (11V)	V	CONUS	6345/4120 MHz	FDM/FM	Telephony: TBB = 5485 kHz	
22 (11H)	H	CONUS and/or Hawaii	6365/4140 MHz		Inactive	
23 (12V)	V	CONUS and/or Alaska	6385/4160 MHz	FM TV	Wold Communications program feeds	6.2 & 6.8 MHz
24 (12H)	H	CONUS and/or Puerto Rico	6405/4180 MHz	FM TV	Occasional video	6.2 & 6.8 MHz

Figure 52: The channel assignment plan for Telstar 301 [13].

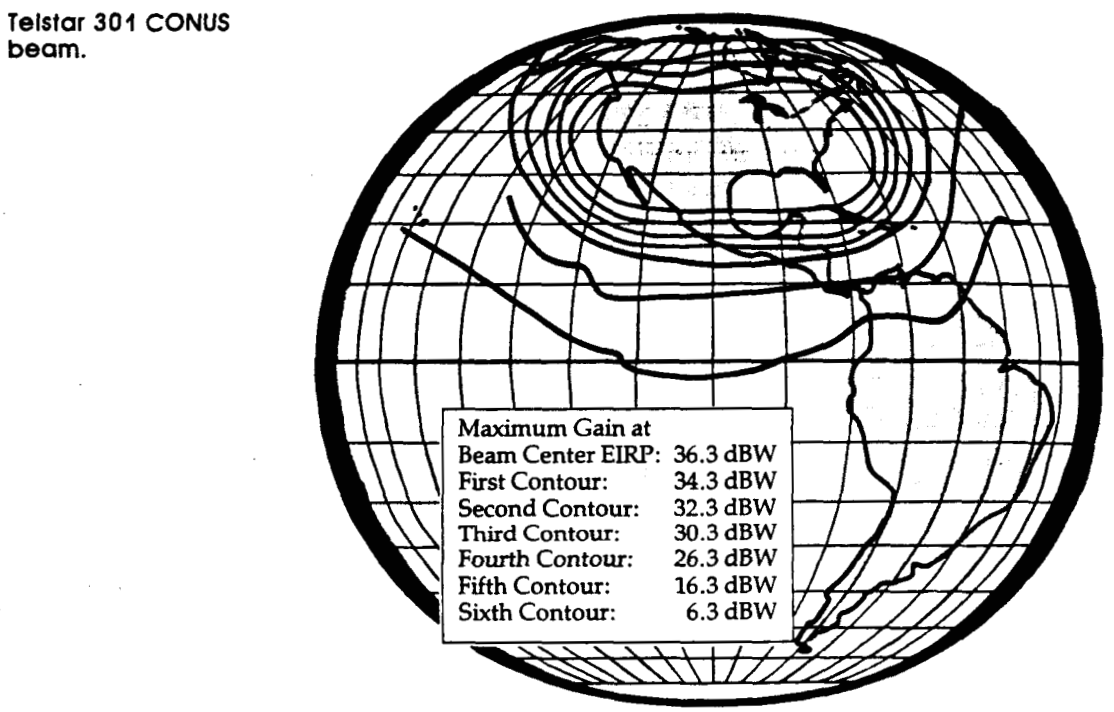

Figure 53: The footprint of the geostationary satellite Telstar 301 [13].

(CONUS). Other antennas produce spot beams which are directed at specific locations, such as Alaska. Each geostationary satellite antenna beam has a specific signal strength in a particular geographical coverage area. This coverage area, or footprint, is described by a contour map of power levels. A power level is expressed in terms of the effective isotropic radiated power (EIRP) of a satellite. Figure 53 shows the footprint for the geostationary satellite Telestar 301. As can be noted, for continental United States, in the main beam of this satellite, the EIRP is at least 36.3 dBW. However, the level of this signal strength varies with various geostationary satellites. For example, Westar 4 has an EIRP of at least

39.75 dBW in Columbus, Ohio. Next a detailed description of an example of a specific interference scenario using geostationary satellites is given.

5.3.1 The Satellites Used in the Experiments

In order to receive two interfering signals and a desired signal simultaneously, all three satellites are required to be spatially close to each other (within 3.8° due to the dimensions of the feed platform). Moreover, they must simultaneously carry television programming on the same center frequency (channel). For these reasons the adaptive array experiments use Telstar 301 at 96° West Longitude as the desired satellite, and used Galaxy 3, at 93.5° West Longitude, and Westar 4, at 99° West Longitude as the two adjacent interfering satellites.

The parabolic reflector is positioned to receive Telstar 301 by the servo-motor controlled mounts. In practice, since the shape of the earth is not uniform, a geostationary satellite will not appear perfectly stationary. Furthermore, satellites are allowed to wander in a figure eight pattern of 0.1° extent [7]. This accounts for the inaccuracy of position of a satellite and thus the need for reestablishing the position of the parabolic reflector over a long term period.

The angular separation of various satellites and their television programming is shown in Figure 54. In this figure the three satellites employed are emphasized by the vertical rectangle box. Channel nine (with center frequency of 3880 MHz) is used since it consistently provided concurrent programming on all three satellites. It should be noted that the same channel on adjacent satellites are normally at opposite polarization. This cross-polarization reduces cross-talk between adjacent satellites in both uplink and downlink. In the experimental system, user controlled sidelobes of the correct polarization are exploited to create a specific interference scenario during performance evaluation.

TRANS H/V	S2 69° SpaceNet 2	F2 72° Satcom F2R	G2 74° Galaxy 2	F4 82° Satcom F4	T2 85° Telstar 302	S3 87° SpaceNet 3	W3 91° Westar 3	G3 93.5° Galaxy 3	T1 96° Telstar 301	W4 99° Westar 4	D1 104.5° Anik D
1	ZAP MOVIES (PPV/S)		UVA TELECOURSES (O/V)		OCCASIONAL VIDEO				OCCASIONAL VIDEO		OCCASIONAL VIDEO
2		*WRBW (S) (CBS) (CHICAGO)	STARSHOT THEATER (S) BEGINS 7/4/86	*BRAVO 6.8/5.8 MN RAJENCI	OCCASIONAL VIDEO			BUENA VISTA (O/V)	CBS (PACIFIC FEED) 6.2/6.8MN		TSN (S) 6.8MN
3	ZAP MOVIES (PPV/S)	OCCASIONAL VIDEO		* KTVT (SCRAMBLED) (DALLAS-FT.W)		CARIBBEAN SUPERSTATION (COMING SOON)			ABC (O/V) 6.2/6.8MN		OCCASIONAL VIDEO
4		*WABC (S) (ABC) (NEW YORK)	*FIRST RUN PAY-PER-VIEW (SCRAMBLED)						ABC (LA/VT FEED) 6.2/6.8 MN		* GLOBAL TV (O/V) 6.8 MN
5	CHANNEL AMERICA 6.8 MN		VTU NASA (O/V)	AVN 6.8 MN		OCCASIONAL VIDEO		* CABLE VIDEO PPV/S (S) (PAY-PER-VIEW)	KBL ENTERTAINMENT (PITTSBURGH)	LATTER-DAY SAINTS (O/V)	OCCASIONAL VIDEO
6				* MSG TELSHOP BISNET					ABC (O/V) 6.2/6.8 MN	* MCN SERVICES CORP 6.8MN	* MUCH MUSIC 6.7MN 5.41/6.17 DB
7			OCCASIONAL SPORTS	* LIBERTY BROADCAST 6.8 MN	OCCASIONAL VIDEO			* ACTS 6.8 MN	*CBS (REG FEED) 6.2/6.8)		CBC (LAB/NEWF) 6.8 MN
8				SUPERSTAR GUIDE	OCCASIONAL VIDEO			HSN 1 5.2/6.8 MN		OCCASIONAL VIDEO	CHCH-TV (S) (HAMILTON ONTARIO)
9	* SELECTV (SCRAMBLED)			*SPORTSVISION 6.8 MN SHOP CHICAGO	ABC (O/V) 6.2/6.8 MN	OCCASIONAL VIDEO		CVN 6.8 MN	* WOLD US SHOPPING NETWORK	* WOLD (O/V) 6.2/6.8 MN	WDIV-TV (S) (DETROIT)
10	SHIPBOARD SATELLITE NETWORK		*TUXXEDO NETWORK (SCRAMBLED)	* KMC (SCRAMBLED) HOME BUYERS	* KMC (PACIFIC FEED) 6.2/6.8 MN			* EWTV 6.2/6.8 MN	* ABC (REG. FEED) 5.8/6.8 MN	*TVSC (O/V) WTN/CNN BRIGHTSTAR	WXYZ-TV (S) (DETROIT)
11	ZAP ENTERTAINMENT ADULT THEATER		NHK WTN (O/V)	HIT VIDEO USA (2 AM-9 AM ET)	ABC (O/V) 6.2/6.8 MN		OCCASIONAL VIDEO	MIND EXT. UNIVERSITY 6.8 MN	ABC (O/V) 6.2/6.8 MN	OCCASIONAL VIDEO	* CBC HOME (PACIFIC FEED) 6.2 MN
12		*WXIA (S) (NBC) (ATLANTA)		*SPORTS CHNL NEW YORK ESPN				OCCASIONAL VIDEO	ABC (REG. FEED) 5.6/6.8 MN	AMSAT 5.2/6.8 MN	
13		NASA (O/V) 6.8 MN	OCCASIONAL SPORTS	* NESN 6.8 MN	OCCASIONAL VIDEO			*WEATHER CHANNEL 6.8 MN	VTC (O/V) CHANNEL 1 (O/V)		* SUNSAT HOLLYWOOD 6.8 MN
14			OCCASIONAL SPORTS	*SPORTS CHNL FLORIDA 6.8 MN	OCCASIONAL VIDEO			C-SPAN 2 6.8 MN	* NBC WEST 5.6/6.2/6.4 MN	BCNZ (O/V) WTN (O/V) BRIGHTSTAR	TCTV (S) MONTREAL
15			OCCASIONAL SPORTS	SHOP AT HOME 6.8 MN	CBS TEST CHN 5.8/6.2 MN			* VH-1 SCRAMBLED	CBS (O/V) 6.2 MN	* PBS (A) 6.8 MN	* CBC FRENCH 6.8 MN
16	OCCASIONAL VIDEO		OCCASIONAL SPORTS	*KTLA (S) INDEPENDENT LOS ANGELES	CBS PACIFIC FEED (O/V)			HOME PREMIER TELEVISION (PPV-S)	OCCASIONAL VIDEO	CNN (O/V) TBS (O/V)	CBC FRENCH CBC NORTH (P)
17			OCCASIONAL SPORTS	*WSBK-TV (S) INDEPENDENT BOSTON	CBS TORONTO (O/V)		OCCASIONAL VIDEO	* MTV SCRAMBLED	OCCASIONAL VIDEO	* PBS (E) 6.8 MN	OCCASIONAL VIDEO
18	OCCASIONAL VIDEO		OCCASIONAL SPORTS		* CBS REG. FEED 6.2 MN			VIEWER'S CHOICE 2 (PPV-S)	OCCASIONAL VIDEO	TELEMUNDO * HBC 6.2/6.8 MN	CITV-TV (S) EDMONTON ALBERTA
19			OCCASIONAL SPORTS	* WPIX (S) NEW YORK 6.8 MN	CBS LA/NY 6.2 MN			NICKELODEON EAST SCRAMBLED	CBS (O/V) 6.2/6.8 MN	* ITN BONNEVILLE SPORTS (O/V)	CBC NORTH ATLANTIC 6.8 MN
20	OCCASIONAL VIDEO	SKI OCCASIONAL HOME NEWSCAST	OCCASIONAL SPORTS	PRIME TICKET * 6.8 MN	* CBS REG. FEED 6.2/6.8 MN			* LIFETIME WEST SCRAMBLED	OCCASIONAL VIDEO	TREASURE CHN HOME TERMINAL SHOW (O/V)	* CBMT (ENG) MONMTREAL 6.8 MN
21		JSIO (O/V) 6.2/6.8 MN	OCCASIONAL SPORTS	*NOSTALGIA CHANNEL 6.8 MN	OCCASIONAL VIDEO	BASS DETROIT 6.8 MN	OCCASIONAL VIDEO	*VIEWER'S CHOICE 1 (PPV-S)	ABC (O/V) 6.2/6.8 MN	* PBS (C) 6.8 MN	WTVS-TV (S) DETROIT
22		AFRTS 6.8 MN	OCCASIONAL SPORTS	* HTS MARYLAND 6.6 MN	OCCASIONAL VIDEO			NICKELODEON WEST SCRAMBLED		OCCASIONAL VIDEO	SCTV (S) VANCOUVER BC
23	ZAP MOVIES (PPV (S)		OCCASIONAL SPORTS	*SPORTS CHN. NEW ENGL. SILENT NET.	OCCASIONAL VIDEO			FAMILY NET. 5.98/5.74 DB	* WOLD (O/V) COMPUTER SHOW TUES/10pm ET	*PBS (D) BONNEVILLE SPORTS (O/V)	WJBK (S) DETROIT
24		OCCASIONAL VIDEO	*TELECABLE CHNEL PAY-PER-VIEW SCRAMBLED	*PLAYBOY CHANNEL SCRAMBLED	SCOLA SATELLITE CHANNEL			*C-SPAN 1 6.8 MN	* PBS (ALB) 5.8/6.2/6.8 MN	BONNEVILLE (O/V) 6.2/6.8 MN	CBC PARL. ENGLISH CBC FRENCH

Figure 54: The transponder programming for Western Hemisphere geostationary satellites.

Prior to performing an adaptive array experiment the user has to choose values for the loop gain and the number of signal samples to be used for each weight update. The procedure used to determine these two values is described next.

5.4 The Loop Gain and Number of Samples

In this section two parameters, the loop gain γ and the number of samples, N, taken for each weight iteration, are discussed. To ensure the stability of the weights, the loop gain must be bounded by

$$0 < \gamma < 1/P_t \tag{5.1}$$

where P_t is the total power received by the array [3]. This ensures that the discrete feedback loop pole is inside the unit circle, and greater than zero. For each test with the experimental system, both γ and N become a direct software input. Values for both are determined empirically through the observation of system performance. The values settled upon are a compromise between weight variance and convergence time (number of iterations until the array weights reach steady state). A small value of loop gain tends to keep the weight variance small about the steady state weight values, but the number of iterations required to reach the steady state may be large. The convergence time is also highly dependent on the interference power received by the array. For a fixed loop gain the time required for the array weights to reach steady state decreases as the interference power received by the array increases.

A similar trade-off exists with the number of samples taken for each iteration. Since the noise components of the two branches of each feedback loop are uncorrelated, with a perfect correlation estimate (i.e. with an infinite number of

samples), noise will have no affect on the array weights, and there will be no random weight jitter. For a correlation estimate based on a finite number of samples, the estimate improves as the number of samples is increased. Thus, increasing N reduces the effect of noise on the array weights. Acquiring a large number of samples for each iteration, however, requires more time and the convergence time of the array is increased. Fortunately, in a typical earth station receive environment, the signal scenario is stationary, or very slowly varying. Since the desired and interfering signal locations change very little, the adaptive array weights will reach their steady state values and remain there, until either the interference ceases, or until other interfering signals become incident on the array. Thus, rapid weight updates are not necessary. In other words, since the auxiliary branch signals arrive from quasi-stationary sources the duration of the convergence time is not critical.

Typical values of γ used in the experiments range from 0.5 to 2.0, and N=640 is typical of the number of samples used to compute each correlation c_i. Thus, since sixty-four samples are taken during a scan, the weights are updated after every ten scans. In practice, 8.8 seconds are required to complete the sampling for each weight update (iteration). The procedure used to perform experiments using geostationary satellites is described next.

5.5 Experimental Procedure

The experimental procedure is described in the following steps.

1. Equipment set up:

   (a) Turn-on:

      i. Parabolic parabolic mount controller (let amplidynes warm up).

ii. Adaptive array processor, VCR, TV monitor, spectrum analyzer satellite receiver, power meter with amplifier, downconverter chassis, TV rotator control boxes, and VCLO control voltage power supply.

(b) Unlatch the parabolic reflector from its stow position.

(c) Wait 30 minutes for electronic components to warm-up. This is needed so that the calibration values later determined for the VMODs, D/A, VDMs, and A/D will be consistent over time.

2. System Calibrate:

(a) Manually measure the detector offset voltages. Null the offset voltage using the amplifier potentiometers on the array processor chassis.

(b) Perform a software calibration of voltage offsets. The computer samples the VDMs for each array branch and calculates their respective DC offsets (detailed in Section 2.4).

(c) Enter phase calibration values into software.

3. Measure system noise:

(a) Position the parabolic reflector with servo-controllers to 52° elevation and 0° azimuth. (This is a position not pointed at the GSO or the ground.) Any power received from land based microwave links is lumped with the thermal noise power.

(b) Measure noise powers of auxiliaries and main channel.

4. Position parabolic reflector so it is directed at the desired satellite (Telstar 301):

(a) Its initial position is determined mathematically (see Figure 32) and then optimized by manually peaking the received signal power.

(b) Set the control voltage on the VCLO to 'tune-in' TVRO satellite channel nine.

5. Set up signal/noise scenario:

(a) If one interfering signal is desired, disconnect one Offset Feed of the main channel. To model an adaptive array with only one degree of freedom, disconnect one auxiliary branch.

(b) If no desired signal is present, turn off the LNA which corresponds to the prime feed. Note that, turning off a LNA in the main channel also reduces the noise level in the main channel. This change in level is taken into consideration when signal-to-noise ratios are measured. Since the noise in the main channel is uncorrelated with the noise in the correlator branch, the array performance is not affected by an increase or decrease in the noise level in the main channel. This will be shown later in this chapter.

(c) Set the interference power of the auxiliaries by sliding the auxiliary channel feed clusters in or out using the TV rotator control boxes.

(d) Set the interference power in the main channel by changing the amount of attenuation of the signals received by Offset Feed #1 and Offset Feed #2.

(e) Measure signal powers in the auxiliary and in the main channel with and without the desired signal present. From these measurements compute the SNR in the main channel, the interference-to-noise ratio in each

auxiliary channel (INR_1 and INR_2), the array output SIR, and the array output SINR. Since the weights are initially zero the SIR and the SINR at the array output are the same as in the main channel. With the weights set at zero it was observed that the array output power is 7.0 dB greater than the main channel power. This gain is due to an amplifier (gain of 28 dB) at the array output which counteracts the insertion loss of the array processor.

(f) Qualitatively characterize the unadapted array output video image, which is the same video image as the main channel output.

6. Algorithm execution:

(a) Set the loop gain, γ, and the number of samples per iteration, N.

(b) Set the VCR into the record mode.

(c) Start adaptation; the computer automatically updates array weights. Continue to adapt until steady state is reached.

7. Performance evaluation:

(a) Measure array output power with and without the desired signal present.

(b) Calculate the interference suppression, output SIR, and output SINR.

(c) Qualitatively characterize the resulting video image.

(d) Go to step 5 for additional experiments, or stop.

5.6 Adaptive Array Experiments

In this section the results of adaptive array experiments with actual satellite signals are summarized. Since the power of a signal cannot accurately or reliably

be measured in the presence of an equal or larger amount of noise power, signal power measurements were done only when the signal was above the receive system noise floor. For this reason, all adaptive array experiments initially have an interference-to-noise ratio (INR) in the main channel of at least 0 dB. Furthermore, all experiments are carried out when the interference-to-noise ratio in the auxiliaries is greater than 0 dB, as established by pointing the main beam associated with a auxiliary channel in the general direction of the interfering signal. Each experimental scenario is characterized by the INR and the SIR in the main channel and the INR in the auxiliaries.

The INR in the main channel is typically between 0-10 dB. Since the INR in the main channel establishes the maximum measurable suppression, the value of suppression obtained is misleadingly small. For this reason the results of adaptive array experiments are characterized not by a quantitative interference suppression measurement but instead by a qualitative description of the array performance in regards to the quality of the steady state video picture.

The original voltage controlled local oscillator used to downconvert the received signals had an excessive amount of phase noise which caused a "noisy" television picture in the receive system. For this reason in the adaptive array experiments the VCLO was replaced by a synthesized signal generator (HP 8672 A) which removed this undesirable disturbance.

In all the experiments to be presented, Telstar 301 at 96° West Longitude is used as the source of the desired signal, Galaxy 3, at 93.5° West Longitude is used for the source of I_1, and Westar 4, at 99° West Longitude is used for the source of I_2.

5.7 Experiments With No Desired Signal in the Main Channel

The first series of tests were done to confirm that each of the modified feedback loops was functional. In other words, for these experiments there is only one interfering signal and only one feedback loop activated. The inputs to the feedback loop which are not activated are terminated into matched loads. Therefore there is no signal in the inactive auxiliary channel and the weight for that channel is equal to zero. Furthermore, no desired signal is included in the main channel. There are two reasons for this. First, a steering vector is not needed when there is not a strong desired signal in the main channel. Second, to determine that the array is operating correctly one has to visually ascertain when the interference is indeed suppressed. An interfering signal contaminates the picture quality of the desired picture. As the array adapts this contamination should no longer be observable. Judging when the interference is no longer objectionable is a subjective process, and thus not precise or definite. However, with the desired signal not present one can clearly see when the interference is suppressed. After the interference is suppressed only noise should be discernable on the television monitor. Moreover, a spectrum analyzer should show only noise once the interference is suppressed. Otherwise, with the desired signal present, the spectral components of the desired signal would mask the weaker interfering signals. Therefore, in the absence of a desired signal one can be more accurate in concluding when the interference is suppressed.

5.7.1 Experiments With One Feedback Loop Activated

Tables 12 and 13 summarize experiments performed to validate the operation of auxiliary channel #1. Each of these tables corresponds to a different signal scenario, and the tables indicate the state of the array after adaptation. The

tables list respectively from left to right: the interference power (I) plus the noise power (N) and the noise power only in the main channel, the interference plus the noise power and the noise power in the signal branch of auxiliary channel #1, the interference plus the noise power and the noise power in the correlator branch of auxiliary channel #1, the steady state weight value for feedback loop #1, and finally the quality of the video picture after adaptation. In the experiments validating the operation of feedback loop #1 there were two types of pictures observed after adaptation, either a black and white video picture which was just visible (represented by B & W in the tables) or noise. In the experiments for Table 12 and 13 the LNAs for Offset Feed #2 and the prime feed were turned off. Thus, the main channel is receiving an interfering signal from interfering satellite source #1 (I_1).

The data in Table 12 show the behavior of the feedback loop weights as the interference power in the main channel is reduced while the INR in the main channel is held constant. There are two sets of experiments listed in Table 12, each with a different INR in the main channel. The INR in the main channel for the first set of experiments is approximately 3.9 dB while its value in the second set of experiments is approximately 6.9 dB. A step attenuator with four relays, as described in Section 4.2, reduces the interference power in the main channel due to Offset Feed #1. The values of attenuation used are 0 dB, 6 dB, 15 dB, and 21 dB. A change in the value of this attenuation, however, will not affect the INR in the main channel. One can observe this in Table 12. Note that, as expected, the magnitude of the weight values decrease as the interference power decreases in the main channel, while the interference power in the signal branch of an auxiliary channel remains constant. In all of the tests shown, except for two cases, the adaptive array successfully suppressed an interfering signal to a level

Table 12: Interfering source I_1, auxiliary loop #2 not activated, a constant INR in the main channel, no desired signal present (all powers are in dBm).

Main Channel		Sig. Branch #1		Corr. Branch #1		Weight	Final
I+N	N	I+N	N	I+N	N	#1	Picture
-35.9	-41.3	-33.3	-45.2	-23.6	-33.3	0.251-1.0j	B & W
-41.9	-47.3	-33.3	-45.2	-23.6	-33.3	0.188-0.841j	Noise
-50.9	-56.3	-33.3	-45.2	-23.6	-33.3	0.099-0.297j	Noise
-56.9	-62.3	-33.3	-45.2	-23.6	-33.3	0.013-0.010j	Noise
-42.0	-43.0	-39.9	-44.0	-27.4	-34.3	1.0+0.183j	B & W
-47.5	-49.0	-39.9	-44.0	-27.4	-34.3	0.730+0.192j	Noise
-55.2	-58.0	-39.9	-44.0	-27.4	-34.3	0.238+0.073j	Noise
-63.0	-64.0	-39.9	-44.0	-27.4	-34.3	0.079+0.015j	Noise

where it was no longer observable, and only noise could be seen on the television monitor. This was true as long as the gain of the auxiliaries was sufficient to keep the magnitude of the weight values from saturating. The two examples when this was not true and the weights saturated are shown on rows one and five of Table 12. In these two cases the interference was only partially suppressed and there was still a black and white video picture present. The reason for this behavior is as follows. The vector modulators used to implement the weights are passive components, so the relative voltage transmission ranges from 0.0 to a maximum of 1.0. Within a VMOD a signal will pass through two power dividers, resulting in an inherent 6 dB loss in the vector modulators. There is also a measured insertion loss of 2.4 dB in the vector modulator. Thus, since the phase of the weights can be between 0° and 360°, the interference power in the auxiliaries has to be greater

Table 13: Interfering source I_1, auxiliary loop #2 not activated, the attenuation of Offset Feed #1 is 6.0 dB, no desired signal present (powers are in dBm).

Main Channel		Sig. Branch #1		Corr. Branch #1		Weight	Final
I+N	N	I+N	N	I+N	N	#1	Picture
-47.5	-49.0	-39.9	-44.0	-27.4	-34.3	0.730+0.192j	Noise
-41.9	-47.3	-33.3	-45.2	-23.6	-33.3	0.188-0.841j	Noise
-43.2	-52.2	-26.8	-35.5	-36.4	-43.4	0.095+0.310j	Noise
-34.5	-50.0	-26.5	-35.5	-38.0	-45.0	0.451-0.741j	Noise

than the sum of these losses, or at least 8.4 dB larger than the interference power in the main channel. This is not the case for row one and five of Table 12, thus the weight saturation and incomplete nulling of the interference.

Another important point one should note from Table 12 is that the gain of the correlator branch is greater than the gain of the signal branch of auxiliary channel #1. Since the interference power in the signal branch has to be larger than the interference power in the main channel, the two branches were interchanged for later experiments. Consequently the adaptive array is able to suppress a larger amount of interference in the main channel without the weight values saturating in feedback loop #1.

For Table 13 the INR in the main channel is varied while the attenuation of the signal received by the Offset Feed #1 is held constant. The value of this attenuation is 6 dB for this experiment. Otherwise, Table 13 is organized the same as Table 12. Even though the attenuation in Offset Feed #1 is held constant, the interference power in the main channel is not constant. In the experimental system the user has control over the received interference power but not the over thermal

noise power. Therefore, in order to change the INR in the main channel, the interference power in the main channel must be adjusted. The INR in the main channel is adjusted by moving the feed cluster which includes Offset Feed #1. By moving the feed cluster the amount of interference power received by Offset Feed #1 varies. However the interference power in auxiliary channel #1 will also vary since the associated feeds are also moved along with the Offset Feed #1. Thus as one can note in Table 13 the interference power in the auxiliaries changes as the INR in the main channel is varied. Again, the adaptive array was successful in suppressing the signal so only noise was visible on the television monitor, in this case irrespective of the INR in the main channel. One may note that there is a discontinuity in the power measurements between rows two and three in Table 13. The reason for this, as described previously, is that the signal branch and the correlator branch of auxiliary channel #1 were interchanged in the receive system.

A more detailed example of a test with one interfering signal and with one feedback loop activated is shown in Figure 55. In this test the computer reads 320 samples before a weight update (N = 320) and the loop gain is set equal to 1.0 (γ = 1.0). Figures 56 through 61 show snapshots of the performance of the adaptive array. The first frame shows the array output before adaptation. Later frames show the array output after given amounts of weight iterations. There is a noticeable distortion of the picture after two weight iterations. After four weight iterations there is bleeding of the colors. There is a loss of color in the picture after six weight iterations. There is only noise observable at fifteen and thirty weight iterations. Thus, the array has converged to the optimum weights to null the interference by this time.

The spectrum analyzer, like the television monitor, also graphically showed the suppression of an interfering signal in real time as the weights adapted. Although

Test I **A modified feedback loop with one interfering signal and no desired signal.**

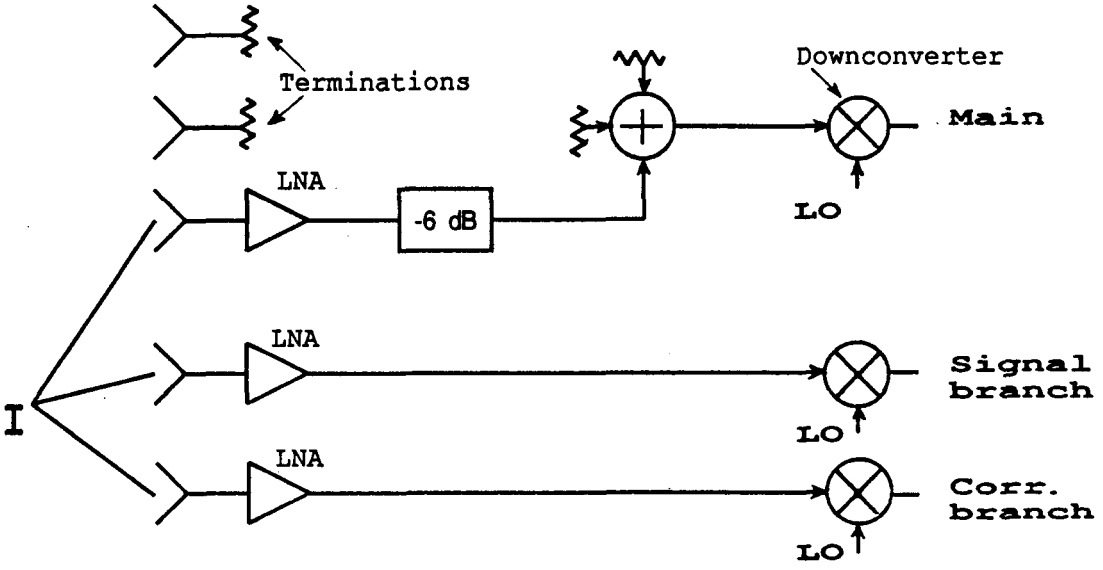


```
I=Interference signal from Galaxy 3
   at 93.5 degrees longitude.


  Array output power (sig. + noise)
   due to the interference.
        before=-32.4 dBm
        after =-40.4 dBm
            =>at least 8 dB suppression



  After 30 iterations the weight
   values are:
        WI=-.330
        wQ=-.482
```

Figure 55: An example test of an interfering signal but no desired signal.

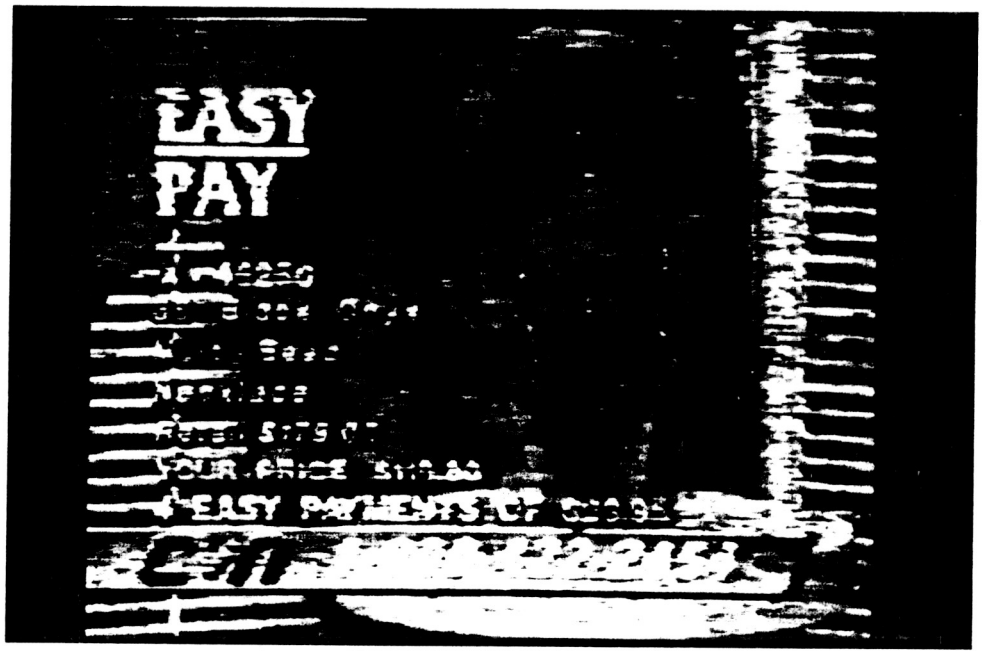

Figure 56: A sequence of television frames showing the array output as the array adapted for the test shown in Figure 55 (Frame A before adaptation).

Figure 57: Frame B after 2 weight iterations.

Figure 58: Frame C after 4 weight iterations.

Figure 59: Frame D after 6 weight iterations.

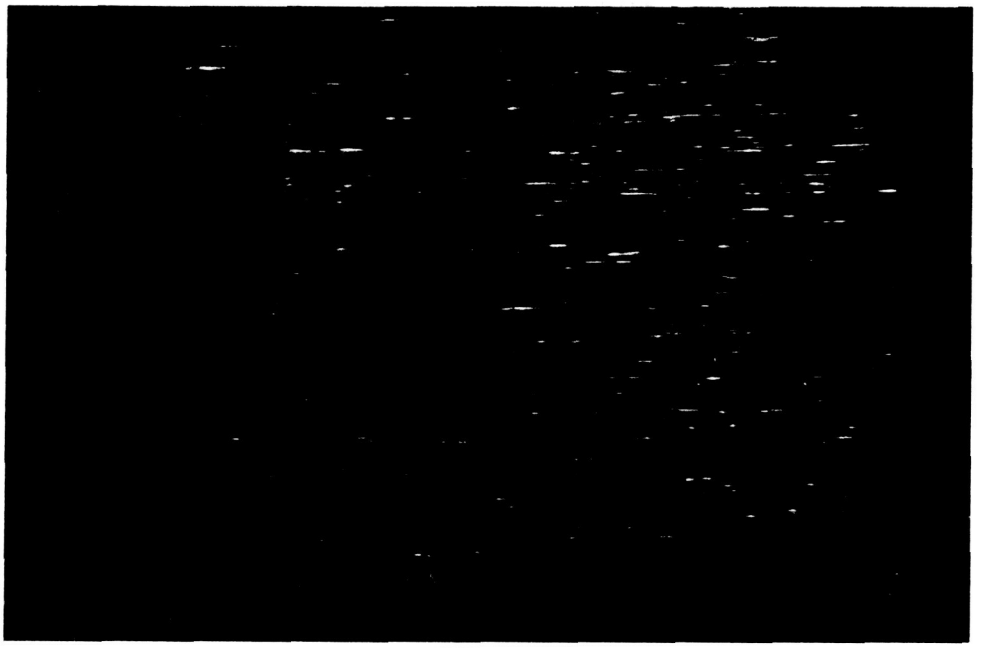

Figure 60: Frame E after 15 weight iterations.

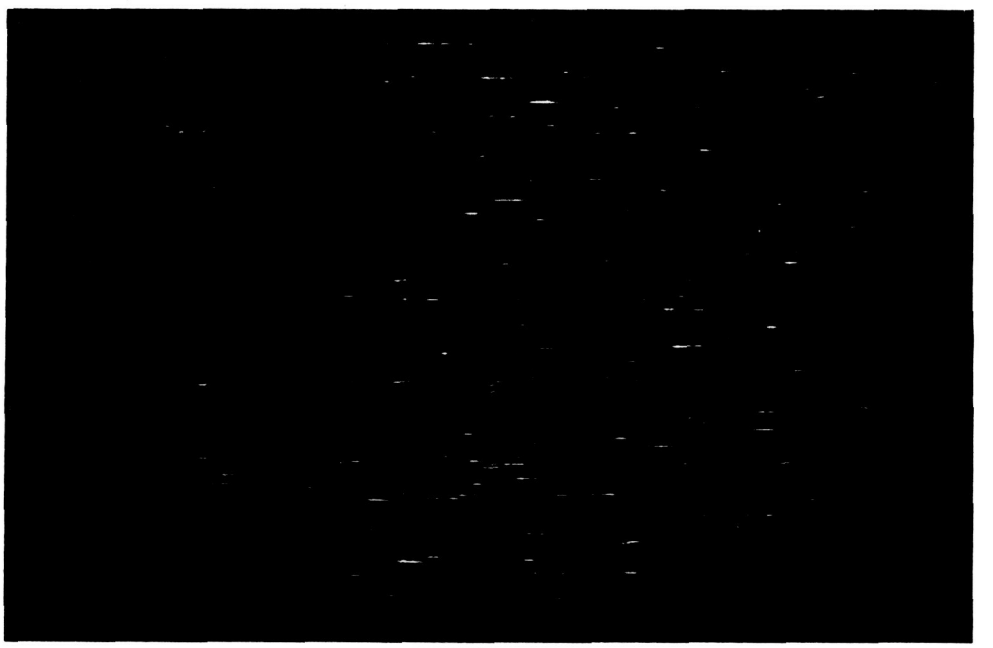

Figure 61: Frame F after 30 weight iterations.

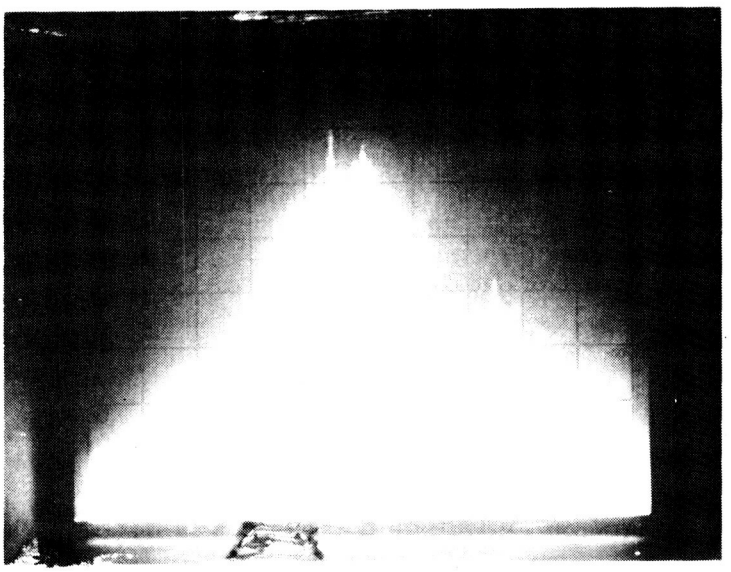

Figure 62: Picture of the spectrum analyzer grid before adaptation.

we are unable to determine the true interference suppression, it was again observed that the weight values continued to adapt well past the point where the interference was no longer visible above the noise floor. The power spectral density of a signal could not be determined below this noise floor. Since the weight values arrived at steady state well past the time when the suppressed interference reached the noise floor threshold, it may be surmised that the interference was suppressed below the system noise level. Figures 62 and 63 show respectively pictures of the spectrum analyzer (HP 8565 A) grid before and after adaptation with one interfering signal and in the absence of the desired signal. The controls of the spectrum analyzer were set for a reference level of -30 dBm, 5 dB per vertical division, 5 MHz per horizontal division with a center frequency of 70 MHz, and a resolution bandwidth of 100 KHz. Note that the interference is suppressed to the noise level across the full 40 MHz bandwidth.

Table 14 represents experiments performed in the same manner as above but in this case for auxiliary channel #2. In this experiment, the input to the auxiliary

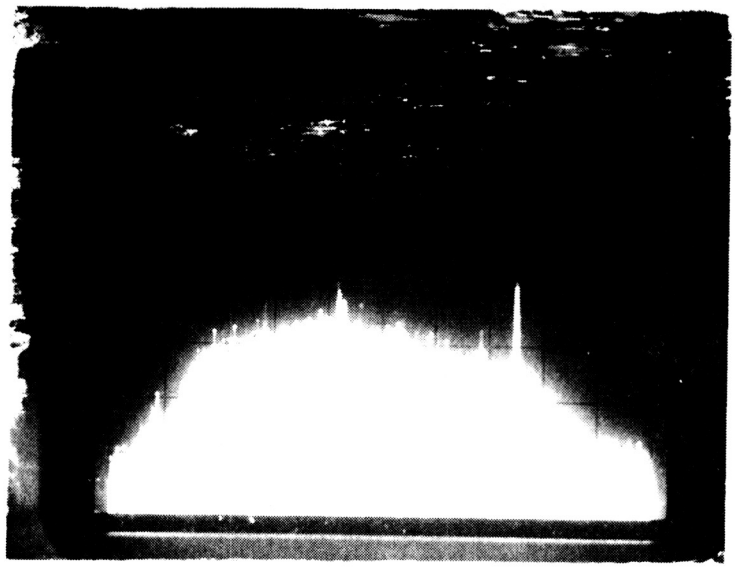

Figure 63: Picture of the spectrum analyzer grid after adaptation.

channel #1 was terminated into matched loads and the LNA for Offset Feed #1 was turned off. Again, the LNA of the prime feed of the main channel was also turned off. Thus, the main channel is receiving an interfering signal from interfering satellite #2. In this experiment the signal received by Offset Feed #2 are always attenuated by 10 dB. In Table 14 results are shown for various values of INR in the main channel and auxiliary channel #2. Note that for all values of INR the final picture after adaptation consists primarily of noise, so the interference was suppressed. Thus, in this subsection we have determined that the two modified feedback loops are indeed independently functional with one interfering signal.

5.7.2 Experiments With Both Feedback Loops Activated

In the next series of experiments there is still one interfering signal and no desired signal present in the main channel. However in this case both feedback loops are activated. Tables 15 and 16 show the obtained results for one interfering signal, in this case I_1. Therefore for this adaptive array experiment the LNAs for

Table 14: Interfering source I_2, auxiliary feedback loop #1 is not activated, no desired signal present, the attenuation of Offset Feed #2 is 10 dB (power measurements in dBm).

Main Channel		Sig. Branch #2		Corr. Branch #2		Weight	Final
I+N	N	I+N	N	I+N	N	#2	Picture
-44.5	-53.4	-31.6	-43.8	-33.2	-41.8	-0.431-0.149j	Noise
-46.8	-51.0	-31.8	-40.5	-34.7	-39.2	-0.334-0.199j	Noise
-49.3	-51.0	-33.4	-43.5	-41.5	-42.5	-0.223-0.026j	Noise

Offset Feed #2 and the prime feed were turned off. Each of these tables corresponds to a different signal scenario, and the tables indicate the state of the array after adaptation. The tables list respectively from left to right: the interference power (I) plus noise power (N) and the noise power in the main channel from Offset Feed #1 after attenuation, the interference plus noise power and the noise power in correlator branch #1, the magnitude of the steady state weight values for feedback loop #1 and #2, and finally the quality of the video picture after adaptation. We take the INR of the auxiliaries to be that of the correlator branch since the weight control algorithm directly samples the signals and noise present in this branch. In Table 15 the INR in the main channel is constant, $\approx$2.3 dB, while the interference power received by Offset Feed #1 is attenuated by 0, 6, and 15 dB. In Table 16 the attenuation of the signal received by Offset feed #1 is held constant while the INR in the main channel varies. Note that for all values of INR in the main channel and auxiliary channel #1, the final picture after adaptation contains only noise. Thus the interference has been suppressed. Also in Table 15, as the interference level in the main channel is reduced by an increase in the received signal attenuation, the weight value for auxiliary channel #1 decreases, which is expected. Note that the

Table 15: Interfering source I_1, both auxiliary loops are activated, no desired signal present, INR(Main Channel)$\approx$ 2.3 dB, (powers are in dBm).

Main Channel		Corr. Branch #1		Mag.(Weight #)		Final
I+N	N	I+N	N	#1	#2	Picture
-44.2	-45.5	-38.5	-44.5	0.359	0.023	Noise
-50.2	-51.5	-38.5	-44.5	0.275	0.007	Noise
-59.2	-60.5	-38.5	-44.5	0.070	0.025	Noise

Table 16: Interfering source I_1, both auxiliary loops are activated, no desired signal present, the attenuation of Offset feed #1 is 6.0 dB, (powers are in dBm).

Main Channel		Corr. Branch #1		Mag.(Weight #)		Final
I+N	N	I+N	N	#1	#2	Picture
-43.2	-52.2	-36.4	-43.4	0.326	0.008	Noise
-50.2	-51.5	-38.5	-44.5	0.275	0.007	Noise
-39.8	-50.4	-44.2	-48.7	0.842	0.172	Noise

weight of feedback loop #2 is very small in magnitude. Moreover, it was observed that if the weight was set to zero there was no visible difference in the interference suppression. The reason for such a low magnitude of weight for auxiliary channel 2 can be attributed to the fact that the level of I_1 in auxiliary channel #2 is very small. The antennas associated with auxiliary channel #2 are pointed in the general direction of I_2, and not I_1. It should also be noted that both auxiliaries also received the desired signal from the geostationary satellite Telstar 301 through their sidelobes. However, with there being an extremely weak desired signal in the main channel (received through the sidelobes of Offset Feed #1) the correlation of

the desired signal components is much lower in magnitude than the correlation of the interfering signal components. Therefore, the array suppression is not affected. Note that the interference power measured in auxiliary channel #1 is actually the sum of three signals ($I=I_1+I_2+D$), however the powers of I_2 and D (the desired signal) are both very small in comparison to power of I_1; therefore, $I \approx I_1$. Thus, one may approximate the INR of auxiliary channel #1 (INR_1) as the INR in auxiliary channel #1 due to I_1 (I_1NR_1). Likewise since the beam associated with auxiliary channel #2 is pointed in the general direction of I_2, the INR of auxiliary channel #2 is approximately equal to the INR of auxiliary channel #2 due to I_2 ($INR_2 \approx I_2NR_2$). In all of the above experiments, except for the test on row three of Table 16 auxiliary channel #2 received signals from satellite source #2.

Table 17 shows the results obtained for an interfering signal from satellite source #2. Here, the LNAs for Offset Feed #1 and the prime feed were turned off while the LNA for Offset Feed #2 is operational. The signals received by Offset Feed #2 are attenuated by 10 dB. The INR in the main channel and also in auxiliary channel #2 is adjusted by the linear displacement of the feed cluster #2 in the focal plane. Again note that the magnitude of the weight value of the inactive auxiliary channel, which in this case is auxiliary channel #1, is very small. The same reasoning holds as before in that in this case auxiliary channel #2 receives a small amount of interference from satellite source #1 through its sidelobes. As in prior experiments, only noise was visible after the interference was suppressed for all obtainable values of INR in the main channel.

Next, the array performance was tested in the presence of two interfering signals. To suppress two interfering signals, both feedback loops must be activated. This is because the adaptive array needs two degrees of freedom which, as described in Chapter II, requires at least two auxiliary channels. These experiments were

Table 17: Interfering source I_2, both auxiliary loops are activated, no desired signal present, the attenuation of Offset Feed #2 is 10 dB, (powers are in dBm).

Main Channel		Corr. Branch #2		Mag.(Weight #)		Final
I+N	N	I+N	N	#1	#2	Picture
-44.5	-53.4	-33.2	-41.8	0.007	0.451	Noise
-47.3	-50.3	-33.3	-38.2	0.049	0.392	Noise
-46.8	-51.0	-34.7	-39.2	0.017	0.345	Noise
-49.3	-51.0	-41.5	-42.5	0.020	0.206	Noise
-51.0	-53.4	-36.4	-41.8	0.008	0.208	Noise

again done with no desired signal present from the prime feed of the main channel. Tables 18 and 19 shows the results for two interfering signals, from the two Offset Feeds. Each of these tables corresponds to a different signal scenario, and the tables indicate the state of the array after adaptation. The tables list respectively from left to right: the interference plus noise power in the main channel from Offset Feed #1 after attenuation and the interference plus noise power in the main channel from Offset Feed #2 after attenuation and the noise power in the main channel after the attenuation of each Offset Feed, the interference plus noise power and the noise power in correlator branch #1, the interference plus noise power and the noise power in correlator branch #2, and finally the quality of the video picture after adaptation. In Table 18 the INR in the main channel due to Offset Feed #1 was constant while the attenuation of its contribution to the total interference power in the main channel varied in fixed steps of 6, 15, and 21 dB. However the INR and interference power in the main channel due to Offset Feed #2 is constant. In these experiments the attenuator in the Offset Feed #2 is always set at 10 dB.

Table 18: Interfering sources I_1 and I_2, both auxiliary loops are activated, no desired signal present, the INR(Main channel) is constant for Offset Feed #1, the attenuation is 10 dB and the INR(Main channel) is constant for Offset Feed #2 for two sets of experiments (powers in dBm).

Main Channel			Corr. Branch 1		Corr. Branch 2		Final
$(I+N)_1$	$(I+N)_2$	N	I+N	N	I+N	N	Picture
-39.1	-47.0	-47.5	-43.4	-44.8	-34.7	-42.5	Noise
-48.1	-47.0	-50.4	-43.4	-44.8	-34.7	-42.5	Noise
-54.1	-47.0	-50.8	-43.4	-44.8	-34.7	-42.5	Noise
-39.1	-49.3	-47.5	-43.4	-44.8	-41.5	-42.5	Noise
-48.1	-49.3	-50.4	-43.4	-44.8	-41.5	-42.5	Noise
-54.1	-49.3	-50.8	-43.4	-44.8	-41.5	-42.5	Noise

Therefore, in Table 18 the INR in the main channel varied with the attenuation of Offset Feed #1 while the INR of the auxiliaries was constant. For the two sets of experiments shown the INR in the main channel due to Offset Feed #1 was the same at approximately 3.2 dB while due to Offset Feed #2 was approximately 1.8 dB and 0.5 dB respectively. In Table 19 the attenuation of the Offset Feed #1 is set at 15 dB and Offset Feed #2 is set at 10 dB while the INR in the main channel varies. In the main channel the INR due to the interfering signal I_1 (I_1NR) and INR due to interfering signal I_2 (I_2NR) vary independently. In these experiments with two interfering signals it was observed that both weight values adapted and were of significant magnitude. Both interfering signals were suppressed in these tests regardless of the INR used in the main channel and the auxiliaries.

In the experiments, it was observed that the adaptive array determined the appropriate phase of the weights very quickly (usually within ten weight iterations).

Table 19: Interfering sources I_1 and I_2, both auxiliary loops are activated, no desired signal present, the attenuation is 15 dB for Offset Feed #1, the attenuation is 10 dB for Offset Feed #2 (powers in dBm).

Main Channel			Corr. Branch #1		Corr. Branch #2		Final
$(I+N)_1$	$(I+N)_2$	N	I+N	N	I+N	N	Picture
-47.5	-47.3	-50.0	-44.3	-43.0	-33.3	-37.2	Noise
-52.2	-44.5	-55.2	-36.4	-43.4	-33.2	-41.8	Noise
-48.1	-47.0	-50.4	-43.4	-44.8	-34.7	-42.5	Noise
-53.4	-51.0	-54.5	-38.2	-43.4	-36.4	-41.8	Noise

On the other hand, determining the correct magnitude of the weight values to create a pattern null was a much longer iterative process. This can be expected since in the experimental system the sampled signals have been phase compensated (see Section 5.2), but there is not an amplitude compensation for the different signal levels of the signal and correlator branches of an auxiliary channel. Therefore, the adaptive array algorithm can determine the phase of the optimal weights directly from the estimate of the correlation of the interfering signal components, which is not also true for the magnitude of the weights.

The first series of experiments were carried out with no desired signal from the feed at the focus of the parabolic reflector in the main channel. There was however, as described before, a very weak desired signal in the auxiliaries and the Offset Feeds. Though weak, its correlation with a strong desired signal from the prime feed can appreciably affect the resulting correlation. Without the strong desired signal, suppression of an interfering signal could be observed on the television monitor or spectrum analyzer while the array adapted. However to be more complete, experiments were carried out with a desired signal present. The inter-

ference suppression should be unaffected by the presence or absence of this desired signal. These experiments are described next.

5.8 Experiments With a Desired Signal Present in the Main Channel

In the next series of experiments a strong desired signal was included in the main channel. In this case, with all the other signal powers the same as in the previous section, the weights always saturated during adaptation. The reason for this is that there is a weak desired signal in the auxiliaries which for the experimental receive system is 50 dB down from that of the main channel. It is 50 dB down due to two factors: 25 dB is due to cross-polarization (auxiliary feeds have horizontal polarization while the prime feed has vertical polarization), and another 25 dB is due to auxiliary sidelobes which are down at least 25 dB at the desired signal source (see Figure 47 at 0.0°). Even though the desired signal in the auxiliaries is very weak (below the noise level), because of the strong desired signal in the main channel, the correlation of the desired signal components influence the overall correlation, c_i. This is especially true when the interference component at the array output is partly nulled. For these reasons, the adaptive array algorithm, which attempts to minimize the output power due to undesired signals, actually suppresses the desired signal. To do this, the adaptive array algorithm attempts to amplify the weak desired signal power in the auxiliary channel to the same magnitude as the desired signal power in the main channel. However, the VMODs of the array processor, being passive components, are incapable of forming weight magnitudes greater than one, so they saturate.

Decreasing the desired signal power in the main channel allows the correlation of the interfering signal to dominate over the correlation of the desired signal. As expected, when the desired signal power in the main channel was reduced, the

weight values suppressed the interference without driving a null in the desired signal direction. Figure 64 shows the results of one representative test. The desired signal power in the main channel was decreased by pointing the beam associated with the prime feed slightly away from the desired signal satellite and more toward the interfering source. This was done by adjusting the position of the parabolic reflector antenna relative to the desired signal source. Since there is a decrease in the desired signal level, the SNR in the main channel likewise decreases. For this reason, this procedure is not recommended for a practical system. The adaptive array however did successfully suppress the interference so that it was no longer objectionable.

A solution to the correlation of the desired signal components is the implementation of a steering vector. The influence of the desired signal correlation is negated by implementing a steering vector. The steering vector can be derived from the correlation of the desired signal components of the correlator branch and the array output [6]. The equation of the estimate of the steering vector, u_{si}, is given by

$$u_{si} = \frac{1}{N} \sum_{k=1}^{N} \{y_{di}(k)(m_d(k) + \sum_{j=1}^{2} w_j s_{dj}(k))^*\} \tag{5.2}$$

where $y_{di}(k)$ is the desired signal component sampled at the i^{th} correlator branch, $m_d(k)$ is the desired signal component sampled at the array output from the main channel, and $s_{dj}(k)$ is the desired signal component sampled at the array output from the j^{th} signal branch, and w_j is the complex weight of the j^{th} auxiliary channel. Here, N is the number of samples used for the correlation estimate and * denotes the complex conjugate. Typically the SIR in the auxiliaries is less than -30 dB and there is a strong desired signal in the main channel; therefore $m_d(k) \gg$

Test II A Modified feedback loop with desired+interference

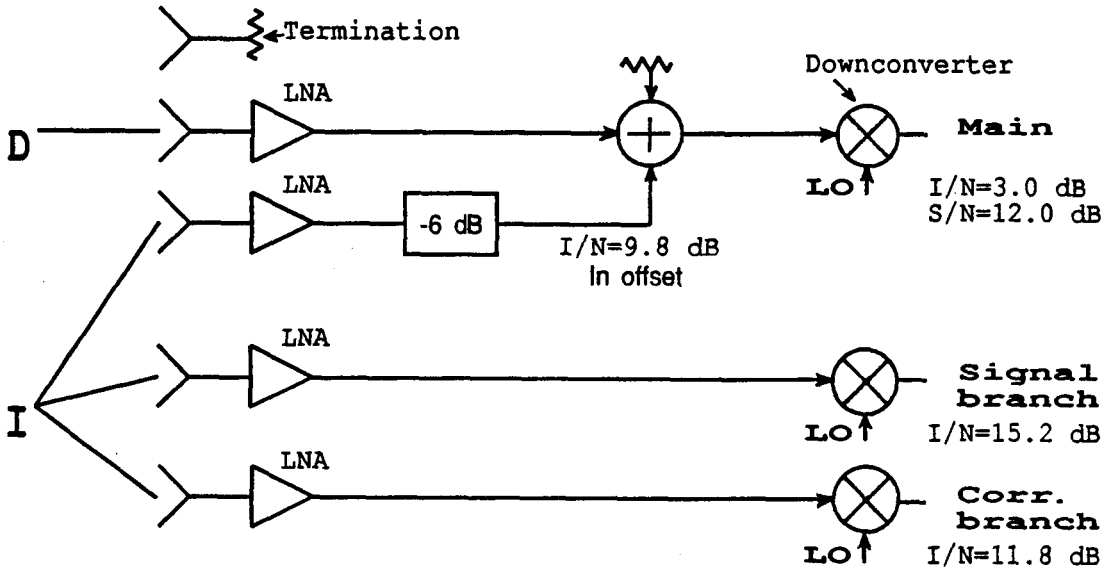


```
D=Desired signal from Telstar 301
   at 96.0 degrees longitude.

I=Interference signal from Galaxy 3
   at 93.5 degrees longitude.


  Array output power (sig. + noise)
   due to the interference.
        before=-31.5 dBm
        after =-39.5 dBm
              =>at least 8 dB suppression


  Array output power (sig. + noise)
   due to the desired signal.
        before=-22.8 dBm
        after =-22.8 dBm


  After 55 iterations the weight
   values are:
        WI=-.273
        WQ=-.569
```

Figure 64: An example test of an interfering signal with a desired signal.

$\sum_{j=1}^{2} w_j s_{dj}(k)$. In this case, one can simplify Equation (5.2) to

$$u_{si} \approx \frac{1}{N} \sum_{k=1}^{N} y_{di}(k) m_d^*(k). \tag{5.3}$$

Note that Equation (5.3) represents the conventional steering vector used in an Applebaum adaptive array [1]. To obtain the above steering vector, one needs to know the magnitude and phase of the desired signal in the main channel and in the correlator branches. Several methods of determining the above conventional steering vector are described next.

5.8.1 Determining the Steering Vector

The first method to determine the steering vector is to calculate the steering vector by knowing the position of the desired satellite with respect to the array elements. For this approach, the relative phase and field pattern magnitudes of each of the array elements has to be known. Of these quantities, the phase is the only one not measured in this thesis. The relative phase could be measured in a similar manner as that done to determine the field pattern - that is, by sweeping the reflector antenna past a point source while measuring its phase referenced to another antenna pointed at the same source. However, in practice there would be measurement errors with this method. Moreover, a potential downfall is that the absolute power received from the desired satellite has to be known. Since this value fluctuates, an exact steering vector may not be able to be calculated.

The second possible method to compute a steering vector is to skew the reflector antenna to a position in the sky where there is only one satellite and no interference. Next, by using the data obtained by the array processor, the steering vector is determined. The steering vector in this case is equal to the correlation of the correlator branch and the array output. Finally the reflector is moved back to

a position such that the desired signal again has an identical orientation relative to the antenna. However because of gear backlash, the final antenna orientation is somewhat inexact, and there will not be identical orientation. Furthermore, the absolute power of one satellite may differ from that of another; indeed, even different transponders on the same satellite have different output powers. As in the first method, this method potentially could involve implementing an inexact steering vector.

The third method is to adapt while employing another channel which is not being used on the same satellite. In other words, by exploiting the fact that a transponder on a desired satellite is not on, or the chosen frequency band is a guard band, one can null the interference without knowing the steering vector. Obviously, with this method the weight values will have to be adjusted to compensate for the difference in frequency of the two channels if the channel selected is widely separated from the desired channel.

A fourth method is to adapt, without using a steering vector, while the signal from the desired satellite is "turned off" at its source for a short period of time. However, this solution might be disagreeable as a universally accepted option. Likewise if the interfering signals are temporarily turned off at the satellite, a steering vector can be derived, and then later used.

From previous work it has been determined that the modified sidelobe canceler is very sensitive to an inexact steering vector [18]. If the steering vector used is inexact, then its magnitude should be greater than the expected optimum steering vector $|u_{si}|$. In this way, the desired signal power in the auxiliaries is enhanced, and so the output array signal power due to the desired signal is increased, which makes up for the thermal noise added by the auxiliary elements. Thus, there is less degradation of the output SINR of the adaptive array as long as there are at

least moderate amounts of desired signal in the auxiliaries.

Performance fluctuations were observed during the adaptive array experiments. Variations in adaptive array performance and system limitations are described next.

5.9 General Comments Concerning the Adaptive Array Experiments

In the experiments presented, as can be noted, the noise powers of the correlator and signal branch as well as the main channel are not the same and vary between tests. The noise power varies between array processor inputs since each LNA exhibits a different thermal noise power which varies with the received frequency. Also, the gain of the various downconverters and LNAs are not the same. Since the gain of the downconverters and LNAs vary with time and temperature one should be aware that a measurement of a signal power prior to an experiment for one array processor input may change to a different value at the end of the experiment. For example, the noise power of an auxiliary branch was observed to vary by approximately 3 dB over a period of three hours. Furthermore, there are variations in the power measurement over time from the same array processor input since the level of the noise is very low and at the sensitivity limit of the power meter. While making noise power measurements the power meter was observed to fluctuate continually within a range of approximately ± 1 dB. This can be expected since the noise level is a random process. Since the noise power varies with time and with separate branches, its measured value is explicitly in the tables. As can be noted, the noise power measurements have significant variation.

In these tests the suppression of the interference was evaluated as a function of the INR in the main channel and the INR in the auxiliaries (auxiliary gain). As described in Chapter II, the INR in the main channel is expected to be initially

between -18 dB and 5 dB. However, because of dynamic range limitations when actual satellite signals are used with the experimental system one is unable to obtain such a wide range of INR. There are several factors which constrain the dynamic range of the signal levels. First, as mentioned before, the interference power in the auxiliaries must be at least 8.4 dB larger than the interference power in the main channel. This constraint establishes the upper bound of the INR in the main channel. For example if we assume for the moment that the noise power in the main channel is equal to the noise power in the auxiliaries, then the INR in the main channel should be at least 8.4 dB lower in the INR in the signal branch. The maximum INR in the auxiliaries is on the order of 13 dB, thus with these assumptions the maximum INR in the main channel that the adaptive array can successfully suppress is about 4.6 dB. Additional amplification of the received signal in the signal branch to counteract the vector modulator insertion loss would solve this problem.

The second limitation in dynamic range is due to the physical dimensions of the feeds on the feed platform; specifically, the center of the feed for each Offset Feed is 4.62 inches away from the center of the auxiliary channel feeds. This distance is critical since the main beam associated with each feed is narrow. For this reason, beams associated with various feeds in a feed cluster cannot be pointed directly at the interfering signal source. Thus there is a trade-off between the interference power received in the auxiliaries versus the interference power received in the Offset Feeds. For example, if the beams associated with an auxiliary channel are pointed directly at the interfering signal source, then the interference power in the Offset Feed will be reduced by at least 20 dB (note Figure 48). The result of this is that if one maximizes the INR in the auxiliaries, then the INR in the main channel will be reduced, and the measurable suppression will be

correspondingly reduced. However, if the INR in the main channel is maximized for the maximum measurable adaptive array suppression, the INR in the auxiliaries must be reduced. In this case, with a low interference power in the auxiliaries and about the same amount of noise power in the auxiliaries, the weights will be large in magnitude and considerable amounts of noise will be added to the array output from the signal branch. This noise will significantly increase the overall noise floor at the array output and thus again reduce the measurable suppression. Thus, in these experiments it is important to consider the allowable dynamic range of the interference powers available.

A third limitation in dynamic range occurs because the power meter/amplifier cannot provide accurate power measurements when the signal levels are less than about -50 dBm. Therefore, when the interference power in the Offset Feeds is attenuated by a large amount, the signal level which results is below this minimum detectable signal threshold. However, in many cases the same signal can be measured without attenuation, and one can calculate the interference power after attenuation by knowing the amount of attenuation used.

In the above experiments the INR in the main channel was required to be above 0 dB. The reason for this requirement was our inability to measure an interference power below the system noise level. In an actual satellite communication link environment the interference may be below the system noise level. In the next subsection further tests are proposed to investigate the operation of the modified feedback loop when the INR in the main and auxiliary channels are less than 0 dB.

5.9.1 Noise Injection Experiments

Presently interference powers cannot be established accurately when the interfering signal is obscured by the system noise floor. For this reason, it is impossible to determine if the interference is truly suppressed below the ambient noise level with a modified sidelobe canceler. Also, one cannot test the ability of the experimental system to null interfering signals below the noise level. One can simulate a signal scenario where the INR in the main channel and the auxiliary channels are less than 0 dB by injecting controlled amounts of noise during an adaptive array experiment and not injecting the noise during performance evaluation. Specifically, before the signals from the actual antenna array enter the array processor, they are combined with controlled levels of noise generated by the noise sources in the array simulator. The array simulator is described in Subsection 2.3.2. Removing the injected noise allows one to measure the suppression of signal below the injected noise level. Still however, the measurable suppression will not be larger than the initial interference-to-noise ratio in the main channel before noise injection. Once the adaptive array suppresses the interference to the receive system noise floor, the interference powers can no longer be measured, even if the artificially injected noise is turned off.

Table 20 shows some representative tests with a desired signal absent in the main channel for one and two interfering signals. This table lists respectively from left to right: the interference plus noise power in the main channel from Offset Feed #1 after attenuation and the interference plus noise power in the main channel from Offset Feed #2 after attenuation and the noise power in the main channel which includes the injected noise power, and the INR in correlator branches #1 and #2 after injection of noise, and finally the quality of the video picture after adaptation.

Table 20: Noise injection tests, both auxiliary loops are activated, no desired signal present.

Main Channel (dBm)			INR(Corr. Branch #) (dB)		Final
$(I+N)_1$	$(I+N)_2$	N	#1	#2	Picture
-44.2	—	-30.7	-8.8	-5.0	Noise
-50.2	—	-30.9	-8.8	-5.0	Noise
-59.2	—	-31.0	-8.8	-5.0	Noise
-49.0	—	-31.0	-4.6	-17.3	Noise
—	-46.8	-31.0	-13.2	-1.5	Noise
-47.8	-47.3	-31.0	-13.3	-2.3	Noise
-48.1	-49.3	-31.0	-13.2	-10.5	Noise

In all experiments the injected noise power is the same for each of the auxiliary channel branches and for the main channel. The power of the injected thermal noise is -31.0 dBm with a 6 MHz bandwidth. Since the power of the injected noise is greater than 10 dB above the system noise, one can approximate the total noise power as only the injected noise power. Because of this approximation, one can calculate the INR in the main and auxiliary channels. The injected noise was removed prior to judging the video picture quality after adaptation. Otherwise the injected noise may mask a weak interfering signal to a point where it is not visible. Note that the interference is suppressed below the injected noise level even if the INR in the auxiliary channels is less that 0 dB. As can be noted from Table 20, the modified feedback loops are able to suppress interference below the noise level even when the INR in the auxiliaries is less than 0 dB.

In preliminary noise injection tests it was observed that if the noise power

in the auxiliaries is greater than the corresponding interference power in the auxiliaries, as in the case of a very low gain auxiliary antenna, a modified feedback loop sidelobe canceler is needed rather than the conventional sidelobe canceler to suppress an interfering signal in the main channel below the noise level. However, if the interference-to-noise ratio in the auxiliaries is more than 10 dB, either type of adaptive antenna array will suffice. Therefore, the modified feedback loop sidelobe canceler is useful in the situation where the INR in the auxiliaries is less than 0 dB, and it is desirable to suppress the interference in the main channel below the system noise floor.

5.10 Summary

In this chapter, the calibration and operation of the experimental system was discussed. The results of two categories of experiments (with and without a desired signal) were also summarized. It was shown that in the absence of a desired signal in the main channel the experimental system can suppress two interfering signal below the noise level for various values of INR in the auxiliaries. Since satellite signals were used, there are dynamic range limitations of the measurable signal and noise powers. It was also shown that with a desired signal present in the main channel, but with a steering vector not implemented, the weights saturated. This problem can be solved by implementing a steering vector. Several possible methods of steering vector implementation were proposed. The next chapter summarizes the work and provides ideas for future investigations.

CHAPTER VI

SUMMARY AND CONCLUSIONS

In this thesis, the performance of an experimental adaptive array was evaluated using the signals received from geostationary satellites. To do so, an earth station was built to receive signals simultaneously from three geostationary satellites. The earth station antenna is a 30 ft diameter parabolic reflector with multiple defocused scalar feeds. The defocused feeds are employed to produce multiple beams which can be pointed in the direction of the desired satellite source and in the general direction of interfering satellite sources. Because of the narrow beamwidths and low sidelobes of the center-fed 30 ft diameter parabolic reflector, two more offset feeds were added to the original five feed adaptive array. The interfering signals received by these two additional feeds are summed with the prime feed to form the main channel. The user has control over the interference scenario by varying the attenuation of the signals received by the Offset Feeds prior to their summation with the prime feed signal. Because of size constraints, the outer rings were cut off of the scalar feeds. A study presented showed that the performance of the feeds was not significantly degraded when their outer rings are removed. The scalar feeds were further modified to obtain the desired aperture illumination for the parabolic reflector.

The received signals are television receive only direct broadcast frequency modulated signals in the 3.7-4.2 GHz band. The received signals are downcon-

verted by the receive system to a 69 MIIz intermediate frequency and fed directly into the array processor. In order to keep the signals coherent a common local oscillator is used for the downconverters. Because of this, the commercially built downconverters had to be modified, and this modification was discussed. A commercial satellite receiver is used to demodulate the frequency modulated TV pictures. A video monitor, spectrum analyzer, and power meter are used for performance evaluation.

Tests were performed both with and without a strong desired signal in the main channel. Initial experiments were performed without a desired signal. First, it was determined that each of the modified feedback loops was functional. As long as the level of the interfering signal in the main channel was below that in the auxiliaries, the adaptive array was successful in suppressing the interference. Once the interference was suppressed, only noise was observed on the television monitor and spectrum analyzer. With both feedback loops activated, it was also observed that the interference was suppressed over the 36 MHz wide satellite transponder bandwidth.

The adaptive array was equally successful in suppressing two interfering signals with various values of INR in the main and auxiliary channels. With a strong desired present the adaptive array attempted to suppress the desired signal. In this case, a steering vector is required for proper operation of the adaptive array. Several methods of implementing a steering vector were discussed. In experiments with a moderate desired signal present in the main channel, the adaptive array was able to null the interfering signal without a steering vector. Thus, we have shown experimentally that with modified feedback loops, an adaptive array can be used to suppress the weak interfering signals encountered in broadcast satellite communications systems if a suitable steering vector is implemented.

In the future there are many avenues of possible research. These include changes in the hardware and/or software of the experimental adaptive array system. Some ideas for future research are given below.

- The most immediate experiments for the future involve implementing a steering vector and injecting decorrelated noise into each branch of the adaptive array. A study should be performed to determine an applicable method of calculating a steering vector in an actual satellite communication environment. Noise injection tests should be carried out to further observe the operation of the modified feedback loop in the presence of weak interfering signals in a high noise level. Moreover, quantitative performance differences of the modified versus the unmodified feedback sidelobe canceler could be investigated using actual satellite signals.

- With the hybrid experimental receive system, one can easily implement various weight control algorithms without a hardware revision. Thus the performance of algorithms such as the modified sample matrix inversion (SMI) technique and the steepest descent method can be investigated using actual satellite signals. Another possible alternative is to use the LMS algorithm when each geostationary satellite has an electronic "tag". This tag could be included with the other information located at the end of each television field during vertical blanking.

- A possible alternative adaptive array scheme is to use a single antenna with each feedback loop. However one can still use two separate amplifiers for each branch of an auxiliary channel to decorrelate the internally generated thermal noise [5]. Even though the external noise would be correlated it was found that the internal noise was the dominant source of the system noise (see Appendix A), so the use of two separate amplifiers would decorrelate much of the system noise. In addition, the gain of the auxiliary elements would increase significantly (9.6 dB for this experimental system) because the beams associated with the feeds can be

pointed directly at the interfering signals. This increase in gain should result in a more effective interference suppression. Therefore, the overall suppression may not be degraded [18, p13]. As a result, the receive system would be less complex and less costly.

APPENDIX A

THE SYSTEM LINK CALCULATIONS

Link calculations:

The system temperature (T_{sys}) referenced to the antenna is given by

$$T_{sys} = T_A + T_{LNA} + \frac{(L-1)T_o}{G_{LNA}} + \frac{LT_{Downconverter}}{G_{LNA}} \qquad (A.1)$$

where

T_A = Antenna Temperature

= 25 K from [13]

(approximate spillover illuminating the Earth)

T_{LNA} = LNA Noise Temperature = 75 K

T_o = Standard Temperature = 290 K

$T_{Downconverter}$ = Noise temperature of the downconverter

$= (F-1)T_o = (31.62-1) \times 290K = 8900$ K

F= Downconverter Noise Figure

= Antilog(15 dB/10) = 31.62

G_{LNA} = Gain of LNA

= antilog(49 dB/10)

$= 7.94 \times 10^4$

L = Loss of 39 feet of RG-9/U transmission line

= antilog(7 dB/10) = 5.0

thus

$$T_{sys} = 25K + 75K + \frac{(5.0-1)290K}{7.94 \times 10^4} + \frac{8900K \times 5.0}{7.94 \times 10^4} = 100.6 \text{ K.} \qquad (A.2)$$

From T_{sys} the system noise can be calculated as

N = Noise referenced to the antenna = kTB

k = Boltzmann's constant = $1.38 \times 10^{-23}\ JK^{-1}$

B = System Bandwidth = 32 MHz

$= 1.38 \times 10^{-23} \times 100.6 \times 32 \times 10^6$

$= 4.44 \times 10^{-14}$ Watts.

Finally,

$$SNR = \frac{(EIRP)\lambda^2 G_R}{(4\pi R)^2 N} \qquad (A.3)$$

where

SNR = Signal-to-noise ratio of the receiving system

EIRP = Effective Isotropic Radiated Power

(Telstar 301) = 36.0 dBW

R = Height = 36000 Kilometers

G_R = Gain of a 30 ft diameter reflector antenna

= (from Table 1) = 48.6 dBi

λ = Wavelength = 0.075 meters at 4.0 GHz.

Thus,

$$SNR = \frac{10^{\frac{(36+48.6)}{10}} \times 0.075^2}{(4 \times \pi \times 36.0 \times 10^6)^2 \times 4.44^{-14}} = 22.5 \text{ dB.} \qquad (A.4)$$

The measured SNR is 21.8 dB for this system, which agrees closely with the calculated value of 22.5 dB.

REFERENCES

[1] S.P. Applebaum, "Adaptive Arrays," *IEEE Transactions on Antennas and Propagation*, Vol. AP-24, No. 5, pp. 585-598, September 1976.

[2] B. Widrow, et al., "Adaptive Antenna Arrays," Proc. IEEE, Vol. 55, No. 12, pp. 2143-2159, December 1967.

[3] R.T. Compton, Jr., *Adaptive Antennas – Concepts and Performance*, Prentice-Hall, Englewood Cliffs, NJ., 1988.

[4] R.T. Compton, Jr., R.J. Huff, W.G. Swarner and A.A. Ksienski, "Adaptive Arrays for Communication Systems: An Overview of Research at The Ohio State University," *IEEE Transactions on Antennas and Propagation*, Vol. AP-24, No. 5, pp. 599-607, September 1976.

[5] I.J. Gupta and A.A. Ksienski, "Adaptive Arrays for Weak Interfering Signals," *IEEE Transactions on Antennas and Propagation*, Vol. AP- 34, No. 3, pp. 420-426, March 1986.

[6] J. Ward, "Adaptive Arrays for Weak Interfering Signals – An Experimental System," M.Sc. Thesis, The Ohio State University, Department of Electrical Engineering, Columbus, Ohio, 1987.

[7] D.M. Jansky and M.C. Jeruchim, *Communication Satellites in the Geostationary Orbit*, Artech House Inc., Norwood, Ma., 1987.

[8] Y. Yamamura and C. Levis, "Calculation of Allowable orbital spacings for the Fixed Satellite Service," Technical Report 716548-1, The Ohio State University ElectroScience Laboratory, Department of Electrical Engineering, July 1985.

[9] J.W. Eberle, "High Gain Antenna Array Facilities at the Ohio State University," Technical Report 1072-3, The Ohio State University Antenna Laboratory, Department of Electrical Engineering, page 5, 22 September 1961.

[10] R.C. Rudduck and Y.C. Chang, "Numerical Electromagnetic Code-Reflector Antenna Code, Part I: User's Manual (Version 2)," Technical Report 712242-16 (713742), The Ohio State University ElectroScience Laboratory, Department of Electrical Engineering, December 1982.

[11] Y.C Chang and R.C. Rudduck, "Numerical Electromagnetic Code-Reflector Antenna Code, Part II: User's Manual (Version 2)," Technical Report 712242-17 (713742), The Ohio State University ElectroScience Laboratory, Department of Electrical Engineering, December 1982.

[12] C.W. Chuang and T.H. Lee, "Calculation of Fields Radiated by Rotationally Symmetric Horn Antennas Using Moment Method," Technical Report 717822-6, The Ohio State University ElectroScience Laboratory, Department of Electrical Engineering, May 1987.

[13] M. Long, *World Satellite Almanac* - The complete guide to Satellite Transmission and Technology, Howard W. Sams and Company, Indianapolis, Indiana, 1987.

[14] R. Wohlleben, H. Mattes, and O. Lochner, "Simple, Small, Primary Feed for Large Opening Angles and High Aperture Efficiency," *Electronic Letters*, Vol 8, No 19, Sept. 1972.

[15] P.J.B. Clarricoats and A.D. Olver, *Corrugated Horns for Microwave Antennas*, Peter Peregrinus Ltd., London, UK, 1984.

[16] J.D. Kraus, *Antennas*, 2^{nd} Edition, McGraw-Hill, 1988.

[17] A.J. Simmons and A.F. Kay, "The Scalar Feed - A High Performance Feed For Large Paraboloid Reflectors," IEE Conf. Pub. no 21, pp 213-217, 1966.

[18] I.J. Gupta, "Adaptive Antenna Arrays For Weak Interfering Signals," Technical Report 716111-2, The Ohio State University ElectroScience Laboratory, Department of Electrical Engineering, Jan. 1985.

[19] J. Ward, et al., "An Experimental Adaptive Array To Suppress Weak Interfering Signals," *IEEE Transactions on Antennas and Propagation*, Vol. AP-36, No. 11, pp. 1551-1559, November 1988.

[20] I.J. Gupta, W.G. Swarner, E.K. Walton, "Adaptive Antenna Arrays For Satellite Communications - Design and Testing," Technical Report 716111-3, The Ohio State University ElectroScience Laboratory, Department of Electrical Engineering, Sept. 1985.

[21] E.K. Walton and J.D. Young, "The Ohio State University Compact Radar Cross-Section Measurement Range," *IEEE Transactions on Antennas and Propagation*, Vol. AP-32, No. 11, pp. 1218-1223, November 1984.